

**Biochemical Analysis of the Phosphatase Domain of the  
Human Soluble Epoxide Hydrolase (sEH)**

**D i s s e r t a t i o n**  
zur Erlangung des Grades  
„Doktor der Naturwissenschaften“

am Fachbereich Biologie  
der Johannes Gutenberg-Universität in Mainz

**Shirli Homburg**  
geboren in Tel-Aviv

Mainz 2010

**Dekan:**

**1. Berichterstatter:**

**2. Berichterstatter:**

**Tag der mündlichen Prüfung:**

# Contents

Acknowledgments .....	1
Abbreviations.....	2
1 Abstract .....	3
2 Introduction.....	7
<b>2.1 Epoxides, epoxide hydrolases (EH) and xenobiotic Metabolism .....</b>	<b>7</b>
2.1.1. Epoxides.....	7
2.1.2. Xenobiotic metabolism and Epoxide hydrolases .....	7
2.1.3. Members of the epoxide hydrolase family .....	9
<b>2.2 The general structure of the sEH and the structure and catalytic mechanism of the epoxide hydrolase located in the sEH C-terminal domain .....</b>	<b>10</b>
2.2.1 Substrate selectivity of the sEH (the C-terminal domain enzyme).....	11
2.2.2 Genomics and Evolution .....	12
<b>2.3 Roles of human sEH (currently assigned to the epoxide hydrolase activity) .....</b>	<b>12</b>
2.3.1 sEH in Arachidonic acid (AA) metabolism and in regulation of blood pressure.....	13
2.3.2 sEH and inflammation .....	13
2.3.3 sEH in cytotoxicity and cancer .....	14
2.3.4 sEH in stress conditions.....	14
<b>2.4 The sEH N-terminal domain.....</b>	<b>14</b>
2.4.1 The N-terminal domain of the sEH is a phosphatase .....	14
2.4.2 The structure of the sEH phosphatase and its homology to the HAD superfamily of enzymes .....	15
2.4.3 Substrates and potential roles of the sEH phosphatase.....	17
<b>2.5 Distribution of mammalian sEH .....</b>	<b>18</b>
2.5.1 Distribution in different species and sexes.....	18
2.5.2 Tissue distribution .....	18
2.5.3 Distribution in the cell .....	18
3 Aims .....	20
4 Materials and methods .....	21
<b>4.1 Materials .....</b>	<b>21</b>
4.1.1 Chemicals and reagents .....	21
4.1.2 Standard buffers and solutions .....	21
4.1.3 Instruments.....	22
4.1.4 Kits .....	23
4.1.5 Software .....	23
4.1.6 Antibodies.....	24
4.1.7 Enzymes.....	24
4.1.8 Oligonucleotides.....	24
4.1.9 Vectors .....	25
4.1.10 Molecular weight markers .....	26
4.1.10.1 Protein markers (Prestained SDS-Marker) .....	26
4.1.10.2 DNA-Molecular weight standards.....	26

4.1.11	Bacteria .....	27
4.1.12	Culture media .....	27
<b>4.2</b>	<b>Methods .....</b>	<b>27</b>
4.2.1	Constructions of mutants .....	27
4.2.1.1	Site directed mutagenesis .....	27
4.2.1.2	Digestion with Dpn 1.....	28
4.2.1.3	Agarose gel electrophoresis.....	28
4.2.1.4	Cloning of the mutants: Transformation, bacteria culture and selection, plasmid isolation .....	29
4.2.1.5	DNA concentration and purity measurement .....	29
4.2.1.6	Sequencing.....	29
4.2.1.7	Restriction digestion .....	30
4.2.2	Generation of recombinant proteins.....	30
4.2.2.1	Expression of the sEH-phosphatase mutant proteins in <i>E.coli</i> : Transformation of bacteria, bacterial culture and induction of protein expression, lysis of Bacteria cells and the use of the FrenchPress system.....	30
4.2.2.2	Purification of the sEH phosphatase mutant proteins using a metal chelate affinity chromatography and the use of the BioLogic Duo-Flow system.....	30
4.2.2.3	Protein analysis .....	31
4.2.2.3.1	Quantifying proteins by the Bradford method .....	31
4.2.2.3.2	SDS polyacrylamide gel electrophoresis .....	31
4.2.2.3.3	Coomassie staining.....	32
4.2.2.3.4	Immunoblot analysis (western blots) by semi-dry blotting and tank-blotting .....	32
4.2.3	Enzymatic assays and calculations .....	33
4.2.3.1	Activity assay: Screening assay for product formation (4-nitrophenol) and kinetic assay .....	33
4.2.3.2	Determination of the kinetic parameters: The four calculating methods.....	33
4.2.3.3	Processing the kinetic assay results and calculations of the kinetic parameters in four calculating methods.....	35
<b>5</b>	<b>Results .....</b>	<b>40</b>
<b>5.1</b>	<b>Selection of candidate phosphatase active-site amino acids.....</b>	<b>40</b>
<b>5.2</b>	<b>Construction of sEH phosphatase active site mutants .....</b>	<b>40</b>
5.2.1	Proving the success of the site directed mutagenesis process .....	42
<b>5.3</b>	<b>Expression of the recombinant human sEH phosphatase proteins (the human sEH phosphatase active site mutant and WT proteins).....</b>	<b>45</b>
<b>5.4</b>	<b>Purification of the recombinant human sEH phosphatase proteins .....</b>	<b>46</b>
<b>5.5</b>	<b>Characterization of the human sEH phosphatase mutants .....</b>	<b>50</b>
5.5.1	Activity-screening assay.....	50
5.5.2	Kinetic activity measurements and calculations.....	50
<b>6</b>	<b>Discussion .....</b>	<b>54</b>
<b>6.1</b>	<b>The kinetic properties of the sEH phosphatase mutant proteins further characterize the catalytic mechanism of phosphorylation.....</b>	<b>54</b>
<b>6.2</b>	<b>The deduced enzymatic reaction mechanism .....</b>	<b>60</b>
<b>6.3</b>	<b>Comparison between the activity results of the sEH phosphatase active site mutants and the activity results of the active site mutants of few other HAD enzymes .....</b>	<b>61</b>

<b>6.4</b>	<b>Current knowledge on the sEH phosphatase (other than the catalytic mechanism) and possibilities for further investigations .....</b>	<b>63</b>
6.4.1	A suggestive role for the sEH phosphatase in regulation of blood pressure through the eNOS enzyme.....	65
<b>6.5</b>	<b>Processing the kinetic assay results: via which technique should the kinetic determinants be calculated? .....</b>	<b>65</b>
<b>7</b>	<b>References .....</b>	<b>67</b>
<b>8</b>	<b>Appendix .....</b>	<b>72</b>
<b>8.1</b>	<b>The amino acid exchanges .....</b>	<b>72</b>
<b>8.2</b>	<b>The different combinations of the amino acids genetic code.....</b>	<b>73</b>
<b>8.3</b>	<b>The oligonucleotide primers.....</b>	<b>74</b>
<b>8.4</b>	<b>Table of results .....</b>	<b>76</b>
<b>8.5</b>	<b>Declaration .....</b>	<b>77</b>
<b>8.6</b>	<b>Curriculum Vitae .....</b>	<b>78</b>

## **Acknowledgments**

Very special thanks to my supervisor, my husband and kids.

## Abbreviations

### Amino acids

<b>A</b>	alanine	<b>Ala</b>
<b>C</b>	cysteine	<b>Cys</b>
<b>D</b>	aspartic acid	<b>Asp</b>
<b>E</b>	glutamic acid	<b>Glu</b>
<b>F</b>	phenylalanine	<b>Phe</b>
<b>G</b>	glycine	<b>Gly</b>
<b>H</b>	Histidine	<b>His</b>
<b>I</b>	isoleucine	<b>Ile</b>
<b>K</b>	lysine	<b>Lys</b>
<b>L</b>	leucine	<b>Leu</b>
<b>M</b>	methionine	<b>Met</b>
<b>N</b>	asparagine	<b>Asn</b>
<b>P</b>	proline	<b>Pro</b>
<b>Q</b>	glutamine	<b>Gln</b>
<b>R</b>	arginine	<b>Arg</b>
<b>S</b>	serine	<b>Ser</b>
<b>T</b>	threonine	<b>Thr</b>
<b>V</b>	valine	<b>Val</b>
<b>W</b>	tryptophan	<b>Trp</b>
<b>Y</b>	tyrosine	<b>Tyr</b>

### DNA bases

<b>A</b>	adenine
<b>C</b>	cytosine
<b>G</b>	guanine
<b>T</b>	thymine

<b>ARDS</b>	adult respiratory distress syndrome
<b>GSH</b>	reduced glutathion
<b>GST</b>	glutathion-s-transferase
<b>HAD1</b>	haloacid dehalogenase
<b>(His)<sub>6</sub></b>	six histidine-tag
<b>HLD1</b>	haloalkane dehalogenase
<b>LEH</b>	limonene epoxide hydrolase
<b>LTA<sub>4</sub></b>	leukotriene A <sub>4</sub>
<b>mEH</b>	microsomal epoxide hydrolase
<b>PMM</b>	phosphomannomutase
<b>PSP</b>	phosphoserine phosphatase
<b>sEH</b>	soluble epoxide hydrolase
<b>WT</b>	wild type

## 1 Abstract

The soluble epoxide hydrolase (sEH) is a member of the epoxide hydrolase family of enzymes. Its “classic” role is detoxification, by converting potentially harmful epoxides to their vicinal diols. Furthermore, its main function is the metabolism of endogenous arachidonic-acid- derived signalling molecules such as epoxyeicosatrienoic acids to the corresponding diols. Hence, the sEH has evolved as a target for therapy of hypertension, inflammation and in therapy of a growing number of other pathologies.

The sEH is a homodimer in which each subunit is composed of two domains. The catalytic center for the epoxide hydrolase activity is located in the 35kD C-terminal domain which has been well studied and nearly all catalytic properties of the enzyme and its known roles have been exclusively related to this part of the enzyme. In contrast, little is known about the sEH 25kD N-terminal domain. It belongs to the haloacid dehalogenases (HAD) superfamily of hydrolases and for a long time the function of the N-terminal domain was unclear. In our working group, we were able to show for the first time that the mammalian sEH is a bifunctional enzyme as, in addition to the well known enzymatic activity in the C-terminal domain, it possess another active site in its N-terminal domain, with a  $Mg^{2+}$ -dependent phosphatase activity. Based on the homology with other HAD enzymes a two-step mechanism for the newly discovered sEH N-terminal phosphatase has been proposed.

To enlighten the catalytic mechanism of dephosphorylation, a biochemical analysis of the human sEH phosphatase catalytic process was performed by constructing active site mutants by site directed mutagenesis. Thus, identifying the active site amino acids that take part in the catalytic process and investigating their role in the catalytic mechanism.

On the basis of structural and possible functional similarities between the sEH and other members of the HAD superfamily, candidate catalytic amino acids (conserved and partly conserved amino acids) in the active site of the sEH phosphatase domain were predicted to be crucial to its catalytic activity.

Thus, of the amino acids in the phosphatase domain, eight amino acids (Asp9 (D9), Asp11 (D11), Thr123 (T123), Asn124 (N124), Lys160 (K160), Asp184 (D184), Asp185 (D185), Asn189 (N189)) were selected to be exchanged to nonfunctional amino acids by site-directed mutagenesis. At least two alternative amino acids, either alanine or an amino acid structurally similar to the one in the wild type enzyme (WT) were introduced for each amino acid candidate. In total, 18 different recombinant clones were constructed encoding mutant sEH phosphatase proteins with a single amino acid residue substitution. The 18 mutants and the WT (N-terminal domain sequence without mutation), constructed in an expression vector, were cloned, verified by restriction and sequencing and recombinantly expressed in *E.coli*. The constructed mutants and the WT proteins (the soluble 25kD subunit) were successfully purified on metal affinity chromatography and tested for phosphatase activity towards the generic phosphatase substrate 4-nitrophenyl phosphate. Mutants that exhibited any degree of activity were subjected to kinetic assays. From the processed results of the kinetic assays, kinetic parameters were calculated in four well- established calculating methods and interpretation was made according to one method the direct linear plot.

Most of the 18 mutant proteins were inactive or lost a major part of the enzyme's activity ( $V_{max}$ ) in comparison to the WT enzyme (WT:  $V_{max}=77.34 \text{ nmol}^{-1} \text{ mg}^{-1} \text{ min}$ ). Loss of activity was unlikely to be due to a loss of structural integrity in any of the mutants (as the WT and the mutated proteins had kept the same behaviour upon chromatography). All replacements of residues Asp9 (D9), Lys160 (K160), Asp184 (D189) and Asn189 (N189) resulted in a complete loss of phosphatase activity proving their



vital function in catalysis. Part of the amino acid exchanges performed for Asp11 (D11), Thr123 (T123), Asn124 (N124) and Asp185 (D185) resulted in mutant proteins that lost a substantial part of their activity but still exhibited detectable activity to different extent (2 -10% and 40% of the WT enzyme activity). Mutant proteins of this group showed altered kinetic properties (only in  $V_{max}$  or  $V_{max}$  and  $K_m$ ). The analysis of the mutant Asp11  $\rightarrow$  Asn kinetic result was of special interest, showing a sole combination of a strong reduction in  $V_{max}$  ( $8.1 \text{ nmol}^{-1} \text{ mg}^{-1} \text{ min}$ ) and a significant reduction in  $K_m$  (Asp11:  $K_m=0.54 \text{ mM}$ , WT:  $K_m=1.3 \text{ mM}$ ), implying a role for the Asp11 (D11) in hydrolysis, the second step of the catalytic cycle.

Altogether, the results indicate that all examined amino acids are required for the enzyme's catalytic activity and participate in forming the sEH phosphatase active site. Moreover, with these results we were able to add information to the possible roles of the examined amino acids supporting a two-step catalytic mechanism of dephosphorylation. We can therefore propose a combined reaction mechanism which is related to other members of the HAD family. This mechanism was based on the elucidated 3D structure, the results of this work and results of further biochemical investigations.

The two-step catalytic mechanism of dephosphorylation involves a nucleophilic attack of the substrate phosphorous by the active site nucleophile Asp9 (D9) under formation of an acylphosphate enzyme intermediate followed by release of the dephosphorylated substrate. In the second step, hydrolysis of the enzyme phosphate intermediate supported by Asp11 (D11), and release of the phosphate group take place. The other examined amino acids are involved in binding of  $\text{Mg}^{2+}$  and/or substrate.

As the catalytic mechanism has been elucidated with the contribution of this work, other themes, which are left to be investigated were discussed in this work: the physiological role of the sEH phosphatase, its endogenous-physiological substrates and the way it functions as a bifunctional enzyme (the way the two catalytic sites communicate and on what level).

## Zusammenfassung

Die lösliche Epoxidhydrolase (sEH) gehört zur Familie der Epoxidhydrolase-Enzyme. Die Rolle der sEH besteht klassischerweise in der Detoxifikation, durch Umwandlung potenziell schädlicher Epoxide in deren unschädliche Diol-Form. Hauptsächlich setzt die sEH endogene, der Arachidonsäure verwandte Signalmoleküle, wie beispielsweise die *Epoxyeicosatrienoic acid*, zu den entsprechenden Diolen um. Daher könnte die sEH als ein Zielenzym in der Therapie von Bluthochdruck und Entzündungen sowie diverser anderer Erkrankungen eingesetzt werden.

Die sEH ist ein Homodimer, in dem jede Untereinheit aus zwei Domänen aufgebaut ist. Das katalytische Zentrum der Epoxidhydrolaseaktivität befindet sich in der 35 kD großen C-terminalen Domäne. Dieser Bereich der sEH wurde bereits im Detail untersucht und nahezu alle katalytischen Eigenschaften des Enzyms sowie deren dazugehörige Funktionen sind in Zusammenhang mit dieser Domäne bekannt. Im Gegensatz dazu ist über die 25 kD große N-terminale Domäne wenig bekannt. Die N-terminale Domäne der sEH wird zur *Haloacid* Dehalogenase (HAD) Superfamilie von Hydrolasen gezählt, jedoch war die Funktion dieser N-terminalen Domäne lange ungeklärt. Wir haben in unserer Arbeitsgruppe zum ersten Mal zeigen können, dass die sEH in Säugern ein bifunktionelles Enzym ist, welches zusätzlich zur allgemein bekannten Enzymaktivität im C-terminalen Bereich eine weitere enzymatische Funktion mit  $Mg^{2+}$ -abhängiger Phosphataseaktivität in der N-terminalen Domäne aufweist. Aufgrund der Homologie der N-terminalen Domäne mit anderen Enzymen der HAD Familie wird für die Ausübung der Phosphatasefunktion (Dephosphorylierung) eine Reaktion in zwei Schritten angenommen.

Um den katalytischen Mechanismus der Dephosphorylierung weiter aufzuklären, wurden biochemische Analysen der humanen sEH Phosphatase durch Generierung von Mutationen im aktiven Zentrum mittels ortsspezifischer Mutagenese durchgeführt. Hiermit sollten die an der katalytischen Aktivität beteiligten Aminosäurereste im aktiven Zentrum identifiziert und deren Rolle bei der Dephosphorylierung spezifiziert werden.

Auf Basis der strukturellen und möglichen funktionellen Ähnlichkeiten der sEH und anderen Mitgliedern der HAD Superfamilie wurden Aminosäuren (konservierte und teilweise konservierte Aminosäuren) im aktiven Zentrum der sEH Phosphatase-Domäne als Kandidaten ausgewählt.

Von den Phosphatase-Domäne bildenden Aminosäuren wurden acht ausgewählt (Asp9 (D9), Asp11 (D11), Thr123 (T123), Asn124 (N124), Lys160 (K160), Asp184 (D184), Asp185 (D185), Asn189 (N189)), die mittels ortsspezifischer Mutagenese durch nicht funktionelle Aminosäuren ausgetauscht werden sollten. Dazu wurde jede der ausgewählten Aminosäuren durch mindestens zwei alternative Aminosäuren ersetzt: entweder durch Alanin oder durch eine Aminosäure ähnlich der im Wildtyp-Enzym. Insgesamt wurden 18 verschiedene rekombinante Klone generiert, die für eine mutante sEH Phosphatase Domäne kodieren, in dem lediglich eine Aminosäure gegenüber dem Wildtyp-Enzym ersetzt wurde. Die 18 Mutanten sowie das Wildtyp (Sequenz der N-terminalen Domäne ohne Mutation) wurden in einem Expressionsvektor in *E.coli* kloniert und die Nukleotidsequenz durch Restriktionsverdau sowie Sequenzierung bestätigt. Die so generierte N-terminale Domäne der sEH (25kD Untereinheit) wurde dann mittels Metallaffinitätschromatographie erfolgreich aufgereinigt und auf Phosphataseaktivität gegenüber des allgemeinen Substrats 4-Nitrophenylphosphat getestet. Diejenigen Mutanten, die Phosphataseaktivität zeigten, wurden anschließend kinetischen Tests unterzogen. Basierend auf den Ergebnissen dieser Untersuchungen wurden kinetische Parameter mittels vier gut etablierter Methoden berechnet und die Ergebnisse mit der „direct linear blot“ Methode interpretiert.

Die Ergebnisse zeigten, dass die meisten der 18 generierten Mutanten inaktiv waren oder einen Großteil der Enzymaktivität ( $V_{max}$ ) gegenüber dem Wildtyp verloren (WT:  $V_{max}=77.34 \text{ nmol}^{-1} \text{ mg}^{-1} \text{ min}$ ). Dieser Verlust an Enzymaktivität ließ sich nicht durch einen Verlust an struktureller Integrität erklären, da der Wildtyp und die mutanten Proteine in der Chromatographie das gleiche Verhalten zeigten. Alle Aminosäureaustausche Asp9 (D9), Lys160 (K160), Asp184 (D184) und Asn189 (N189) führten zum kompletten Verlust der Phosphataseaktivität, was auf deren katalytische Funktion im N-terminalen Bereich der sEH hindeutet. Bei einem Teil der Aminosäureaustausche die für Asp11 (D11), Thr123 (T123), Asn124 (N124) und Asn185 (D185) durchgeführt wurden, kam es, verglichen mit dem Wildtyp, zu einer starken Reduktion der Phosphataseaktivität, die aber dennoch für die einzelnen Proteinmutanten in unterschiedlichem Ausmaß zu messen war (2 -10% and 40% of the WT enzyme activity). Zudem zeigten die Mutanten dieser Gruppe veränderte kinetische Eigenschaften ( $V_{max}$  allein oder  $V_{max}$  und  $K_m$ ). Dabei war die kinetische Analyse des Mutanten Asp11  $\rightarrow$  Asn aufgrund der nur bei dieser Mutanten detektierbaren starken  $V_{max}$  Reduktion ( $8.1 \text{ nmol}^{-1} \text{ mg}^{-1} \text{ min}$ ) und einer signifikanten Reduktion der  $K_m$  (Asp11:  $K_m=0.54 \text{ mM}$ , WT:  $K_m=1.3 \text{ mM}$ ), von besonderem Interesse und impliziert eine Rolle von Asp11 (D11) im zweiten Schritt der Hydrolyse des katalytischen Zyklus.

Zusammenfassend zeigen die Ergebnisse, dass alle in dieser Arbeit untersuchten Aminosäuren für die Phosphataseaktivität der sEH nötig sind und das aktive Zentrum der sEH Phosphatase im N-terminalen Bereich des Enzyms bilden. Weiterhin tragen diese Ergebnisse zur Aufklärung der potenziellen Rolle der untersuchten Aminosäuren bei und unterstützen die Hypothese, dass die Dephosphorylierungsreaktion in zwei Schritten abläuft. Somit ist ein kombinierter Reaktionsmechanismus, ähnlich denen anderer Enzyme der HAD Familie, für die Ausübung der Dephosphorylierungsfunktion denkbar. Diese Annahme wird gestützt durch die 3D-Struktur der N-terminalen Domäne, den Ergebnissen dieser Arbeit sowie Resultaten weiterer biochemischer Analysen. Der zweistufige Mechanismus der Dephosphorylierung beinhaltet einen nukleophilen Angriff des Substratphosphors durch das Nukleophil Asp9 (D9) des aktiven Zentrums unter Bildung eines Acylphosphat-Enzym-Zwischenprodukts, gefolgt von der anschließenden Freisetzung des dephosphorylierten Substrats. Im zweiten Schritt erfolgt die Hydrolyse des Enzym-Phosphat-Zwischenprodukts unterstützt durch Asp11 (D11), und die Freisetzung der Phosphatgruppe findet statt. Die anderen untersuchten Aminosäuren sind an der Bindung von  $\text{Mg}^{2+}$  und/oder Substrat beteiligt.

Mit Hilfe dieser Arbeit konnte der katalytischen Mechanismus der sEH Phosphatase weiter aufgeklärt werden und wichtige noch zu untersuchende Fragestellungen, wie die physiologische Rolle der sEH Phosphatase, deren endogene physiologische Substrate und der genaue Funktionsmechanismus als bifunktionelles Enzym (die Kommunikation der zwei katalytischen Einheiten des Enzyms) wurden aufgezeigt und diskutiert.

## 2 Introduction

The mammalian soluble epoxid hydrolase is a homodimeric enzyme that combines two separate catalytic domains in each monomer. The C-terminal domain functions as an epoxide hydrolase and has been well studied, whereas a novel phosphatase activity was located in the N-terminal domain. The phosphatase of the sEH N-terminal domain (termed sEH phosphatase) which is responsible to this activity was the subject of research in this work.

### 2.1 Epoxides, epoxide hydrolases (EH) and xenobiotic Metabolism

#### 2.1.1. Epoxides

Epoxides (oxiranes) are compounds with a three-membered ring system that contain one oxygen three-membered cyclic ether). Epoxides are generally considered to be reactive compounds (electrophiles) due to the polarization of the C-O bonds combined with the tension of the epoxide ring. However, factors such as solubility of the epoxide and the substituents surrounding the epoxide will determine the reactivity. Accordingly, epoxides have the potential to bind covalently to nucleophilic compounds such as DNA, RNA and proteins, thereby leading to cytotoxic and/or genotoxic effects. Epoxides occur in nature and we are exposed to them through the air we breathe and the food we eat. They can be found in natural products, food additives, industrial chemicals, and pollutants. Few epoxides are entering the body as epoxidized compounds but many of them are formed endogenously in mammalian cells as a result of biotransformation of compounds. Epoxides entering the body as epoxidized compounds or transformed to epoxides after entering the body are part of what is defined as xenobiotic metabolism. Xenobiotics are small foreign molecules such as drugs. When they enter the body, they are being metabolized by cytochrome P-450 system to different metabolites among them epoxides. Other epoxides are endogenous substances that are formed frequently as epoxidized intermediates metabolites in normal metabolism (e.g. fatty acids epoxides)

Enzymatic degradation of epoxides to their less reactive intermediates is considered, in general, protective. All epoxide compounds (all of them containing an unsaturated bond), once taken up or formed in the body during oxidative metabolism, are under the control of the relevant detoxifying enzymes, among them epoxide hydrolases (EH's) (Oesch, 1973).

#### 2.1.2. Xenobiotic metabolism and Epoxide hydrolases

Epoxide hydrolases (EC 3.3.2.3) are a group of functionally related enzymes. As implied by their name, they catalyze the addition of water to a wide variety of compounds that contain an epoxide moiety, thereby generating from the epoxides the corresponding vicinal trans diol metabolites.

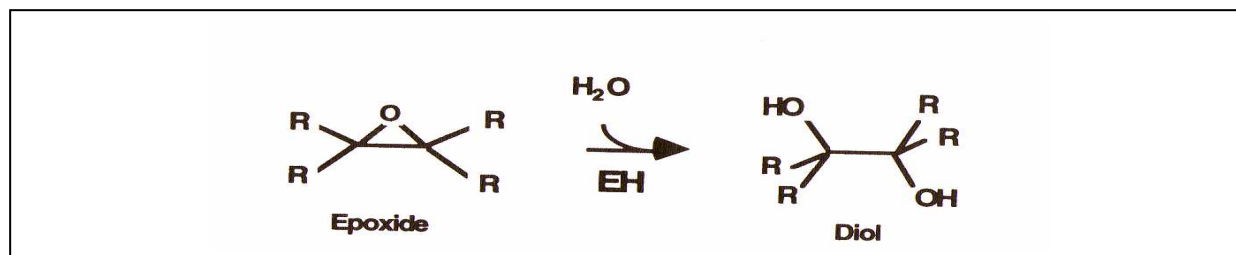


**Fig. 1. Prototypic enzymatic reaction catalyzed by epoxid hydrolases (EH)** (Arand et al., in "Control mechanism of carcinogenesis", Hengstler & Oesch (ed.), 1996)

Hydrolysis of the epoxide ring leads to more stable and less reactive metabolites. In addition, catalysis of epoxides to diols increases the water solubility of the compound and provides functional groups that can be conjugated, causing a rapider elimination and excretion from the body. Thus, this enzymatic reaction has been regarded as a detoxification step.

EHs are part of a group that contains a limited number of enzymes that catalyze xenobiotic compounds, drugs and chemical carcinogens, with broad substrate specificities, therefore termed xenobiotic metabolizing enzymes or biotransformation enzymes. Transformation of lipid soluble xenobiotics, as was mentioned above regarding the epoxide hydrolases, increases the hydrophilicity of the compounds and their ability to undergo significant ionization at physiological pH, facilitating transport in the blood stream and excretion from the body. It occurs mainly in the liver and can be divided into two-steps:

Phase 1: predominantly oxidation but also reduction and hydrolysis; phase 2: conjugation. The phase 1 reactions entail introduction of reactive/functional groups into lipophilic compounds, which are often being catalyzing sites, exposed for phase 2 enzymes. In most cases, it is achieved by the introduction of an oxygen atom into a compound as a first step towards detoxification and elimination. Phase 2 involves addition of an endogenous moiety to that functional group to increase water solubility. The main phase 2 reactions are addition of glucuronic acid, sulphate, glutathione (glutathione conjugation is an important detoxification reaction), amino acids and acetylation catalyzed by transferases. Phase 1 is processed mainly by CYP450s enzymes and its isoforms, a group of enzymes capable of catalyzing several dozen types of chemical reactions, including dealkylation, aromatic and aliphatic hydroxylations, N- and S- oxidations and reductions as well as epoxidation, exposing or introducing a functional group (e.g., -OH, -NH<sub>2</sub>, -SH, or -COOH). Other oxidative enzymes like alcohol dehydrogenase, reduction by reductases in gut bacteria and hydrolysis, like hydration of epoxides by epoxide hydrolases are also taking part in the first phase of biotransformation (Friedberg, 1994).

Most of the EH's function can be attributable to the two major EHs, the microsomal epoxide hydrolase (mEH) and the soluble epoxide hydrolase (sEH) which detoxify a large variety of xenobiotic-derived epoxides with complementary yet overlapping substrate specificity (Thomas *et al.*, 1990). Catalysis of different xenobiotic substances, by the mammalian EH enzymes results in different effects as described in Fig. 1.1. The vast majority of substrates are chemically inactivated by EHs and thus detoxified by these enzymes. In specific cases, epoxide hydrolysis can directly or indirectly increase the toxicity of the respective epoxide substrate, as in the case of the product leukotoxin diol being the cause for adult respiratory distress syndrome (ARDS) which can be developed after extensive burns (Moghaddam *et al.*, 1997).

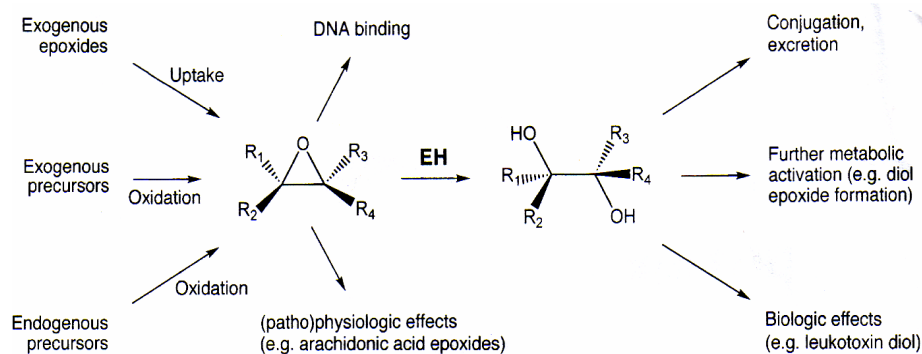


**Fig. 2. Effects and fate of exogenous and endogenous epoxides and consequently the epoxide hydrolase (EH) reaction product (diol).** The diagram is taken from Arand & Oesch, 2002.

Benzo[a]pyren and aflatoxin are known examples of compounds, of which the epoxide metabolites have the capacity to bind DNA, form DNA adducts and cause DNA damage that can initiate chemical carcinogenesis, if not quickly enough eliminated by the EH. Both genotoxins are also an example for substances which are chemically inert with respect to their reactions with DNA but are activated to their toxic form, the epoxide form of aflatoxin and the oxidized epoxide of benzo[a]pyren during the process of xenobiotic metabolism, when the body tries to eliminate and excrete the lipophilic parent compounds of these genotoxins (Arand and Oesch, 2002).

### 2.1.3. Members of the epoxide hydrolase family

EHs are a ubiquitous group of enzymes. They can be found in all types of living organisms, including mammals, invertebrates, plants, fungi, and bacteria.

Five enzymes that catalyze the hydrolytic cleavage of epoxides have been biochemically characterized in humans. Two membrane bound forms, mEH and cholesterol 5,6-oxide hydrolase (Watabe *et al.*, 1981) and three soluble forms- sEH, Leukotriene A<sub>4</sub> hydrolase (Samuelsson *et al.*, 1983) and hepoxilin hydrolase (Pace-Ascis and Lee, 1989). These forms are distinguished by their molecular weight, substrates and pI specificities, immunological reactivities, subcellular localization and roles (Norris *et al.*, 1998). Another division in this group presents three enzymes with a high specificity against a single endogenous substrate, and other two, namely microsomal and soluble epoxide hydrolases (mEH and sEH), that are involved in the turnover of multiple substrates. mEH is perhaps the most extensively studied EH (the sEH has become a subject for intensive investigations not before 1980) (Ota and Hammock, 1980). It is characteristically the most similar EH member to the sEH. mEH is particularly important for the efficient detoxification of highly reactive epoxides that occur in minute concentrations in our body. This enzyme has an unusual combination of a broad substrate specificity with high detoxification efficacy which is probably due to the catalytic nucleophile of mEH, an aspartate side chain, which is apparently rather mobile, suggesting that mEH can much better adapt to the spatial position of the epoxide ring of different substrates (congress book, MDO 2004-Arand *et al.*, 2004).

## 2.2 The general structure of the sEH and the structure and catalytic mechanism of the epoxide hydrolase located in the sEH C-terminal domain

The mammalian sEH is a homodimer in solution with a subunit molecular mass of 62.5 kD, consisting of 555 amino acids (Beetham *et al.*, 1993). sEH contains two distinct domains. Each subunit is composed of two domains, the C-terminal and the N-terminal domain. The sEH-C-terminal domain is connected via a proline-rich linker to the smaller N-terminal domain.

The structure of the mouse soluble epoxide hydrolase

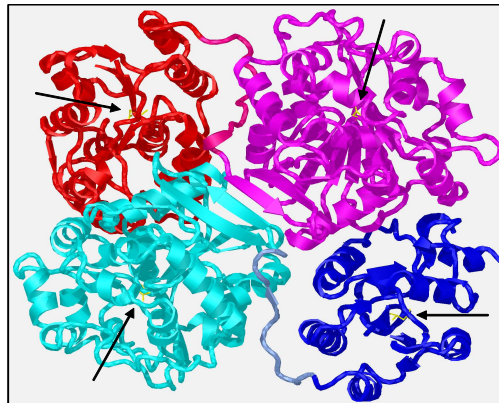


**Fig. 3. The 3D structure of mouse sEH, elucidated by Arigiriadi *et al.*, 1999.** The enzyme is a homodimer. Dimer formation is the result of interactions between the two C-terminal domains (in light blue and pink colours), as well as the association between the N-terminal domain of one subunit (in red and blue colours) and the C-terminal of its dimerization partner. No interactions between the two N-terminal domains were observed. The figure was taken from Cronin *et al.*, (2003).

The 35kD C-terminal domain (320 amino acids) has been well studied. When the first mammalian sEH was cloned (Knehr *et al.* 1993), it became evident that the EH activity of the enzyme was attributable to a large C-terminal domain which has a sequence similarity to the bacterial haloalkane dehalogenase and a typical  $\alpha/\beta$  hydrolase fold (Arand *et al.*, 1994).

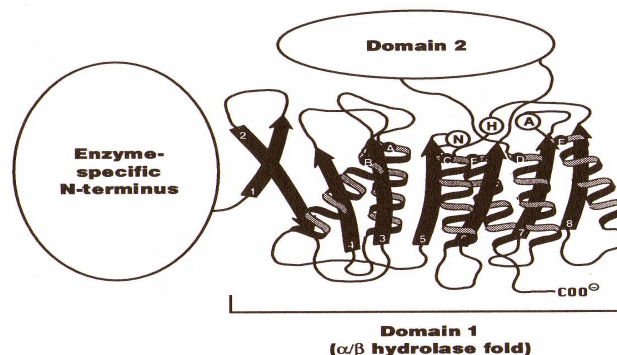


**Fig. 4. The general structure of the  $\alpha/\beta$  hydrolase fold-enzymes.** The C-terminal epoxide hydrolase belongs to the family of the  $\alpha/\beta$  hydrolase fold-enzymes. In the figure, the  $\alpha$ -helical regions are symbolized with letters and the  $\beta$ -strands in numbered arrows. The location of the amino acids involved in catalysis are pointed out in the figure, surrounded in a circle. The picture is taken from Arand *et al.*, 1996. from "Control mechanisms of carcinogenesis". Ed., Hengstler and Oesch.

The  $\alpha/\beta$  hydrolase fold family of enzymes is a group of proteins that has a widespread substrate specificities, such as lipids, haloalkane, peptides and more. They are related by same 3D core structure, and enzymatic mechanism. These hydrolytic enzymes have a catalytic triad, functionally similar to that of many proteases, which is constituted by specific residues of the so-called domain 1 (Fig.4). This is the core of each enzyme and it is conserved and similar between different enzymes from different (sub) families (e.g., haloalkane dehalogenase, EH and bromoperoxidase). Members of the  $\alpha/\beta$  hydrolyse fold family are composed of eight central  $\beta$ -sheet flanked and connected by alpha helices (barrel-in Fig.4). All of them have a similar three-dimensional arrangement of the central eight strands. These enzymes are bearing three conserved amino acid residues forming a catalytic triad, that in the native folded enzyme are in close proximity to each other. These enzymes have diverged from a common ancestor so as to preserve the arrangement of the catalytic residues (not the binding site) (Ollis et al., 1992). The identity of the amino acid residues constituting the catalytic site of sEH and their essential role in the hydrolysis of epoxides were proven by biochemical analysis and site-directed mutagenesis (Lacourciere and Armstrong, 1994, Hammock et al., 1994, Pinot et al., 1995, Arand et al., 1996). The catalytic mechanism of the sEH a two-step reaction, is characteristic to the  $\alpha/\beta$  -hydrolase fold enzymes. The amino acids, involved in the catalysis are concentrated in the triad as shown in Fig.4. The first step of the enzymatic reaction involves a formation of a substrate ester bond by a covalent binding of a nucleophilic amino acid (N, in fig 4.) – Asp or Ser or Cys to the substrate. In the second step the ester intermediate is hydrolysed by a water molecule that has been activated via proton abstraction by a histidine (H, in Fig.4). The histidine is supported by a third member of the catalytic triad, an acidic residue (A in Fig.4) (Verschueren et al., 1993).

In the first step of the sEH catalytic mechanism, the epoxide, after entering the active center is polarized by hydrogen bonding to proton donors, Tyr465 and Tyr381. Both Tyr act as acid catalysts, facilitating in ring opening of the catalytic nucleophile and thereby in formation of a covalent enzyme intermediate. On nucleophilic attack by Asp333, the epoxide ring opens under proton abstraction, forming a covalent hydroxyl ester. In the second step, water, activated by His523 coupled with Asp495/Glu in a charge relay system, hydrolyzes the ester bond, which results in the release of the corresponding diol product (Arand *et al.*, 1994, 1996), Gomez *et al.*, 2004).

An imperfect targeting signal was detected in the C-terminal domain. This kind of imperfect targeting signal is believed to be the reason for an incomplete import into peroxisomes, leading to the observed bicompartamental cellular distribution of the sEH in cytosol and peroxisomes (Arand *et al.*, 1991).

### 2.2.1 Substrate selectivity of the sEH (the C-terminal domain enzyme)

sEH together with mEH detoxify a large variety of xenobiotic-derived epoxides with complementary yet overlapping substrate specificity. Both mEH and sEH metabolize most monosubstituted epoxides such as styrene oxide and octane oxide. Arene oxides, such as benzo[a]pyrene 4, 5, are poorly metabolized by sEH and are better substrates for mEH. Bulky compounds, like the epoxides of polycyclic aromatic hydrocarbons, are, in general, better substrates for the mEH, while trans-substitution at the oxirane ring leads to selective substrates for the sEH (Thomas *et al.*, 1990). Typical examples of this group of compounds are trans-stilbene oxide and trans-benzyl styrene oxide. Treatment with this compound leads to sister chromatid exchanges in human lymphocytes (Krämer *et al.*, 1991).



mEH is able to detoxify most of the xenobiotic-derived epoxides, whereas sEH preferentially acts on endogenous compounds that play a role in the regulation of physiological processes. Results show that most fatty acid epoxides are hydrolyzed by sEH, 1000 times the rate of mEH (Moghaddam *et al.*, 1997). The clear domain of sEH is epoxides derived from fatty acids, such as epoxides of stearic, (Halarnkar *et al.*, 1989), linoleic (Moghaddam *et al.*, 1996) and arachidonic acids (Chacos *et al.*, 1983), which are among its best substrates (Boran *et al.*, 1995). These substrates have implied of (patho) physiological endogenous functions for the sEH (Sinal *et al.*, 2000). sEH has also been reported to hydrate oxygenated steroids such as squalene oxide, squalene dioxide and lanosterol epoxide (Hammock *et al.*, 1997).

## 2.2.2 Genomics and Evolution

The human sEH gene (EPHX2) has been found in chromosome 8, localized in chromosomal region 8p21-p12 (Larsson *et al.*, 1995). The gene is approximately 45 kb in size and contains 19 exons (Sandberg and Meijer, 1996).

Beetham *et al.*, (1995) proposed that the mammalian sEH is composed of two evolutionary distinct regions, the amino part showing structural homology to bacterial HAD1 (haloacid dehalogenase) and the carboxy terminal part resembling the bacterial HLD1 (haloalkane dehalogenase), mEH and sEH from plants. They suggested that mammalian sEH is a result of a fusion between the ancestral genes of HAD1 and HLD1, giving rise to a primitive monomeric protein that underwent stabilization, followed by dimerization through domain swapping (Agridardi *et al.*, 1999). In addition they have also suggested that the homology of mEH to sEH might be a result of a gene duplication of an ancestral bacterial gene.

## 2.3 Roles of human sEH (currently assigned to the epoxide hydrolase activity)

Most of the established sEH functions are currently assigned to the epoxide hydrolase activity. The sEH is an enzyme with multiple roles. The reaction done by epoxide hydrolases is historically related only to detoxification processes of xenobiotic epoxides. The involvement of mammalian sEH in endogenous compound metabolism (other than detoxifications of endogenously induced epoxides), has been more appreciated only in the last few years, as in the case with several other xenobiotic metabolizing enzymes. Apart from its classic role in detoxification processes, the main function of sEH is certainly in the metabolism of endogenous arachidonic- acid-derived signalling molecules such as epoxyeicosatrienoic (EET) acids to the corresponding diols (Yu *et al.*, 2000). This metabolic path is the base for the observed involvement of sEH in regulation of important physiological processes such as blood pressure (Yu *et al.*, 2000., Fang *et al.*, 2001), inflammation (Schmeltzer *et al.*, 2005) and in their potential therapy (by sEH inhibitors) (Imig *et al.*, 2005).

Lately the sEH, attracted attention as a novel treatment in diabetes and stroke (using sEH inhibitors that results in increased levels of EETs) (Ohtoshi *et al.*, 2005., Schmeltzer *et al.*, 2006., Zhang *et al.*, 2007)

### 2.3.1 sEH in Arachidonic acid (AA) metabolism and in regulation of blood pressure

Arachidonic acid (AA) undergoes oxidative metabolism that generates a variety of physiologically important metabolites, with important cell signalling roles. (Sinal, 1997). One of the pathways in AA metabolism involves the microsomal cytochrome P450 (CYP450) monooxygenases that catalyze from AA three types of reactions: (1) allylic hydroxylation resulting in *cis*- *trans*- conjugated hydroxyeicosatetraenoic acids, (2)  $\omega$ -oxidation yielding 19/20-hydroxyeicosatetraenoic acids and (3) epoxidation forming four regioisomeric epoxyeicosatrienoic acids (EETs), (5,6-, 8,9-, 11,12-, and 14,15-EET) (Capdevila *et al.*, 1992). The EETs are further degraded by sEH to their corresponding dihydroxyeicosatrienoic acid. The EETs were found to be among the sEH best endogenous substrates (Borhan *et al.*, 1995). Evidences exist for a variety of renal functions attributable to EETs and DHETs generated by CYP- dependent epoxygenase and sEH activity. Most notably, they function as modulators of salt and water regulation in the kidney (renal hemodynamics and natriuresis regulation) (Capdevila *et al.*, 1992)

EETs have antihypertensive, vasodilatory properties (Hu and Kim, 1993, Ominato *et al.*, 1996). Since sEH efficiently degrades EETs, one could expect an association between sEH and blood pressure. Yu *et al.*, (2000), showed in SHR (spontaneously hypertensive rat) that the hydrolysis of EETs to their corresponding DHETs by sEH is a mechanism for regulation of blood pressure. sEH displayed a dominant pro-hypertensive action, thereby identifying it as a possible therapeutic target (sEH inhibition) for control of blood pressure (Imig, 2005). Few other works implied the same; in sEH knock-out mice blood pressure from male mice is lower compare to WT (blood pressure went down to female levels) (Sinal *et al.*, 2000). Results of this work are in line with earlier findings showing a higher expression of sEH in male mice than in females (Inoue *et al.*, 1993) and a higher blood pressure in male than in female mice (Imig *et al.*, 2002), in addition, Zhao *et al.*, (2004) demonstrated an increased sEH expression in Angiotensin (Ang) injected rats (Ang elevates blood pressure) which led to an increase in EET hydration, inhibition of sEH in the Ang 2 hypertension mice had an antihypertensive effect.

### 2.3.2 sEH and inflammation

Several biological effects have been reported on leukotoxin-diols in mediating inflammatory responses including induction of NOS (Ishizaki *et al.*, 1995). sEH was demonstrated to be present in rat inflammatory cells (neutrophils and macrophages) (Draper and Hammock, 1999b). It was shown that cytochrome P450 epoxygenases -derived eicosanoids (processed by sEH) have anti-inflammatory properties (Node *et al.*, 1999). Davis *et al.*, (2002) suggested that the urea class of sEH inhibitors may be useful in the therapy of atherosclerosis characterized by vascular smooth muscle cell proliferation and vascular inflammation. Schmelzer *et al.*, (2005) suggested that sEH inhibitors have therapeutic efficacy in the treatment of acute inflammatory diseases, as sEH inhibitors decreased plasma levels of pro inflammatory cytokines and nitric oxide metabolites while promoting the formation of lipoxins, thus supporting inflammatory resolution.

### 2.3.3 sEH in cytotoxicity and cancer

Epoxides, when reactive enough can bind covalently to proteins and/or DNA, thereby leading to cytotoxic and/or genotoxic effects. Several epoxides are known to be cytotoxic, genotoxic and thus carcinogenic. One such example is the ultimate carcinogen benzo [a]pyrene 7, 8-diol-9, 10-epoxide, a metabolite of a prototypic polycyclic aromatic hydrocarbon, an environmental pollutant (Yang *et al.*, 1997). Microsomal and cytosolic fractions, in rodents, were shown to reduce the mutagenic activity of some epoxides (El-Tantawy and Hammock, 1980). A correlation between the level of sEH and the induction of sister chromatid exchanges was demonstrated in human lymphocytes after addition of different epoxide compounds (Krämer *et al.*, 1991, 1993). In a study by Morisseau *et al.*, (1999) the toxicity of TSO was shown to be reduced in *Spodoptera frugiperda* cells expressing mouse sEH compared to cells expressing  $\beta$ -galactosidase whereas in the presence of a sEH inhibitor (N,N-dicyclohexylurea), the protection was lost and the toxicity of TSO was similar to that obtained with control cells.

### 2.3.4 sEH in stress conditions

Recovery from primary shock in severe stress conditions such as extensive burns is often accompanied by multiple organ failure, including adult respiratory distress syndrome (ARDS). In the search for a non-bacterial toxin, an ether soluble substance, toxic to mitochondrial function was isolated from burned skin. This substance, which was produced by neutrophils, was shown to be linoleate epoxide, 9, 10 epoxy-12-octadecenoate (leukotoxin) (Kosaka *et al.*, 1994). As it was generally believed that the conversion of epoxides to their corresponding diols represents a detoxification step, it was rather surprising when Moghaddam *et al.*, (1997) showed that the leukotoxin diols rather than the precursor epoxides of the linoleic acid (leukotoxin) exhibited the increased toxicity and being by that the inflammatory mediator in multiple organ failure and ARDS.

## 2.4 The sEH N-terminal domain

### 2.4.1 The N-terminal domain of the sEH is a phosphatase

For long, the function of the 25kD N-terminal domain (20 amino acids), other than in structural stabilization of the dimer was unclear (Beetham *et al.*, 1995, Arigiriadi *et al.*, 1999). Nevertheless, some accumulated findings implied that the function of the 25kD N-terminal domain of the sEH was not exclusively structural:

The sEH orthologues in plants has EH activity similar to the mammalian enzymes though sEH in plants lack the N-terminal domain and apparently exists as a monomer (Beetham *et al.*, 1995). Arand *et al.*, (1999) showed that the N-terminal domains of mEH and sEH were not homologous. Koonin and Tatusov (1994) were the first ones to analyse the relationship between haloacid dehalogenases, other enzymes and the EH N-terminal domain. They identified a large group of structural relatives called the haloacid dehalogenase (HAD) superfamily that included among other enzymes a number of phosphatases and shared three conserved motifs with potential catalytic residues in all HAD members. In addition, the work of Collet *et al.*, (1999) and Ndubuisil *et al.*, (2002), showed that the

amino-terminal motif- DXDX(T/V) appears in some of the HAD enzymes, including the sEH N-terminal domain and is being used to describe an HAD class of enzymes that includes mostly phosphatases. It was shown for the first time by Cronin *et al.*, (2003), in our lab, that a dephosphorylation activity is a property of the sEH N-terminal domain, defining by that the sEH as a bifunctional enzyme.

Several biochemical results in Cronin *et al.*, (2003) work proved the above conclusion and supplied fundamental information on the newly described sEH phosphatase activity:

- The native rat sEH displayed a phosphatase activity. Purified rat sEH catalyzed the dephosphorylation of the generic phosphatase substrate, 4-nitrophenyl phosphate (since the physiological substrate is unknown), approximately at the same rate as the reaction observed for sEH with its diagnostic epoxide.
- $Mg^{2+}$  was found to be crucial for the phosphatase activity, which is in agreement with the expectation that a divalent anion would be a necessary cofactor in the catalytic site of the N-terminal domain (as it is with Ser/Thr phosphatases).
- In order to exclude the possibility that the phosphatase activity measured with the native sEH resides in the C-terminal (EH) domain of the enzyme, the human recombinant N-terminal domain (the first 221 amino acid residues) was expressed and purified and showed a phosphatase activity, though much less than in the native rat.
- Recombinant expression of full-length human sEH in *E.coli* has been done showing a moderate 4-nitrophenyl phosphatase activity. This result indicated that the reason for the observed difference between the rat holoenzyme and human N-terminal domain is not stabilization or contribution of the C-terminal domain to the phosphatase activity but rather species difference.
- There was no indication for a cross talk between the two domains. There was no change in the rate constant or  $K_m$  for epoxide hydrolysis in the presence or in the absence of the phosphatase substrate. Likewise the presence of a EH substrate or inhibitor did not affect the kinetics of the phosphate hydrolysis. Thus, the two domains operate independently under these experimental conditions.
- The N-terminal domain of the phosphatase has probably no role in xenobiotic metabolism. The sEH phosphatase can not hydrolyze 4-nitrophenyl sulfate although similar to 7-nitrophenyl phosphate, indicating that the catalytic domain is specifically acting on phosphate esters.

#### **2.4.2 The structure of the sEH phosphatase and its homology to the HAD superfamily of enzymes**

Based on structural similarities, both domains of mammalian sEH are grouped within large and separate superfamilies of hydrolases. While the C-terminal epoxide hydrolase domain adopts a  $\alpha/\beta$ -hydrolase fold and belongs to the haloalkane dehalogenases family of enzymes (Lacourciere *et al.*,

1994, Arand *et al.*, 1994, Van Loo *et al.*, 2006), its smaller N-terminal domain has a different  $\alpha/\beta$  fold and belongs to a distinct family of haloacid dehalogenases (HAD). The HADs are largely composed of phosphatases, dehalogenases, phosphotransferases and other hydrolases (Koonin & Tatusov., 1994). Members of the HAD family are ubiquitously expressed in prokaryotes and eukaryotes, and they cover an exceptionally broad catalytic spectrum in metabolism, membrane transport, signal transduction or nucleic acid repair (Burroughs *et al.*, 2006, Kuznetsova *et al.*, 2006)

Despite an overall low sequence similarity, all enzymes of the HAD superfamily possess a structurally conserved Rossmannoid  $\alpha,\beta$ -core domain containing four loops that represent the catalytic scaffold (see picture in comparison table 1) As displayed in Fig 5., each of the four loops contains a characteristic sequence motif with some conserved or partly conserved amino acids.

In all HAD members, the catalytic Asp nucleophile located in loop 1 is most highly conserved. Many HADs contain an additional aspartic acid residue two positions downstream of the Asp nucleophile in loop 1 that was suggested to function as a general acid/base in the catalytic cycle of phosphotransferases and phosphatases (Allen *et al.*, 2004, Wang *et al.*, 2002). The loops 2 and 3 position the substrate phosphoryl binding residues Ser/Thr and Lys/Arg, whereas loop 4 either contains the  $Mg^{2+}$  binding pocket formed by two aspartic acids in phosphatases or two Ser residues that stabilise the nucleophile and/or water in the dehalogenases (Baker *et al.*, 1998, Morais *et al.*, 2000).

	loop 1	loop 2	loop 3	loop 4
hsEH	3..AVFDLDGVL...101..TTAILTNTW...32..VKPEPQ...14...EVVFLDDIGANLKP..29			
HAD	4..IAFDLYGTL...97...KLAILSNGS...28..YKPDNR...14...AILFVSSNAWDATG..29			
Phos	3..VIFDWAGTT...101..KIGSTTGYT...29..GRPYPW...15...HMIKVGDTVSDMKE..29			
PSP	5..ILFDFDSTL...75...VVAVVSGGF...37..KENAKGE...14...DTVAVGDDGANDISM..29			
	↑↑	↑	↑	↑↑↑

**Fig. 5. Structure-based sequence alignment of human sEH (hsEH) and other HAD members, HAD from *Pseudomonas* sp. (HAD), phosphonoacetaldehyde hydrolase from *Bacillus cererus* (Phos) and phosphoserine phosphatase from *M. jannaschi* (PSP).** Conserved residues are marked in red and partly conserved residues are marked in green. The figure is taken from Cronin *et al.*, (2008).

The spatial arrangement (in Fig.6) of the conserved and partly conserved residues (indicated in Fig.5) in few members of the HADs, was also examined by Cronin *et al.*, (2003), knowing that the catalysis in the various family members depends on the correct placement of the catalytic active site amino acid residues with respect to the substrate. As it can be seen in Fig 6, almost perfect spatial conservation is observed between the marked residues of all three HAD enzymes that were examined (the same enzymes as in Fig.5) and sEH.

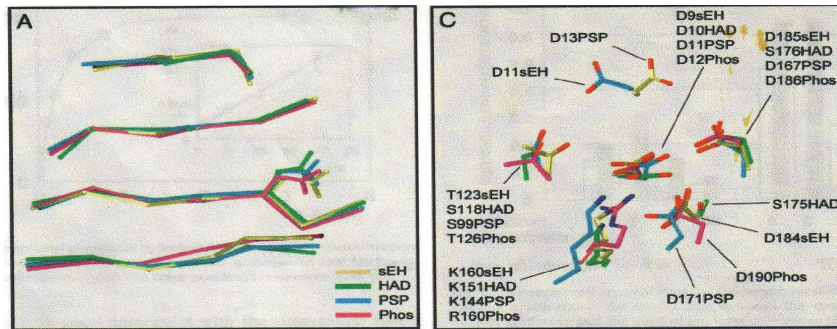


**Fig . 6. The spatial arrangement of the conserved and partly conserved residues.** In A, the alignment of the four central strands of the  $\beta$  sheets including the catalytic nucleophile side chain. In C, a similar spatial arrangement of the conserved and partly conserved amino acid residues of the sEH phosphatase (indicated in Fig. 5) and equivalent residues of few others HAD enzymes (listed in Fig. 5). The pictures are taken from Cronin *et al.*, (2003).

The three- dimensional structure of human sEH has been recently solved with a resolution of 2.6Å (Gomez *et al.*, 2004). It shows domain interactions similar to the murine sEH (Argiriadi *et al.*, 1999), where the phosphatase domain of one homodimer interacts with the epoxide hydrolase domain of the other. The human 3D structure reveals a hexacoordinated  $Mg^{2+}$  bound in the phosphatase active site at the bottom of a 15Å-deep pocket, as well as the product complex with  $HPO_4^{2-}$ . The crystal structure present several residues potentially composing the sEH phosphatase active site, in line with the previous structure based sequence alignments analysis.

Another common feature of the HAD enzyme is the cap domain (see picture in the summary table). All HAD enzymes are grouped within three subfamilies by virtue of the presence and location of an additional cap domain that is implicated in substrate selectivity (Selengut, 2000). The sEH phosphatase is part of class 1 HADs together with phosphonataase and PSP. This group of HAD enzymes contain an insertion between loop 1 and loop 2 of the core domain. Members of the class 2 HAD have a larger cap domain between loop 2 and 3 (Lahiri *et al.*, 2006). The class 3 of HAD members have no cap domain and thus, are better suited to accept large substrates (Peisach *et al.*, 2004).

Based on homology with other HADs, a two-step mechanism for the dephosphorylation reaction has been proposed (Baker *et al.*, 1999, Collet *et al.*, 1999, Wang *et al.*, 2001).

The first step is composed of a nucleophilic attack by the D9 on the substrate phosphoester group, protonation of the leaving group and a phosphoenzyme intermediate formation. In the second step, the phosphoenzyme intermediate is hydrolyzed via a nucleophilic attack by an activated water molecule.

### 2.4.3 Substrates and potential roles of the sEH phosphatase

Phosphatases are enzymes that are able to catalyse the hydrolysis of a large variety of phosphate monoesters using different catalytic strategies. Substrates range from phosphorylated proteins and nucleic acid to a broad range of small phosphorylated metabolites (Bradford *et al.*, 1998, Alonso *et al.*, 2004, Ducruet *et al.*, 2005). The sEH phosphatase has so far been shown to accept generic substrate 4-nitrophenyl phosphate (4-NPP), some lipid phosphates (Newman *et al.*, 2003) and isoprenoid

phosphates (Enayetallah *et al.*, 2006), possibly connecting the sEH phosphatase to cholesterol biosynthesis or lipid metabolism. The physiological role of sEH phosphatase activity remains uncertain to date but the bifunctional character of human sEH implies that the sEH phosphatase may have a regulatory function in connection with the epoxide hydrolase activity.

## 2.5 Distribution of mammalian sEH

### 2.5.1 Distribution in different species and sexes

Meijer *et al.* (1987b), examined few mammals, looking for their sEH activity (using TSO as a substrate). Mouse displayed the highest specific sEH activity, followed by hamster, rabbit, guinea pig, monkey, human and rat. Sexual dimorphism was found and investigated by castration and testosterone addition, in mice and rats, exhibiting higher hepatic sEH activity in males than in females (Delinger and Vessel, 1989, Inoue *et al.*, 1993).

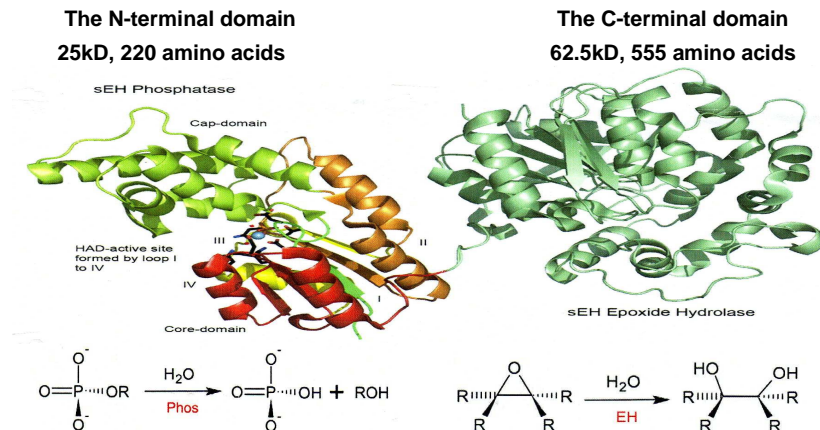
### 2.5.2 Tissue distribution

The major location of sEH in most species (except of the rat) is in the liver, followed by kidney, heart, brain, lung, testes, spleen and lymphocytes (Gill and Hammock 1980; Seidegard *et al.* 1984; Schladt *et al.*, 1986). sEH was also found in pancreatic islets, epithelial cells in the skin, prostatic ducts and the gastrointestinal tract (Enayetallah *et al.*, 2004). In the last few years high expression of sEH was found also in vascular endothelium, some smooth muscle, and the proximal tubule (Zheng *et al.*, 2001, Yu *et al.*, 2000), supporting the role of sEH in regulation of blood pressure. The work results of Priyanka *et al.*, (2008) indicated differential localization of sEH in normal human brain and in its arterioles, suggesting an essential role for sEH in the central nervous system.

### 2.5.3 Distribution in the cell

The subcellular localization of sEH has been controversial. Earlier studies using mouse and rat liver suggested that sEH may be cytosolic and/or peroxisomal (Patel *et al.*, 1986, Erickson *et al.*, 1991). Another evidence supporting the bicompartamental distribution is based on the PTS1 (peroxisomal targeting signal) findings. It is a sequence encoding a tripeptide Ser, Lys, Leu (SKL), that functions as a microbody targeting signal on the C-terminus of the sEH in mammals, plants and yeast (Gould *et al.*, 1987). A variant with isoleucine (SKI) at the extreme C-terminus was found in mouse sEH (Grant *et al.*, 1993) and rat (Arand *et al.*, 1991). Therefore there is a possibility that SKI represents a weak PTS, resulting in a dual cytosolic and peroxisomal distribution as was suggested by Arand *et al.*, (1991). Enayetallah *et al.*, (2006), showed that sEH is both cytosolic and/or peroxisomal in human hepatocytes and renal proximal tubules and exclusively cytosolic in other sEH containing tissues such as pancreatic islet cells, intestinal epithelium, anterior pituitary cells, adrenal gland endometrium, lymphoid follicles, prostate ductal epithelium, alveolar wall, and blood vessels. sEH was not exclusively peroxisomal in any of the tissues evaluated. The data suggest that human subcellular localization is tissue dependent and that sEH may have tissue or cell type-specific functionality.

## sEH and its two catalytic domains: A short summary



- A phosphatase
  - Homolog to the HAD family (Haloacid dehalogenas)
  - Does not participate in xenobiotic metabolism
  - Endogenous-physiological substrates are not known as well as the roles/processes the enzyme is involved in
  - The catalytic mechanism is recently elucidated with the contribution of this work
- An epoxide hydrolase
  - Homolog to haloalkane dehalogenase. Belongs to the  $\alpha/\beta$  hydrolase fold family
  - Participates in xenobiotic metabolism (trans-substituted epoxides)
  - Endogenous- physiological substrates are known. Participate in arachidonic acid (EECs) metabolism and thereby is involved in blood pressure regulation and in few pathophysiological processes
  - Catalytic mechanism is elucidated
- The way and level of communication between the two catalytic sites is not yet clear



### 3 Aims

It was recently discovered within our working group as well as by other researchers, that the N-terminal domain of the human soluble epoxide hydrolase (sEH) displays a novel phosphatase activity. The N-terminal domain of the sEH (the sEH phosphatase) is grouped to a large superfamily of hydrolases, the haloacid dehalogenase (HAD), with which it shares structural similarities. Based on the homology of sEH with other HAD members, a two-step mechanism for the sEH phosphatase dephosphorylation reaction was suggested.

The aim of this work was to elucidate the catalytic mechanism of the human sEH phosphatase. We will therefore perform a biochemical analysis of the sEH phosphatase catalytic mechanism thereby the active-site amino acids will be identified and their role in the sEH phosphatase catalytic mechanism investigated.

For that purpose, amino acids candidates, that were found to be conserved or partly conserved in HAD enzymes, sharing a similar spatial arrangement to equivalent amino acids in few of the examined HAD enzymes, will be chosen to be substituted to a nonfunctional amino acids by site -directed mutagenesis.

At least two alternative amino acids, alanine and an amino acid structurally similar to the one in the wild type (WT) will be introduced to each candidate amino acid, replacing the original WT amino acid in that position. By inducing different kinds of exchanges, wider possibilities in interpretation of the results will be provided.

The resulting mutants obtained from the site directed mutagenesis process constructed in expression vectors will be cloned, confirmed by restriction and sequencing for the correct coding, recombinantly expressed in *E.coli* as soluble proteins, purified and subsequently screened for activity. Mutants with detectable activity will be further analyzed. Therefore, kinetic activity measurement assays will be performed and kinetic parameters will be calculated in four well-established calculating methods and evaluated.

The analysis of the activity results and the calculated kinetic parameters of the mutant proteins will help in enlightening the catalytic mechanism and its required components. With the contribution of the work results a catalytic mechanism for the sEH phosphatase will be suggested.

## 4 Materials and methods

### 4.1 Materials

#### 4.1.1 Chemicals and reagents

Agar (bact. grade)	Gibco BRL (Karlsruhe, D)
Agarose (ultra pure)	Gibco BRL (Karlsruhe, D)
Ammoniumpersulfat (APS)	Serva (Heidelberg, D)
Ampicillin (Na-Salt, p.a.)	Sigma (Deisenhofen, D)
L-Arabinose	Sigma (Deisenhofen, D)
Bactopecton (Select Pepton Nr. 140)	Gibco BRL (Karlsruhe, D)
Bradford-Reagent (Roti-Quant)	Roth (Karlsruhe, D)
Bovine serum albumin (BSA)	Roth (Karlsruhe, D)
Bromphenol blue	Sigma (Deisenhofen, D)
Coomassie Brilliant Blue R250/ G250	Serva (Heidelberg, D)
Diethylether	Riedel-de Haën (Seelze, D)
Deoxy-nucleotid tri-phosphate (dNTP)	Boehringer Mannheim (D)
Dithiothreitol (DTT)	Sigma (Deisenhofen, D)
Ethidiumbromid-solution (10 mg/ml)	Sigma (Deisenhofen, D)
Fetal calfserum (FCS)	Gibco BRL (Karlsruhe, D)
Gelatine	Sigma (Deisenhofen, D)
GSH-Sepharose slurry	Pharmacia Biotec.
n-Hexan	Sigma (Deisenhofen, D)
Imidazol	Sigma (Deisenhofen, D)
Natrium-Dodecylsulfat (SDS)	Sigma (Deisenhofen, D)
Nitroblau-Tetrazolium Salz (NBT)	Boehringer Mannheim (D)
4-Nitrophenyl phosphate	Sigma (Deisenhofen, D)
Phenol (mol.biol.)	Roth (Karlsruhe, D)
Rotiphorese 30 (Acrylamidlösung)	Roth (Karlsruhe, D)
RotiQuant Bradford-Reagent	Roth (Karlsruhe, D)
N,N,N',N'-Tetramethylethylenediamin (TEMED)	Pharmacia (Freiburg, D)
Tween 20	Serva (Heidelberg, D)
Xylencyanol	Sigma (Deisenhofen, D)
Yeast Extract	Gibco BRL (Karlsruhe, D)

#### 4.1.2 Standard buffers and solutions

Ampicillin-solution (50 mg/ml)	500 mg ampicillin (natriumsalt) in 10 ml water filtered.
Blocking buffer	3 g bovine serum albumin (BSA), 50 µl Tween 20 in TBS.
Blot-Transfer-buffer	25 mM Tris, 192 mM glycine and 20 % methanol in water, pH 8.3
Coomassie-staining	0.1% (w/v) Coomassie Brilliant Blue, 50% (v/v) methanol and 10% (v/v) acetic acid in water.
Digi 3-solution	100 mM Tris, 100 mM NaCl, 50 mM MgCl <sub>2</sub> ; with HCl to adjust to pH 9.5

DNA sample buffer	50% glycerin and 10 µl bromophenol blue (1% in ethanol) in 1 ml water.
EDTA 0,5 M	14.6 g EDTA in 50 ml water, to adjust to pH 8.0 with NaOH and fill to 100 ml water, autoclave.
Destaining solution	water/methanol/acetic acid in ratio of 6/3/1.
Colour reaction solution (Western blot)	4.5 µl NBT-solution and 3.5 µl X-Phosphat-solution in 1 ml Digi 3, freshly made.
Incubation buffer (Western blot)	2.5 g gelatine, 250 µl Tween 20 in 200 ml TBS buffer (boiled), filled to 500 ml with TBS, cooled.
Running buffer for SDS-PAGE (10x)	5.1 g Tris, 72 g glycine in 500 ml water, pH 8.3. Before use to add 2.5 ml SDS-solution (20%) to 50 ml running buffer and fill to 500 ml with water.
NBT-solution	75 mg nitroblue-tetrazolium salt in 1 ml dimethylformamid kept in -20°C.
PBS	8 g NaCl, 0.2 g KCl, 1.44 g Na <sub>2</sub> HPO <sub>4</sub> , 0.24 g KH <sub>2</sub> PO <sub>4</sub> in 800 ml of ddH <sub>2</sub> O, adjust to pH 7.4 with HCl, add H <sub>2</sub> O to 1.0 liter.
Sample buffer (Lammeli 5x)	48 g urea, 12.1 g Tris-HCl (pH 6.8), 6 g SDS, 5 ml β-Mercaptoethanol, 5 ml bromophenol blue-solution, 20g glycerin filled to 100 ml water.
TAE-buffer	40 mM Tris-acetat, 1 mM EDTA (pH 8.5).
TBE-buffer	90 mM Tris-HCl, 90 mM boric acid, 2 mM EDTA (pH 8).
TBS-buffer	10 mM Tris-HCl pH 7.4, 0.9% NaCl.
TE-buffer	10 mM Tris-HCl, 1 mM EDTA, pH 8,0 (autoclaved)
Trypsin/EDTA	0.025% trypsin (w/v), 0,2 mM EDTA in PBS.
X-Phosphat-solution	50 mg 5-brom-4-chlor-3-indolylphosphate dissolved in 1 ml Dimethylformamid, kept in -20°C.

Other SDS-PAGE solutions, "lower" (separating) gel and "upper" (stacking) gel are detailed under the method description. Any other solutions and buffers can be found in Sambrook et al., 1989.

### 4.1.3 Instruments

Agarose gel electrophoresis chamber	Work shop Inst. f. Toxikologie, Mainz
BioLogic Duo-Flow system	Bio-Rad
Blotting chamber (Inhalt 3.0 l)	Work shop Inst. f. Toxikologie, Mainz
Centricon Ym-3 3000 MW cut-off	Amico (Kelsterbach, D)
Eagle Eye II Still Video System	Stratagene (Heidelberg, D)
Eppendorfs (1.5 und 2 ml Safe-Lock)	Eppendorf (Hamburg, D)
Expendable -Kivets (1.5 ml, Brand)	Roth (Karlsruhe, D)
Fluoreszenz-Spektralphotometer F2000	Hitachi (Berks, UK)
French Pressure cell press	Sim-Amico Spectronic Instruments
HiTrap chelating HP column (1 ml)	AP Biotech (Freiburg, D)
Kodak Diagnostic Film X-omat AR (35x45 cm)	Nordfoto (Hamburg, D)

Mastercycler gradient	Eppendorf (Hamburg, D)
Minigel Twin – Gel apparatus	Biometra (Göttingen, D)
Nitrocellulose membrane (0,45 µm)	Sartorius (Göttingen, D)
PCR-Reaction tubes (0.5 ml)	Kühn und Bayer (Nidderau)
Petriplates (steril, Ø 82 mm)	Greiner (Nürtingen, D)
Phero-Stab. 500 Powersupply	Fischer-Biotec
Phosphoimager STORM 840	Molecular Dynamics (Sunnyvale, USA)
Power/Pac 300	Bio-Rad
Shaking incubator Certomat H+R	Braun (Melsungen, D)
Sorvall Superspeed RC 2-B Zentrifuge	Du Pont ( Bad Homburg, D)
Spectrophotometer MPS-2000	Shimadzu (Kyoto, Japan)
Spectrophotometer, Mikrotiter Spectramax 25	Molecular Devices (Ismaning, D)
S&S-Sterile filters (0.22 µm/ 0.45 µm)	Schleicher & Schuell (Dassel, D)
Table centrifuge: Biofuge A	Heraeus (Osterode, D)
Table centrifuge: Labofuge 400R	Heraeus (Osterode, D)
Thermocycler PCR Sprint	Thermo Hybaid (Ulm, D)
Thermostat 5320 (Heat block)	Eppendorf (Hamburg, D)
Tissue culture and immunoplate	
maxisorb 96-well plate	Nunc (Wiesbaden,D)
TLC-Plastikfolien 20x20 cm (Kieselgel 60F <sub>254</sub> )	Merck (Darmstadt, D)
Ultrasound-Becherresonator HD 2070	Bandelin (Berlin, D)
Ultra centrifuge: Beckman Model L5.65 UZ	Beckman (München, D)
Ultrospec 3100 pro	Amersham Biosciences (Freiburg, D)
Whatman 3MM Chr-Paper	Bender und Hobein (München, D)

#### 4.1.4 Kits

Qiaex DNA Gel Extraction Kit II	Qiagen (Hilden, D)
Qiagen Plasmid Midi Kit (25)	Qiagen (Hilden, D)
Ready To Go/ T-Primed First-Strand Kit	Amersham PharmaciaBitech (Freiburg)
RNeasy Mini Kit	Qiagen (Hilden, D)

#### 4.1.5 Software

EditSeq (sequencing)	DNASStar (Madison, USA)
EditView (sequencing, “ABI-Traces“)	Perkin-Elmer (Ueberlingen, D)
ImageQuant (phosphoimager)	Molecular Dynamics (Sunnyvale, USA)
MapDraw (restriction)	DNASStar (Madison, USA)
MegAlign (sequences comparison)	DNASStar (Madison, USA)
PrimerSelect (PCR-primer-design)	DNASStar (Madison, USA)
SoftMax Pro (Spectramax 250)	Molecular Devices (Ismaning, D)

### 4.1.6 Antibodies

Rabbit anti-sEH (rat)	Produced in- house (Mainz, D)
Goat anti-rabbit IgG (alk.Phosph.- Konj.)	Sigma (Steinheim, D)
Anti-Diogoxygenin(DIG)-AP	Boehringer (Mahnheim, D)

### 4.1.7 Enzymes

#### Restriction endonucleases:

All restriction enzymes that were used were ordered from New England Biolabs (Frankfurt a.M., D) except for Dpn1 (Stratagene, Heidelberg, D) and DNase1 (Gibco BRL, Karlsruhe, D). All enzymes were delivered with 10x reaction buffer.

#### Other Enzymes:

AmpliTaq DNA-Polymerase	Perkin-Elmer (Ueberlingen, D)
PfuTurbo-DNA-Polymerase	Stratagene (Heidelberg, D)
Alkaline Phosphatase	Amersham (Braunschweig, D)

### 4.1.8 Oligonucleotides

The primers were ordered from MWG-Biotech-AG, (Ebersberg, D.).

In table 2 in results the sequence of the desired mutation is marked in each of the oligonucleotide sequences.

D9Asense
5'-GCC GTC TTC GCC CTT GAC GGG GTG CTG GCG-3'
D9Aanti
5'-CCC CGT CAA GGG CGA AGA CGG CGC CCG GCA-3'
D9Nsense
5'-CGC GCG GCT GTC TTC AAC CTT GAC GGG GTG CTG GCG-3'
D9Nanti
5'-GTC AAG GTT GAA GAC AGC CGC GCG CAG CGT CAT GC-3'
D11Asense
5'-TTC GAC CTT GCG GGC GTG CTG GCG CTG CCA GCG G-3'
D11Aanti
5'-AGC GCC AGC ACG CCG GCA AGG TCG AAG ACG GCC GCG-3'
D11Nsense
5'-CCG TCT TCG ATT TAA ACG GGG TGC TGG CGC TGC C-3'
D11Nanti
5'-GCA CCC CGT TTA AAT CGA AGA CGG CCG CGC GCA-3'
T123Asense
5'-TGC CAT CCT CGC GAA CAC CTG GCT GGA CGA CCG-3'
T123Aanti
5'-AGC CAG TG TTC GCG AGG ATG GCA GTA GTG AAT CC-3'
T123Nsense

5' -CTA CTG CAA TAT TAA ACA ACA CCT GGC TGG ACG ACC-3'
T123Nanti
5' -GGT GTT GTT TAA TAT TGC AGT AGT GAA TCC TTT CTT CC-3'
T123Vsense
5' -TGC CAT CCT CGT TAA CAC CTG GCT GGA CGA CCG-3'
T123Vanti
5' -GCC AGG TGT TAA CGA GGA TGG CAG TAG TGA ATC C-3'
K160Asense
5' -GGG AAT GGT CGC GCC TGA ACC TCA GAT CTA CAA G -3'
K160Aanti
5' -GAG GTT CAG GCG CGA CCA TTC CCA CCT GAC ACG A-3'
K160Nsense
5' -AAT GGT CAA TCC GGA ACC TCA GAT CTA CAA GTT TCT G-3'
K160Nanti
5' -TCT GAG GTT CCG GAT TGA CCA TTC CCA CCT GAC ACG-3'
K160Rsense
5' -GGG AAT GGT GCT CCC TGA ACC TCA GAT CTA CAA G-3'
K160Ranti
5' -AGG TTC AGG GCG CAC CAT TCC CAC CTG ACA CGA-3'
D184Asense
5' -CGT TTT TTT GGC CGA CAT CGG GGC TAA TCT GAA G-3'
D184Aanti
5' -CCC GAT GTC GGC CAA AAA AAC GAC CTC ACT GGG-3'
D184Nsense
5' -CGT TTT TTT GAA TGA TAT CGG GGC TAA TCT GAA GCC A-3'
D184Nanti
5' -AGC CCC GAT ATC ATT CAA AAA AAC GAC CTC ACT GGG-3'
D185Asense
5' -TTT TTG GAT GCG ATC GGG GCT AAT CTG AAG CCA -3'
D185Aanti
5' -T AG CCC CGA TCG CAT CCA AAA AAA CGA CCT CAC T G-3'
D185Nsense
5' -TTT TTG GAT AAT ATT GGG GCT AAT CTG AAG CCA GC-3'
D185Nanti
5' -ATT AGC CCC AAT ATT ATC CAA AAA AAC GAC CTC ACT G-3'
N189Asense
5' -ACA TCG GGG CAG CGC TGA AGC CAG CCC GTG ACT TG-3'
N189Aanti
5' -CTG GCT TCA GCG CTG CCC CGA TGT CAT CCA AAA AAA CG-3'
N189Dsense
5' -ACA TCG GGG CAG ATC TGA AGC CAG CCC GTG AC-3'
N189Danti
5' -GGC TTC AGA TCT GCC CCG ATG TCA TCC AAA AAA A-3'

### 4.1.9 Vectors

Cloning vectors:

pGEFII

pGEF-sEH phos-His

pGEF-sEH phos-GST

## 4.1.10 Molecular weight markers

### 4.1.10.1 Protein markers (Prestained SDS-Marker)

During this work the markers that were used were the prestained SDS-7B Molecular marker (in A) from Sigma (Deisenhofen, D) and the peqGold Prestained Protein-Marker (in B) from peqLab Biotechnologie.

A)

Protein	Natives MW [Dalton]
2-Macroglobulin (human)	180.000
Galaktosidase ( <i>E.coli</i> )	116.000
Fruktose-6-phosphatkinase (rabbit)	84.000
Pyruvatkinase (chicken)	58.000
Fumarase (porcine)	48.500
Laktatdehydrogenase (rabbit)	36.500
Triosephosphatisomerase (rabbit)	26.600

B)

Protein	Natives MW [Dalton]
Galaktosidase ( <i>E.coli</i> )	121.600
Bovines Serum-Albumin	81.400
Ovalbumin (chicken)	46.800
Karboanhydrase (bovine)	32.000
Lactoglobulin (bovine)	24.500
Lysozym (chicken)	20.400

### 4.1.10.2 DNA-Molecular weight standards

#### Lambda DNA, EcoR I / Hind III

The marker was ordered from MBI Fermentas, in a concentration of 200 ng/10 µl. The DNA size fragments and quantity are as follows:

Fragment size [bp]	Quantity of fragment [ng]
21.227	88
5.148 + 4.973	42
4.268	18
3.530	15
2.027	8,3
1.904	7,8
1.584	6,5
1.375	5,7
947	3,9
831	3,4
564	2,3

#### pBR322-DNA, Alu I-Verdau

The marker was ordered from MBI Fermentas, in a concentration of 200 ng /10 µl. The DNA size fragments and quantity are as follows:

Fragment size [bp]	Quantity of fragment [ng]
908	42
659 + 656	60
521	23
403	18
281	13
257	12
226	10
100	4,6

### 4.1.11 Bacteria

The bacteria that were used in this work are exclusively *E.coli* strain.

For cloning:

Stamm DH10B: F<sup>-</sup> mcrA (mrr-hsdRMS-mcrBC) 80lacZ M15 lacX74 deoR recA1 endA1 ara139 (ara/leu) 7697 galU galK - rpsL nupG - tonA

Stamm TOP10: F<sup>-</sup> mcrA (mrr-hsdRMS-mcrBC) 80lacZ M15 lacX74 deoR recA1 araD139 (ara/leu) 7697 galU galK rpsL(Str<sup>R</sup>) endA1 nupG

For expression of the recombinant proteins:

Stamm BL21AI: F<sup>-</sup> ompT hsdS<sub>B</sub> (r<sub>B</sub><sup>-</sup>m<sub>B</sub><sup>-</sup>) gal dcm araB :T7RNAP-tetA

### 4.1.12 Culture media

LB (Luria Bertani)-Medium: 10 g bactopecton, 10 g NaCl, 5 g yeast extract  
Bactopecton, yeast extract and salt, dissolved in 800 ml water, adjusted to pH 7.4 with 5 M NaOH, filled to 1 liter water, autoclaved (121°C, 20 min).

LB/Amp-Medium: 0.1 g ampicillin is added to 1000 ml autoclaved LB (100 µg ampicillin per 1 ml medium).

Agar-Plates: 15 g agar is added to autoclaved LB. When the medium is cooled down (around 60°C), ampicillin (100 µg/ml LB) can be added. 85 mm petri dishes are filled with the agar/LB/amp.

## 4.2 Methods

### 4.2.1 Constructions of mutants

#### 4.2.1.1 Site directed mutagenesis

The site directed mutagenesis technique is basically a PCR method or a variation of it.

A supercoiled double strand vectors- pGEF plasmids (T7 promoter plasmid with ampicillin resistance), cloned before with the sEH N-terminal domain sequence, and a (His)<sub>6</sub> sequence were inserted with the selected mutations during a PCR reaction. The oligonucleotide primers that carried the desired mutation were designed by us and produced by MWG-Biotech AG. Denaturation and annealing of the primers were done using a Pfu Turbo DNA polymerase 2 (Stratagene kit) and a thermal temperature cycler.

The reaction sample contained

5 µl of 10x reaction buffer



1.25  $\mu$ l (5 ng/ $\mu$ l) of dsDNA template

1.25  $\mu$ l (100 ng/ $\mu$ l) of oligonucleotide primer..

5  $\mu$ l (2.5 mM) dNTP mix

ddH<sub>2</sub>O to final volume of 50  $\mu$ l

1  $\mu$ l of PfuTurbo DNA polymerase (2.5 U/ $\mu$ l) – added after one cycle of denaturation.

Except for the primers all materials were taken from the QuickChange site-directed mutagenesis kit (Stratagene)

#### Cycling parameters:

Cycles	Temperature	Time
1	95°C	3 min
16	95°C	30 sec
	55°C	45 sec
	72°C	9 min

Extension and incorporation of the primers by the Pfu Turbo DNA polymerase result in nicked circular strands. The nicks in the mutated plasmids were repaired only after transformation by bacterial competent cells.

#### **4.2.1.2 Digestion with Dpn 1**

Dpn1 endonuclease (Stratagene) is specific for methylated and hemimethylated DNA. Thereby, Dpn1 in the amplification reaction sample digest parental DNA template resulting in a selected mutation-containing synthesized DNA.

1 $\mu$ l of Dpn1 was added directly to each amplification reaction, mixed gently, centrifuged for 1 min and immediately incubated for one hour at 37°C.

#### **4.2.1.3 Agarose gel electrophoresis**

Agarose gel analysis is the most commonly used method for analyzing DNA fragments between 0.1 and 25 kb. The concentration of agarose used in a gel (see table below) depends on the size of the DNA fragments that are analyzed.

Agarose concentration (% w/v)	DNA fragment range (kb)
1	1-30
0.7	0.8-12
1.0	0.5-10
1.2	0.4-7
1.5	0.2-3
2.0	0.05-2

Agarose (Gibco BRL) is added to 0.5 x TAE buffer and boiled until the agarose was dissolved. When the agarose solution was cooled (60°C), it was poured onto the gel and the comb was immediately inserted. After the gel was left to set for 30-40 min, the comb was removed and the tank container was filled with electrophoresis buffer-0.5 x TAE buffer. The markers and the samples (the mutated plasmids which were already nicked and in a linear form as a result of the site directed mutagenesis process) were mixed with 6x probe buffer (50%Glycerin and/ Xylencyanol)) and loaded to the wells.

The gel was run at 40-100 volt, until the dye has migrated to an appropriate distance. The DNA bands were visualized after the agarose gels were stained with ethidium bromide in an ethidium bromide bath (400 µg/ml in 0.5 TAE buffer) for 30 min and examined after under UV light (366 nm). Results were documented by the Eagle Eye video system.

#### 4.2.1.4 Cloning of the mutants:

##### Transformation, bacteria culture and selection, plasmid isolation

1 µl of the amplification sample, after Dpn1 restriction (around 10 ng plasmid) was added to 100 µl of DH-10B competent cells. After the sample was gently mixed and incubated on ice for 5 min., the transformation reaction sample was placed in a 42° C water bath ("heat shock") for 42 sec, and directly placed for 2 min. on ice.

500 µl of LB medium (10 g SELECT peptone 140 (Invitrogen), 5 g yeast extract, 10 g NaCl per 1.0 liter, autoclaved), were added to the reaction mix and incubated while shaking (220rpm) at 37°C for one hour.

100 µl of the transformation reaction sample were plated on LB-agar plates (15 g SELECT agar (Invitrogen) added to 1.0 liter sterilised LB medium and 100 µg/ml ampicillin (Sigma)), at 37°C o/n. A single colony was peaked from the selective plate and inoculated to 100 ml LB-Amp medium (100 µg/ml Amp) for o/n, shaking at RT.

The bacterial cells were harvested by centrifugation at 6000 g for 15 min. at 4° C following plasmid isolation by 50 ml "midi" prep, using the Qiagen plasmid midi/maxi kit.

#### 4.2.1.5 DNA concentration and purity measurement

DNA concentration was determined by measuring the absorbance at 260 nm (A<sub>260</sub>) in a spectrophotometer using a quartz cuvette. An absorbance of 1 unit at 260 nm corresponds to 50 µg plasmid or genomic dsDNA per ml (A<sub>260</sub> =1 → 50 µg/ml). This relation is valid only for measurements made at neutral pH (Tris-Cl, pH 7.0).

The calculation was done by the following formula:

DNA concentration (µg/µl) = OD<sub>260</sub> x dilution factor x 0.05

Oligonucleotide concentration = OD<sub>260</sub> x dilution factor x 0.03

A good indicator for DNA purity (in a slightly alkaline buffer, 10 mM Tris-HCl (pH 7.5)) is the ratio of absorbance at 260 nm to 280 nm. A DNA solution with an A<sub>260</sub>/A<sub>280</sub> ratio of 1.8-2.0 is desirable.

#### 4.2.1.6 Sequencing

After plasmid isolation and DNA-plasmid concentration measurements, samples of 10 µg DNA in 10 mM Tris/HCl (pH 8.0) were sent to GATC Biotech AG in Konstanz for sequencing. The sequencing results were sent back by email as "ABI-Traces" files and were analysed by EditView and MegAlign software.

#### 4.2.1.7 Restriction digestion

Restriction enzymes were ordered from “New England BioLabs” together with suitable enzyme buffers. The following enzymes were used:

Taq1, Eag1, Nae1, Dra1, Nae1, Ssp1, Hpa1, Bst1, Tha1, Bsp1, Hha1, Eae1, EcoR5, Pvu1, Hae2, Bgl2.

0.3 µl of enzyme was added to a reaction mix of 1.0 µl x10 restriction enzyme buffer (suitable for each restriction enzyme), 3.7 ddH<sub>2</sub>O, 5.0 plasmid and 0.1 BSA if needed according to instructions, followed by one hour at 37°C (unless other temperature was noticed).

### 4.2.2 Generation of recombinant proteins

#### 4.2.2.1 Expression of the sEH-phosphatase mutant proteins in *E.coli*: Transformation of bacteria, bacterial culture and induction of protein expression, lysis of Bacteria cells and the use of the FrenchPress system

Transformation of BL21-AI competent cells (Invitrogen) with the expression vectors and the following cultures are as described for cloning and culture in 4.2.1.3.

Colony peaking, culture and induction: One colony was peaked from the selecting plate with sterile pipette tip and inoculated into 100 ml of LB medium with 100 µg/ml ampicillin. When the culture reached O.D600 = 0.6 (mid-log phase) in room temperature while shaking (220 rpm), the expression was induced with 100 µM L-arabinose and left for 16 hours at room temperature, shaking. Cells were harvested by centrifugation at 4°C, 4500 rpm, for 15 min., and pellets were resuspended in 10 ml 20 mM NH<sub>4</sub>HCO<sub>3</sub>-buffer pH 7.4. Cells were broken by one pass through the FrenchPress pressure cell (aminco) at 30,000 psi when the ratio selector control level was on high. The resulting lysates were clarified by centrifugation at 10000g and 4°C for 20 min. analysed by immunoblots and used for further analysis. The FrenchPress system was washed thoroughly by one pass of 150 ml 20 mM NH<sub>4</sub>HCO<sub>3</sub> followed by one pass wash of 70% ethanol after every use, in order to prevent a mixture between the different sEH phosphatase mutant proteins, when loaded to the system one after the other.

#### 4.2.2.2 Purification of the sEH phosphatase mutant proteins using a metal chelate affinity chromatography and the use of the BioLogic Duo-Flow system

Affinity chromatography is one form of liquid chromatography. It relies on the ability of a protein to bind specifically to a complementary molecule (ligand) which is immobilized on insoluble beads packed in a column and to dissociate from it. For the purification of the sEH N-terminal domain -(His)<sub>6</sub>-tagged proteins, we used the immobilised metal (nickel) chelate affinity chromatography technique. The purification was performed with the HiTrap chelating HP column (1 ml) (Ap Biotech) according to the instructions of the manufacturer. The HiTrap chelating HP column is supplied free of metal ions and therefore had to be charged with 1ml of 100 mM nickel chloride (until a blue-green colour appeared throughout the whole column). Elution of bound proteins was done by elution gradient from 0 to 500 mM imidazole in 20 mM phosphate and 500 mM NaCl<sub>2</sub>, pH7.4. Stripping of the column was done with 0.05 M EDTA as a chelating agent in 20mM phosphate and 500 mM NaCl<sub>2</sub>, pH7.4.

The column was operated by the BioLogic Duo-Flow system (Bio-Rad), after programming the system according to the instruction manual of the column. All solutions loaded on the column were of high purity and degassed by filtration through a 0.45 µm filter or when using large volumes, by vacuum. For the kinetic assay, which followed the purification step, all the sEH phosphatase-containing fractions had to be pooled and concentrated by filtration through an anisotropic membrane using the Centricon YM-3, 3000MW cut-off (Amincon) at 4,500 rpm for 10 min.

#### **4.2.2.3 Protein analysis**

##### **4.2.2.3.1 Quantifying proteins by the Bradford method**

The assay is held in a 96 well plate. 0.2 ml of each protein sample was mixed well with 50 µl of Bradford reagent (Roti-Quant-Roth Karlsruhe). The absorbance of the protein sample (OD) was measured at 595 nm by the Microtiter- Spektralphotometer. The quantification of the protein samples were done according to the results of the BSA standard curve. The standard curve was made with known concentrations of BSA (1 mg/ml) – 50 µg, 25 µg, 12.5 µg, 6.25 µg, 3 µg, 1.8 µg, 0.9 µg and 0 µg per ml). Duplicates were made for the different BSA concentrations and the protein samples.

##### **4.2.2.3.2 SDS polyacrylamide gel electrophoresis**

SDS polyacrylamide gel electrophoresis was done according to Laemmli (1970).

10% acrylamide gels were used to separate the sEH phosphatase mutant proteins tagged with GST and 12.5% acrylamide gels were used to separate the sEH mutant proteins and WT tagged with (His)<sub>6</sub>. After the gel plates were assembled ammoniumpersulfate was added to the separating or the stacking gel mixture (for 12.5% separating gel- 2.5ml acrylamide solution (Rotiphorese 30), 1.2 ml of 1.88M Tris/HCl-buffer, pH 8.8, 1.2 ml 0.5% SDS, 1.0 ml water, 5.0 µl TEMED and 30.0 µl 10% ammoniumpersulfat). After the whole mixture was poured into the gap between the plates, a thin layer of water or isopropanol (creating a straight separating line) was added above the separating gel. When polymerization was completed the water/isopropanol was rinsed out and the Stacking gel solution ("upper" gel) was made and mixed (495 µl acrylamide solution, 600 µl 0.625 M Tris/HCl-buffer pH 6.8, 582 µl 0.5%SDS, 1305 µl water, 3 µl TEMED, 15 µl 10% Ammoniumpersulphat) and the comb was inserted. When the stacking gel polymerized, the gel was placed in the electrophoresis chamber. The chamber was filled with 50 ml electrophoresis buffer ("running" buffer)- 10X Electrophoresis buffer (75.5 g Tris, 360 g glycine in 5 l water), 2.5 ml 20% SDS, 447.5 ml water with Tris or glycine fixed at pH 8.0). Protein samples and marker were loaded after addition of sample buffer- 4 x sample buffer (1.89 g Tris, 5 g SDS, 25 ml glycerol, 12.5 ml 2-mercaptoethanol, 0.5 bromophenol blue 1% in ethanol, water is added to 50 ml) heated at 95°C for 5 min. The gel was run at 10 mA during protein migration in the "upper" gel and at 25 mA when proteins migrated in the "lower" gel.

#### 4.2.2.3.3 Coomassie staining

At the end of the electrophoresis the gels were released and transferred to a coomassie staining solution (2 g coomassie blue R250, 0.5 coomassie blue G250, 425 ml ethanol, 50 ml methanol 100 ml acetic acid, 425 ml water) for overnight on a rocking platform. After staining, the gels were removed to a destaining solution (30% methanol, 5% acetic acid) until the background disappeared and the bands were clearly seen.

#### 4.2.2.3.4 Immunoblot analysis (western blots) by semi-dry blotting and tank-blotting

Protein transfer from gels to nitrocellulose sheets and subsequent immunodetection were carried out according to Towbin et al. (1979). Following electrophoresis, proteins in a polyacrylamide gel were transferred to a hydrophobic membrane (a nitrocellulose or PVDF membrane) in a buffer-tank-blotting apparatus or by semi-dry electroblotting. By the semi-dry electroblotting method, the gel and membrane were sandwiched between two stacks of filter paper that have been pre-wet with transfer buffer. The membrane was placed near the anode (positively charged), and the gel was placed near the cathode. SDS-coated negatively charged proteins, were transferred to the membrane when an electric current was applied. In the tank blotting method, a blotting cassette was submerged in a tank for blotting. Tank blotting was performed over extended periods since the buffer capacity is far greater than that with semi-dry transfer systems. 8 pieces of filter paper (Whatman 3MM) and a piece of membrane were soaked in blotting buffer (25 mM Tris, 192 mM glycine and 20% methanol). 4 sheets of filter paper were placed on the cathode side, followed by the gel, the membrane and another 4 sheets of filter paper directed to the anode side. For the tank blotting 2 fiber pads were added, each in both sides of the filter papers and membrane complex. Tank blotting protein transfer was conducted by voltage of 16 V and current of 80 mA O/N.

At the end of the blotting when the proteins were transferred to the membrane, the proteins were probed with epitope-specific antibodies. All incubation and washing steps were done on rocking platform. The membrane was washed twice for 5-10 min. with incubation/washing buffer gelatin buffer (2.5 g gelatin in 200 ml boiled water, 250 µl Tween 20 in 500 ml TBS) and then incubated for 1 hour in blocking buffer (3 g BSA in 100 ml TBS, 50 µl Tween 20). The membrane was washed 3 times for 5 min with gelatin buffer and incubated again for 1 hour with primary antibody (rabbit antiserum for the detection of sEH protein) in a dilution of 1:1000 in gelatine buffer. The Membrane was washed again 3 times for 5 minutes. The second antibody (goat anti rabbit IgG alkaline phosphatase conjugated) diluted 1:20,000 in gelatine buffer, was incubated for 1 hour in RT. After washing (3 times for 5 min), the membrane was equilibrated with the colour reaction buffer – 100 mM Tris/HCl pH 9.5, 100 mM NaCl, 50 mM MgCl<sub>2</sub>. The colour reaction started when the membrane was incubated with NBT/Xphosphate substrates in a colour reaction buffer (4.5 µl NBT (75 mg/ml 70 % DMF) and 3.5 µl X-Phosphate (50 mg/ml DMF) in 1 ml buffer, until violet bands appeared. The color reaction was stopped with EDTA buffer.

## 4.2.3 Enzymatic assays and calculations

### 4.2.3.1 Activity assay: Screening assay for product formation (4-nitrophenol) and kinetic assay

The screening assay for product formation was followed by a kinetic activity assay for mutants that showed detectable enzyme activity in the screening assay.

Both assays were made in a 96 well plate (Nunc) using the substrate 4-nitrophenyl phosphate. The assays measured product formation (absorbance) of 4-nitrophenol at 405 nm by the spectramax 250 microplate reader (Molecular Devices).

The reaction in the first assay starts with addition of 50  $\mu$ l enzyme taken from every eppendorf (23 eppendorfs) that were collected during the purification process to 200  $\mu$ l of assay buffer (50mM Tris-HCL, 50 mM NaCL, 10 mM  $MgCl_2$ , pH 7.8 in a total volume of 250  $\mu$ l) and substrate 2mM 4-nitrophenyl phosphate (1 tablet of 4-nitrophenyl phosphate (Sigma) in 5 ml of assay buffer). Product formation was measured for one hour at 37°C. The blank controls contained assay buffer instead of protein.

In the following kinetic assay for the mutants that showed detectable enzymatic activity, the samples of the fractions/eppendorfs that exhibited product formation and were detected in the former assay were collected and concentrated by filtration through an anisotropic membrane using the Centricon YM-3, 3000MW cut-off (Amincon) at 4,500 rpm for 10 min., and measured for protein concentration determination.

For the kinetic assay, two sub assays were done for scaling use. Different concentrations of the product 4 -nitrophenol (100, 90, 80, 70, 60, 50, 40, 30, 20, 10, 0  $\mu$ M) were measured for absorbance by the Spectramax device, in endpoint mode (not in kinetic mode). Different concentrations of substrate were prepared, by 2 fold dilutions, starting with a concentration of 6.4 mM of 4 -nitrophenyl phosphate (3 tablets of 4 – nitrophenyl phosphate in 5 ml assay buffer).

Reaction started with addition of the purified enzyme- 50  $\mu$ l per well from the concentrated fraction (typically corresponding to 0.5-20  $\mu$ g) to 200  $\mu$ l assay buffer and substrate. Parallel wells were made with the same concentrations of substrate without enzyme. The absorbance of the control-blank wells is later deducted from the absorbance result of the parallel substrate + enzyme in a well.

### 4.2.3.2 Determination of the kinetic parameters: The four calculating methods

First thing to do in order to determine  $V_{max}$  and  $K_m$  is to measure the rate of catalysis at different substrate concentrations. There are four techniques for calculating these kinetic parameters: **Lineweaver-Burk plot**-the most popular one, **Eadie-Hofstee plot**, **Hanes plot**, and the **direct linear**. Basically, all the calculating methods transform the Michaelis-Menten equation to one that gives a straight-line plot by simple but different algebraic conversion that results in an equation with a structure that is similar to the straight-line equation:  $Y=MX+C$  (only the direct linear plot is a very different use of a straight-line technique). This gives a clear advantage, as drawing a straight-line graph, which can be extrapolated to cut both axes, makes the calculations of these kinetic parameters simpler and easier. Each one of the different calculating techniques has some advantages and disadvantages over the other (see in discussion). The kinetic parameters were calculated from the not processed experimental results (as detailed in section 4.2.3.3).

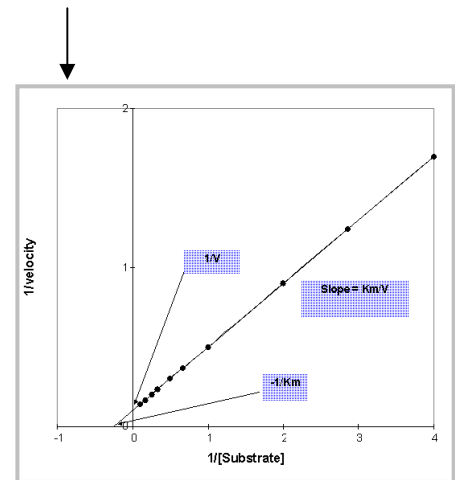
The calculation principles of the calculating methods are elaborated below

The most popular and familiar technique is the **Lineweaver-Burk plot** (also named double reciprocal).

The plot is based on the Michaelis-Menten equation:

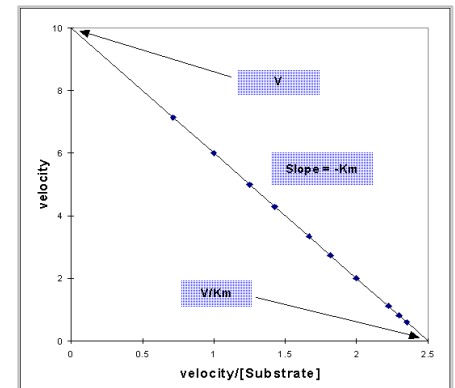
$$1/v = K_m/V_{max} \times 1/[s] + 1/V_{max}$$

In this plot, 1/v versus 1/[s] yields a straight-line with intercepts of 1/V<sub>max</sub> on the vertical axis and -1/K<sub>m</sub> on the horizontal axis, and a slope of K<sub>m</sub>/V<sub>max</sub>. This seems to answer many of the problems involved in calculating kinetic parameters from a curve of velocity against substrate concentration curve: It is a straight-line which is much easier to draw. It does not require a *direct* measurement of V<sub>max</sub> and both V<sub>max</sub> and K<sub>m</sub> are read easily from the graph. Unfortunately it does have some real drawbacks in dealing with data containing significant experimental error.



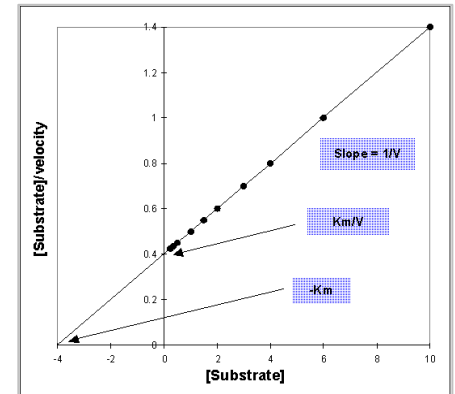
In the **Eadie-Hofstee plot**

The Michaelis-Menten equation is converted to one of a straight-line:  $V = -K_m V/[S] + V_{max}$ . The plot gives a straight-line with a slope of - K<sub>m</sub> and an intercept of V. The intercept on the horizontal axis is V/K<sub>m</sub>.



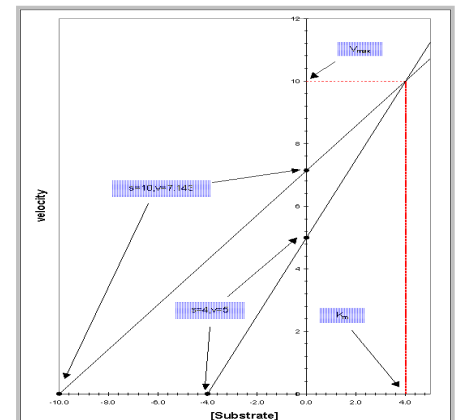
Another conversion of the Michaelis-Menten equation that gives a straight-line is the **Hanes plot**.

This plot follows the equation  $[S]/V = 1/V_{max} \times [S] + K_m/V_{max}$ . Substrate concentration divided by velocity against substrate concentration gives a straight-line with an interception on the horizontal axis of -K<sub>m</sub> and K<sub>m</sub>/V on the vertical axis. The slope is 1/V.



**The direct linear plot:**

The three other methods are rather similar to each other and based on an algebraic conversion of the Michaelis-Menten equation to give a straight-line equation. The direct linear plot is a very different use of the straight-line technique, thus quite different from the other three methods. As seen in the graph the substrate values are marked as points on the negative side of the substrate axis and the velocity values on the velocity horizontal axis. There is no calculation involved at this stage (before plotting the data on



the graph), the data is simply plotted on the graph. Each pair of data (substrate and velocity) are joined with a straight-line. Lines, obtained by data that have no experimental error would meet in one intersection from where a vertical line is dropped to the substrate axis and gives the value of  $K_m$  and the value of  $V_{max}$  when a horizontal line is dropped to the velocity axis. Because experimental data have some errors there will be few intersections. The intersection that will reveal the  $V_{max}$  and  $K_m$  values was calculated as described below (section 4.2.3.3 (12, 13, graph 7)).

#### 4.2.3.3 Processing the kinetic assay results and calculations of the kinetic parameters in four calculating methods

The following description gives a detailed explanation for all the steps from managing the experimental results to calculation of kinetic parameters in different calculating techniques. I have chosen to present it at the same way it was originally done in excel (for the WT as an example). Every explained **stage** is marked with a **red number** and related to the **same number** in the Excel calculating sheet (page 42).

**1** - Concentration of the purified enzyme used for the activity test, measured by Bradford.

**2** – The amount of enzyme per well used for the activity assay was calculated by  
Amount of enzyme (section 1) x volume of reaction sample in a well (35  $\mu$ l-50  $\mu$ l) / 1000

**3** – Absorbance measurements (mO.D for a minute) of the product formation as were read by the spectrophotometer. Each measurement (represents a well) was given to a different substrate concentration. The substrate (4-nitrophenol phosphate) was consequently two times diluted (see kinetic assay). Each well in the column contained the same amount (see section 2) of purified enzyme.

**4** – Same as in section 3 but without an enzyme, thus termed blank (the measurements were all done at the same time)

**5, 6** – The measurement values in section 3 had to be converted to O.D values. The values in section 3 were therefore multiplied by 60 (duration of the assay) and divided to 1000.

**7, 8, graph 1** - For the known concentrations of the substrate (section 7) there were parallel calculations of O.D (section 6 – O.D blank), which constructed graph 1. Setting each different substrate concentration in the straight-line equation evaluated in graph 1 resulted in the “O.D regulated results” in section 8.

**9** – As the substrate has a “self” absorption, it was subtracted from the absorption of the whole sample. At section 9, “O.D blank” is subtracted from O.D sample (in section 5). The O.D values in section 9 show the absorption of the product itself (PNP – 4-nitrophenol)

**10, 11, graph 2** – As a standard was needed for scaling the experimental results, different concentrations of product - PNP (section 10) were measured for O.D (section 11). The results were plotted on a graph (graph 2) showing a linear plot of the data together with an adequate linear equation.



**12** – In section 12 (termed “turnover nmol” although it is not the turnover number) the product (in nmol) of the enzymatic reaction for each substrate concentration was indicated. Calculation was done by setting each O.D value (from section 9) in the linear equation obtained from graph 2. After the values in section 9 were set in the linear equation (as Y), the calculated X values were divided to 4 (a shortcut calculation that depends on the total volume of the reaction in the well- 250  $\mu$ l), thereby getting the amount of product directly in nmol for a given substrate concentration.

**13** – Activity (or velocity or reaction rate) is calculated in section 13 by dividing the values of section 12 to the amount of enzyme per well in mg (indicated in section 2) and to the time in minutes of the assay (usually 60 min).

**Graph 3** – Graph 3 (values in section 7.1 were plotted against the values in section 13) showed the effect of substrate concentration on the reaction rate (or velocity). It exhibited a curve that indicated a typical Michaelis-Menten enzyme catalysed reaction and a rough estimation (with some extrapolation of the curve), of the expected Vmax value.

**14, 15, graph 4**- The Lineweaver–Burk plot and Vmax, Km calculations.

1/substrate (calculated in section 14) versus 1/velocity (calculated in section 15) resulted in the Lineweaver-Burk plot shown in graph 4. As the Lineweaver-Burk equation has a similar structure to the straight-line equation  $Y = M X + C$ , a straight-line (in graph 4) and a straight-line equation were obtained. From this simplified equation the values for X and Y when the line intercepts the vertical axis and the horizontal axis could be obtained. Meaning that the value of X when Y=0 and the value of Y when X=0 could be calculated. These values were set in the Linweaver-Burk equation, thereby the values of Vmax and Km (written under the graph) could be obtained:

**When  $1/S=0$  or  $X=0$ , Y (calculated from the straight-line equation which was written in graph 4) equals  $1/V = 1/V_{max}$**

**When  $1/V=0$  or  $Y=0$ ,  $(-1/X)$  (calculated from the straight-line equation written in graph 4) equals  $-1/K_m \rightarrow K_m = -1/-X$ .**

**15, 16, graph 5**- The Eadie-Hofstee plot and Vmax, Km calculations.

Like the Lineweaver-Burk plot, this technique is based on the conversion of Michaelis equation to a straight-line equation:  $V = -K_m V/S + V_{max}$ . This time the variables are V (velocity or activity) and V/S (velocity/substrate conce.). A plot of them will give a straight-line with intercepts of Vmax on the vertical axis and Vmax/Km on the horizontal axis. From the Eadie-Hofstee plot of the experimental data (calculated data for the plot are in sections 15, 16), a straight-line was obtained (in graph 5) and a straight-line equation (indicated in the graph). After setting the values of the intercepts in the straight-line equation and calculating X and Y values, these values were set in the Eadie-Hofstee equation. Thereby, the values of Vmax and Km (written under the graph) could be obtained:

**When  $X=0$  or  $V/S=0$ , Y (calculated from the straight-line equation written in graph 5)  $=V=V_{max}$**

**When  $Y=0$  or  $V=0$ , X (calculated from the straight-line equation written in graph 5)  $= V_{max}/K_m \rightarrow K_m = V_{max}/X$**

**17, 18, graph 6**- The Hanes plot and Vmax, Km calculations.

Another conversion of the Michaelis-Menten equation that gives an equation of a straight-line:  $S/V = 1/V_{max} S + K_m/V_{max}$ . A straight-line was obtained by plotting substrate conce./velocity [S]/V

against substrate concentration [S] with an intercept on the horizontal axis of  $-K_m$  and  $K_m/V$  on the vertical axis.

**When  $Y=0$  or  $[S]/V=0$ ,  $(-X)$  (a value, calculated from the straight-line equation that was obtained by the Hanes plot of the experimental data) =  $-K_m \rightarrow X=K_m$**

**When  $X=0$  or  $[S]=0$ ,  $Y$  (a value, calculated from the straight-line equation that was obtained by the Hanes plot of the experimental data) =  $K_m/V_{max} \rightarrow V_{max}=K_m/Y$ .**

### **12, 13, graph 7, Table 1** – The direct linear plot and $V_{max}$ , $K_m$ determination

The direct linear plot is a very different use of a straight-line technique. No calculation is involved (at the first stage), the raw experimental data is plotted on the graph although this data (in sections 12 and 13) have to be first written in a certain way (table 7), in order to get the right graph by excel. The X-axis in the graph is substrate concentration; it has a negative side, where all the experimental substrate values are marked. The Y-axis represents velocity (activity). Each pair of data (substrate concentration and activity) produces a straight-line, which was extrapolated into the positive substrate area of the graph. The “trick” that could help getting the right graph in Excel was to write the experimental data given in 12 and 13 as showed in Table 1. At first, values of substrate concentrations were set on the negative side. Second, each pair of data was marked twice on the graph. Each value on the Y-axis had two values marked on the X-axis, one was the substrate concentration and the other was 0, thereby 2 points on each axis were obtained and joined with a straight-line.

The extrapolated straight-lines (in the positive side) intersect with one other, a vertical line dropped from the intersection to the substrate axis gave the value of  $K_m$  and the horizontal line to the velocity axis gave the  $V_{max}$  value. If the experimental data were “perfect” (had no error in it) all the lines would have intersected in one point and the  $K_m$ ,  $V_{max}$  values would have been clear, but normally experimental data contain some error therefore the lines intersect in different points and each intersection is an estimation of the  $V_{max}$  and  $K_m$ .

So what to take as the best value for  $V_{max}$  and  $K_m$ ? The correct method is to select the  $K_m$  and  $v_{max}$  values that were obtained by the intersection that represented the median number (not average!) of the intersections. For calculating the median number of intersections in the direct linear plot the number of intersections is firstly calculated by the equation  $n(n-1)/2$  where  $n$  is the number of lines. For eight lines as in graph 7 there were 29 intersections. The median was then halfway between the 14<sup>th</sup> to the 15<sup>th</sup> line, counted from the bottom of the plot upwards. Because it was difficult to distinguish and count some of the intersections (some were too condensed or not seen in that part of the graph), the intersections were identified by calculations. Each line had a straight-line equation and by equalizing them (8 straight-line equations) with one another, algebraic equations (28!) were obtained in which the calculated X, Y values were numbered from the lowest to the highest until the intersection of the median number (in this example between the 14<sup>th</sup> and the 15<sup>th</sup> X, Y values). An average of the two X values and the two Y had given the  $V_{max}$  (Y) and  $K_m$  (X) values.

**Kcat calculation** – Kcat is calculated by the equation -  $V_{max} = K_{cat} [E]$ .

$V_{max}$  value was taken from the  $V_{max}$  calculation done by the direct linear plot technique. Enzyme concentration in nmol was calculated by the molecular weight of the N-terminal sEH (25,000 gr/mol) and the quantity of the purified protein per well given in section 2.

**Kcat/Km** – The calculated Kcat divided to Km value obtained from the Km calculation done by the chosen technique (the direct linear plot).



## 5 Results

### 5.1 Selection of candidate phosphatase active-site amino acids

Candidate catalytic amino acids in the active site of the sEH phosphatase domain were predicted to be crucial to its catalytic activity. A combination of several investigations was taken as a basis to choose potential catalytic amino acids residues as described by Cronin *et al.*, (2003) (see introduction). The structure based sequence alignments of sEH and selected members of the HAD family revealed conserved and partly conserved amino acids concentrated in characteristic motives. Most of the conserved amino acids were the ones found to be implied in the catalytic mechanism of a few investigated HAD enzymes: the haloacid dehalogenase (Schneider *et al.*,1993), P-ATPase (Aravind *et al.*, 1998, Ridder & Dijkstra 1999), phosphoserine phosphatase (PSP) and phosphomutase (PMP) (Altschul *et al.*,1997, Collet *et al.*,1999, Wang *et al.*, 2002). The prediction/selection was further supported by examination of the sEH murine crystal structure (Argiriadi *et al.*, 1999) and by the similar spatial arrangement that was found between the equivalent conserved amino acids of the sEH and the examined HAD enzymes. The selection results presented here follow the four conserved sequence motifs highlighted in the alignments shown in Fig. 5.

Motif 1 (DXDXT/V) includes the potential nucleophile **Asp9 (D9)** in the sEH phosphatase. This position is highly conserved among all HAD members. Motif 1 displays a second aspartic acid residue **Asp11 (D11)** in the sEH phosphatase that was assumed to act as a general acid/base catalyst in related HAD phosphatases such as the PSP from *Methanococcus jannaschii* (Wang *et al.*, 2002).

In Motif 2 and 3 all HAD members contain a serine or threonine residue in a conserved position as well as a basic amino acid residue in motif 3 – **Thr123 (T123)** and **Lys160 (K160)** in the sEH phosphatase. Both were supposed to hydrogen bond to the negatively charged phosphate substrate. **Asn124 (D124)** was selected as an active site amino acid a candidate in the sEH phosphatase due to its spatial orientation observed in the active site of the murine sEH crystal structure (Argiriadi *et al.*, 1999).

Motif 4 is the least conserved Motif (G/SDXXN/TD) and it contains either two neighboring aspartic acids like in the sEH - **Asp184 (D184)** and **Asp185 (D185)** or separated by three or four amino acids. Both aspartates were implicated in binding the divalent cation within the active site (Wang *et al.*, 2002). In the haloacid dehalogenase as an exception the two neighboring (vicinal) aspartates are replaced by serines to function in stabilization of the catalytic nucleophile (as they have no cation in the active site) (Morais *et al.*, 2000). The **Asn189 (N189)** in Motif 4 was selected for amino acid exchange because it resembles the conserved position of the second aspartic acid in loop 4 in the primary sequence of other phosphatases and it is further oriented towards the active site.

### 5.2 Construction of sEH phosphatase active site mutants

In order to investigate whether the putative candidates of the sEH phosphatase active site are directly involved in catalysis, we substituted the residues in question to non-functional amino acids by site directed mutagenesis of an expression plasmid which encoded the 221 N-terminal amino acids of the

human sEH phosphatase domain together with a C-terminal His<sub>6</sub> – tag, under the control of the T7 promoter (pGEF-HisC-sEH-Nterm).

The selection of amino acids that would substitute the putative active site amino acids was directed by the need to remove the side-chain functionality, yet to maintain structural integrity of the mutant protein. At least two alternative amino acids, either alanine in most cases or an amino acid structurally similar to that in the WT enzyme (also termed a “conservative” exchange/ substitution) were introduced for each candidate amino acid. The different kinds of alternative exchanges enabled us to get a larger scope of kinetic results and therefore to broaden the possible obtained information.

Altogether, 18 amino acid exchanges (mutants) were planned and constructed:

Asp9, 11, 184, 185	→Ala.
Asp9, 11, 184, 185	→Asn
Thr123	→Val
Thr123	→Ala
Thr123	→Asn
Lys160	→Ala
Lys160	→Arg
Lys160	→Asn
Asn124, 189	→Ala
Asn124, 189	→Asp

The amino acids written above are illustrated in the appendix, making it easier to evaluate the difference between the original amino acids and the amino acids they are replaced with. During the site directed mutagenesis process, the oligonucleotide primers were used for introduction of the different point mutations which resulted in mutant sEH phosphatase proteins with a single amino acid residue substitution. To ensure the success of the site directed mutagenesis reaction, we tried, when designing the primers, to make as minimal change as possible in the WT sequence in order to get the desirable amino acid, utilizing the fact that each amino acid is encoded by few possible triplet sequences (table in appendix). The primers were further designed to contain additionally new or deleted existing restriction sites, in order to simplify the identification of correct mutants. The nucleotide bases responsible for the amino acid exchanges and for the modified restriction sites are marked with different colors in the primer sequences in Table 1 in the appendix.

The expression plasmids coding for active-site mutants were isolated and visualized on agarose gels (see Fig. 7). The 18 different recombinant clones were the result of diverse experiments to get a sufficient product from the site directed mutagenesis-PCR reaction, with changes in annealing temperature and time, denaturation duration (up to 3 minutes), number of cycles and even replacement of the thermal temperature cycler machine.

All product-recombinant clones were subjected to Dpn1 restriction as Dpn 1 eliminates the original non-mutated plasmid from each sample by digesting the methylated, non-mutated parental DNA template. After restriction digestion the product was loaded on agarose gels to ensure cloning success before competent cells were transformed with the mutated plasmid products. The differently mutated expression plasmids contained a nick, which occurred through the extension, and incorporation of the primers by the DNA polymerase during the site directed mutagenesis process, thereby there was no need to restrict the expression plasmids before loading the gels. The nicks were later repaired by the competent cells (DH-108) when transformed with the mutated plasmids.

The resulting 18 different recombinant clones (expression plasmids), presented in the figure below were proved later to be inserted with the correct mutation.

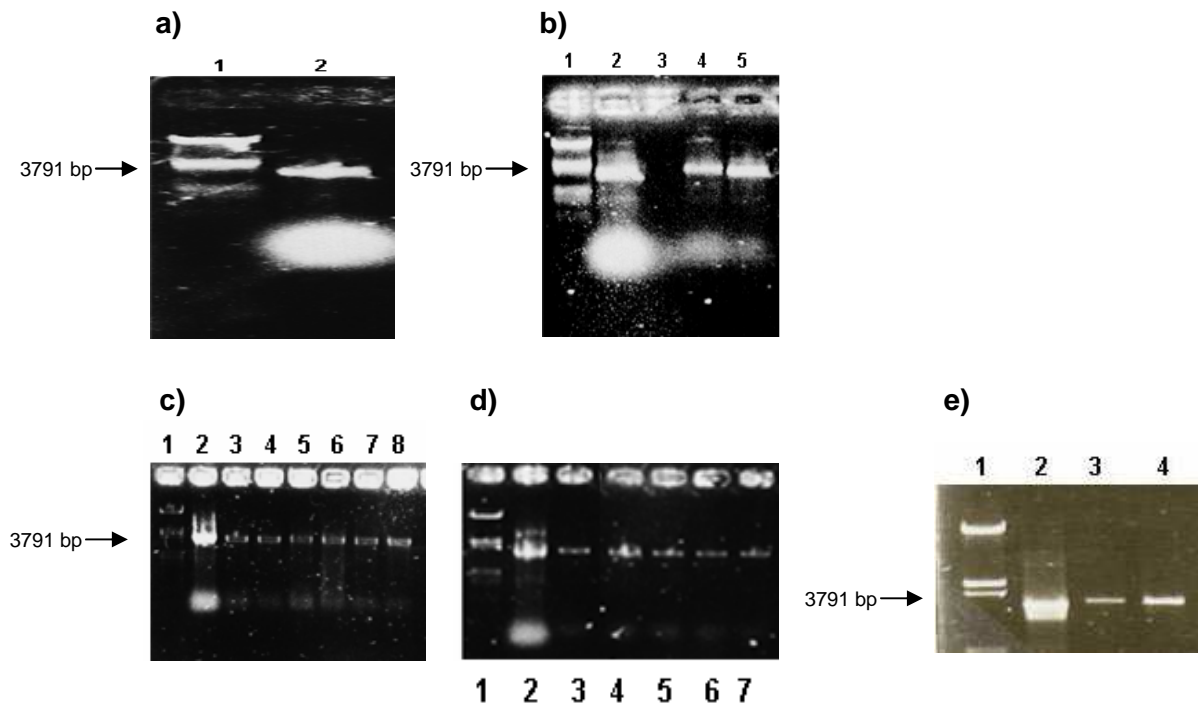


**Fig. 7. The differently mutated expression plasmids (pGEF-HisC-sEH-Nterm), products of the site directed mutagenesis process.** The mutated expression plasmids (3791bp) were run and visualized on 1% agarose gels, encoding for the following amino acid substitutions or mutants: **a)** 2- D11A **b)** 3- D11A (no product by 53°C annealing temp.) 4- K1 60A 5- D185A. **c)** 3- D9A 4- D9N 5- D11N 6- T123A, 7- T123N 8- T123V **d)** 3- K160N 4- D184N 5-D185N 6-N189A 7-N189D **e)** 3- K160R 4- D184A. The presented recombinant clones were proved later to carry the mutations leading to the indicated substitutions. In all gels, lane 1- EcoR1/Hind3 marker (21226bp, a band group of 5148, 4973, 4268, 3530bp, and a band group of 2027, 1904bp), lane 2- control pGEF plasmid containing the limonene EH (LEH) sequence.

### 5.2.1 Proving the success of the site directed mutagenesis process

The recombinant expression plasmids encoding mutant sEH phosphatase proteins were verified by both restriction and sequence analysis to ensure the correctness of the encoded amino acid sequence. As was written before, the primers used in the site directed mutagenesis process were designed to induce an amino acid substitution and to modify a restriction site (eliminate or create a new restriction site). It was assumed that if a mutation which was designed to modify a restriction site, was identified by restriction with a compatible restriction enzyme, it is thereby proving with high probability (like a marker) that the mutation which was designed to lead to an amino acid exchange through the same primer was also inserted. The exact correctness of the inserted bases was proven in a later step by sequencing. The restriction analysis was made before sequencing in order to identify problems in the site-directed mutagenesis process and to make sure that the obtained recombinant clones are the ones that were supposed to be.

In Table 1, the suitable restriction enzymes used for restriction of each mutant plasmid and WT plasmids (which were restricted in parallel by the same restriction enzymes) are indicated together with the expected fragment size to be obtained after the restriction digest. The expected differences

between the restriction results of the mutated plasmids and the WT plasmids were made visible, after running the restriction digest fragments on agarose gel.

**Table 1. The restriction enzymes used for restriction of each mutant and WT plasmid in parallel and the expected fragments size.** Restriction was designed to result in fragments size that would easily show a difference on a gel between restriction fragments of a mutant and a WT plasmid (with the same restriction enzyme). Obtaining the expected fragments had implied of successful results in the site directed mutagenesis process.

Mutation	Restriction enzyme and site of restriction	Expected fragments size (bp)
D9A	Restriction by TaqI at position 122 is eliminated	WT: 1444, 643, 579, 512, 273, 218, 116, 6 Mu.: 1444, 759, 579, 512, 273, 218, 6
D9N	Restriction by EagI at position 112 is eliminated	WT: 3736, 55 Mu.: linear plasmid (3791).
D11A	A new restriction site for NaeI at position 132	WT: linear plasmid (3791) Mu.: 3462, 329
D11N	A new restriction site for DraI at position 128	WT: 3080, 692, 19 Mu.: 2032, 1048, 692, 19
T123A	A new restriction site for NruI at position 466	WT: no restriction site mu: linear plasmid
T123N	A new restriction site for SspI at position 461	WT: linear plasmid 3582, 185, 24 Mu.: 2636, 946, 185, 24
T123V	A new restriction site for HpaI at position 468	WT: linear plasmid Mu.: 3323, 469
K160A	A new restriction site for BstUI at position 577	WT: 890, 581, 493, 376, 341, 332, 330, 8 further fragments below 200 Mu.: 581, 493, 465, 425, 376, 341, 332, 330, 8 further fragments below 120
K160N	A new restriction site for BspEI at position 579	WT: linear plasmid Mu.: 3396, 395
K160R	A new restriction site for HhaI at position 578	WT: 812, 455, 393, 337, 332, 270, 19 further fragments below 200 Mu.: 455, 426, 393, 386, 337, 332, 270, 19 further fragments below 200
D184A	A new restriction site for EaeI at position 646	WT: 2514, 1222, 55 Mu.: 2035, 1222, 479, 55
D184N	A new restriction site for EcoRV at position 654	WT: no restriction site Mu.: linear plasmid
D185A	A new restriction site for PvuI at position 654	WT: 2692, 1099 Mu.: 2008, 1099, 684
D185N	A new restriction site for SspI at position 654	WT: 3582, 185, 24 Mu.: 2443, 1139, 185, 24
N189A	A new restriction site for HaeIII at position 665	WT: 1993, 1086, 370, 286, 48, 8 Mu.: 1993, 613, 473, 370, 286, 48, 8
N189D	A new restriction site for BglII at position 662	WT: linear plasmid Mu.: 3245, 546



Most of the restriction results of the mutant and WT plasmids were in agreement with the expected fragments size detailed in Table 1, except for T123V, N189D mutants (which were later proved for the correctness of the inserted bases by sequencing).

The examples in Fig. 8 emphasize the possibility as described above to distinguish visually if a plasmid was successfully inserted by the site directed mutagenesis process, with a mutation leading to a modification in a restriction site (presumably combined with an insertion of a mutation that substitutes an existing amino acid with another). To make it easier to the eye, a restriction digest of only two differently mutated expression plasmids (D11A and D185A mutant plasmids) and WT plasmids were presented. The WT plasmids and the D11A and D185A mutants were restricted with restriction enzymes indicated in Table 1. If a successful site directed mutagenesis occurred, inducing the desired mutations, a difference would be observed in fragments size from the restriction digest of D11A (by *Naell*) and D185A (by *PvuI*) compare to the fragments size obtained in the restriction digest (by the same restriction enzymes respectively) of the WT plasmids. The mutations were designed in a way that differences in fragments size between a certain restricted mutant and its corresponding restricted WT plasmid would be visible on agarose gel. The restriction of D185A resulted in a significantly visible fragment of 684bp (Fig. 8, lane 4) that does not appear as one of the fragments following a WT restriction with the same restriction enzyme (Fig. 8, lane 5). Same for the D11A restriction, resulting in a 329bp fragment (Fig. 8, lane 2) that does not appear among the fragments obtained in the WT plasmid restriction (lane 3).

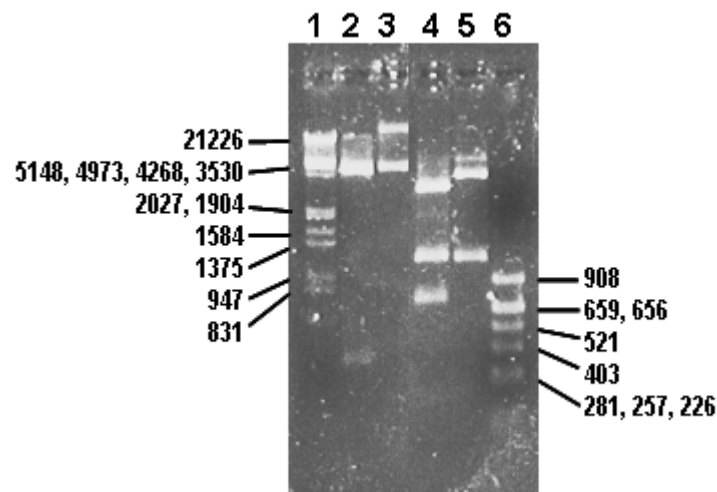


**Fig. 8. Restriction results of two of the mutated expression plasmids, encoding mutants D11A, D185A and the WT plasmids (pGEF-HisC-sEH-Nterm), as visualized on 1% agarose gels.** 1- *EcoR1/Hind3* marker 2, 3 - D11A mutant and WT plasmids respectively 4, 5 - D185A mutant and WT respectively 6 – Alu marker. Restriction of D11A and WT plasmids by *Naell* resulted in the expected fragments size as indicated in Table 1, showing a clear difference by a fragment size of 329bp in lane 2 (D11A restriction) absent in lane 3 (WT restriction). Restriction of D185A and WT plasmid by *PvuI* resulted in the expected fragments size as indicated in Table 1, showing clearly a difference by a fragment size of 684bp (lane 2) absent in lane 3 (WT plasmid restriction). In addition different fragment sizes of 2692bp (lane 5, WT plasmid restriction) compare to 2008bp (lane 4, D185A restriction) could be additionally observed.

After restriction, the expression plasmids were cloned in *E.coli* strain of competent cells (DH-10B) to the minimum required DNA amount of 10  $\mu$ l in 30  $\mu$ l and sent for sequencing (GATC-Biotech). Sequencing results verified, that all the desired mutations were inserted in the exact sequence and site, therefore coding for the specific planned substitutions. The accepted sequencing results were additionally screened and found to be free of random mutations in the amplified sequence, mutations

that could have occurred during the site directed mutagenesis process and shift the reading frame in a way that would result in a different amino acid coding. At this stage, the 18 mutants were readily available for subsequent examinations.

### **5.3 Expression of the recombinant human sEH phosphatase proteins (the human sEH phosphatase active site mutant and WT proteins)**

For the production of the recombinant enzymes, *Escherichia coli* (*E.coli*) BL21-AI competent cells (Invitrogen) were transformed with the expression vector constructs coding for the different sEH active-site mutants and WT. The BL21-AI cells are known to be suitable for recombinant protein expression of any T7 RNA polymerase-based expression vectors and proved before to be successfully expressed several metaloproteases (Pieper, 2000). In addition, the BL21-AI cells were chosen to be used, as the expression results obtained from another examined strain of *E.coli* cells BL21DES, exhibited poor expression results when transformed with the WT and mutant sEH expression plasmids.

After induction of protein expression was by 100  $\mu$ l of L-arabinose, cultures were allowed to grow further overnight. Cells were harvested, centrifuged, resuspended in hydrogen carbonate buffer and subsequently broken by one pass through a French Press pressure cell (Aminco). The resulting lysates were clarified by centrifugation and showed no formation of insoluble proteins (inclusion bodies) in none of the active-site mutants although misfolding or aggregation, causing formation of inclusion bodies, is one of the major problems in expressing foreign eukaryotic proteins in *E.coli* (Achantra et al., 1993). This might be due to the use of the French press system for breaking the cells rather than the use of sonication ([www.ivaan.com/protocols/111](http://www.ivaan.com/protocols/111)).

The expression of the recombinant proteins was examined on denaturing 12% polyacrylamide gels followed by immunoblots (semi-dry blotting) and protein detection using an anti -sEH first antibody that was produced in our lab. As can be seen in the immunoblots in Fig. 9, transformation of *Escherichia coli* BL21 with WT and mutant sEH vector constructs and induction of proteins with L-arabinose resulted in production of soluble recombinant proteins in the expected size of 25-kDa, corresponding to the phosphatase domain of the human sEH. The expression level was of approximately 5% of the cellular protein content (results not shown). Only one mutant out of the 18 mutants, the K160A, failed to express in the system used (Fig. 9, lane 3). The mutation had probably a drastic effect on the enzyme structure/ integrity that prevented it to form as a whole protein, therefore no purification and further investigations were possible with this mutant. After expression, 17 mutants and WT were available for purification for the subsequent enzymatic activity tests and kinetic assays.

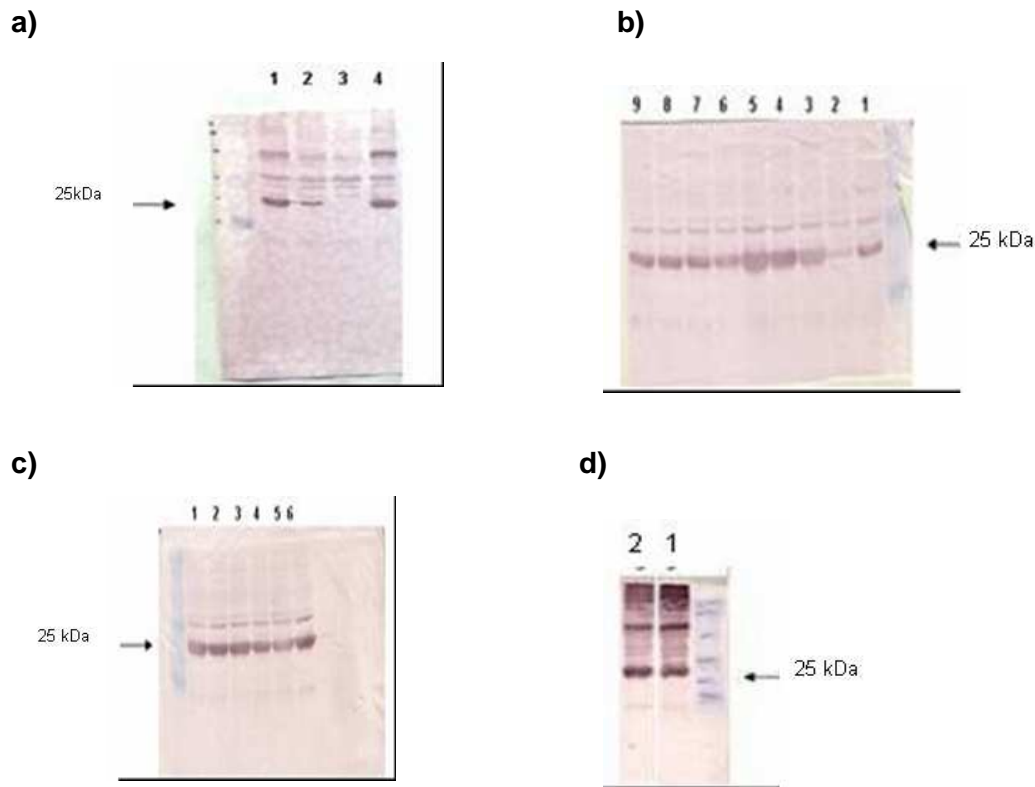


**Fig. 9. Expression of the human sEH phosphatase active-site mutant proteins and WT in *E. coli* cells (BL21-AI).** All mutants were successfully expressed except for the K160A mutant. The expression results were examined by immunoblots (12% polyacrylamide gels) and compared to a molecular weight standard, showing expression of soluble proteins in the expected size (25kDa) corresponding to the following sEH active-site mutants: **a)** 1- WT 2- D11A 3- K160A 4- D185A **b)** 1- WT 2- D9A 3- D9N 4- D11N 5- T123A 6- T123N 7- T123V 8- K160N 9- K160R **c)** 1- D184A 2- D184N 3- D185A 4- D185N 5- N189A 6- N189D **d)** 1- N124A 2- N124D.

## 5.4 Purification of the recombinant human sEH phosphatase proteins

The purification method depending on the peptide tag was already determined when the expression vector was designed. The His<sub>6</sub>- tag was used as a peptide tag because it has been already proven not to interfere with the catalytic activity of the enzyme (Cronin et al., 2003). The sEH phosphatase WT and mutant proteins were purified using a metal (nickel) chelate affinity chromatography (HisTrap chelating HP columns (AP-Biotec)). The purification steps were operated by the BioLogic Duo-Flow system after suitable programming and buffer preparations, which made the purification process accurate and adherent. Since there were no significant problems with generation of inclusion bodies, the purification process was directly assessed after the cells were broken by one pass through the French Press and followed by centrifugation.

The purification results of the mutant and WT proteins and thereby the efficiency of the purification process was examined by SDS-PAGE analysis in which proteins were separated on 12% polyacrylamide gel, coomassie stained and compared to a molecular weight standard). In addition, compatibility of the purification chromatograms ("run report"), the activity-screening test results and the coomassie stained gels of the WT and the relatively active mutant proteins was examined (termed,

“cross information”), contributing by that in identifying clearly or assuring the fractions (and lanes) that contained the sEH phosphatase.

The SDS-PAGE gels (denaturing 12% (W/V) polyacrylamide gels) in Fig. 10 are of two representative examples of SDS-PAGE analysis, the WT and the active mutant D185N. The gels contain all the fractions that were collected during the metal chelate chromatography purification process by the BioLogic Duo-Flow system, therefore, exhibiting a “follow up” of the purification-isolation process. Additionally, as the the WT and D185N mutant proteins exhibited enzymatic activity, their respective gels could be used for “cross information” between the results of the gels the results of the activity screening test and the chromatograms. The purification results in Fig. 10 show that along the purification process or in parallel to the raise in the imidazol concentration (used for elution of the sEH phosphatase- (His)<sub>6</sub> tagged), a clear band at the expected size of the sEH phosphatase protein, 25 kDa, appeared from around the 12<sup>th</sup>/ 13<sup>th</sup> collected fraction onward. This band was gradually isolated to be the only observed band.

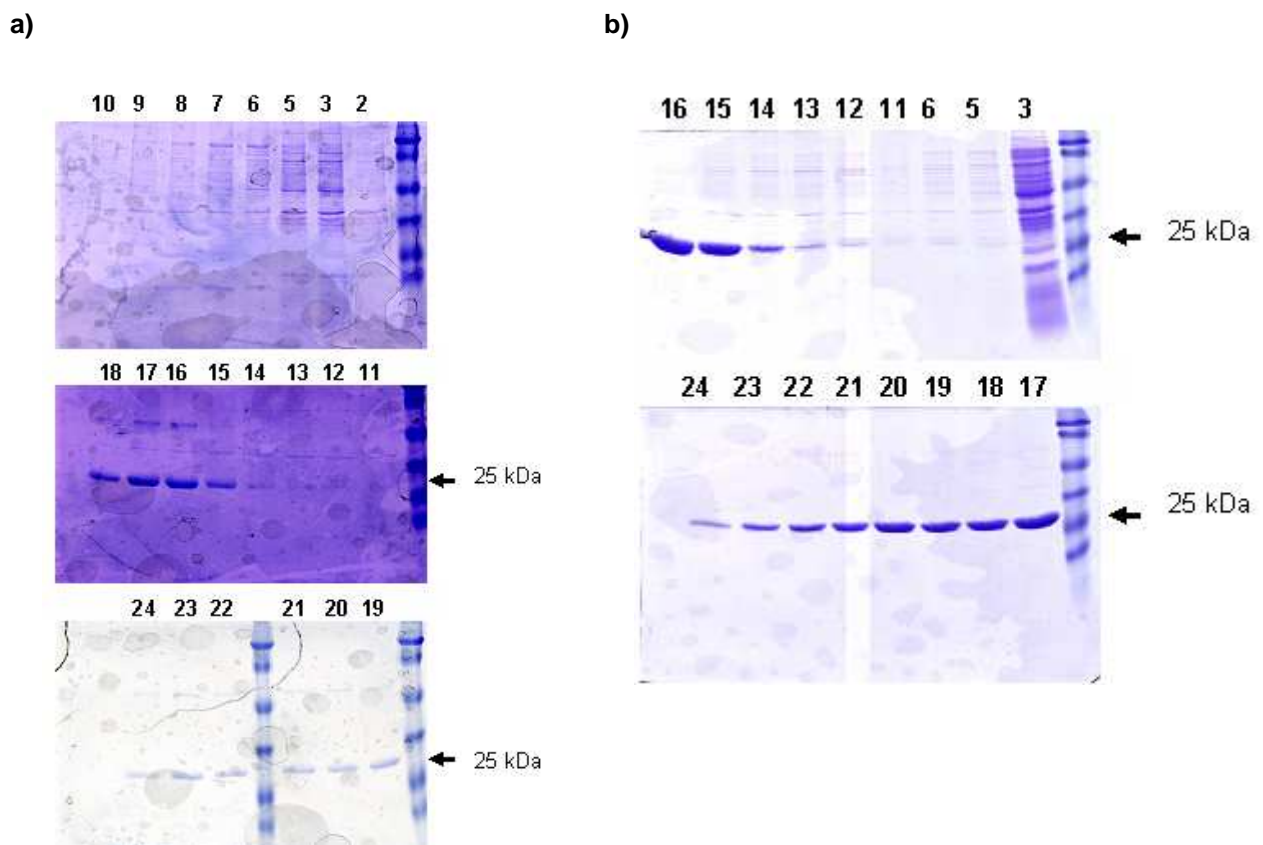


**Fig. 10. SDS-PAGE analysis of two representative examples of the purification/ isolation of the sEH phosphatase proteins, WT proteins (a) and D185N mutant proteins (b).** The presented SDS gels were loaded with all the fractions, which were collected during the metal chelate chromatography purification process. The proteins were separated on 12% polyacrylamide gel, coomassie stained and compared to a molecular weight standard. The lane numbers represent the numbers of the fractions that were collected during the purification process, (and marked in the chromatogram below). The 25 kDa sEH phosphatase band was detected from the 12<sup>th</sup>/ 13<sup>th</sup> sample onwards and evolved to a single clear band in parallel to the raise in the imidazol concentration. This phase corresponded to the third protein peak in the chromatogram (Fig. 11) and to the activity raise observed in the activity-screening test (Fig. 12).

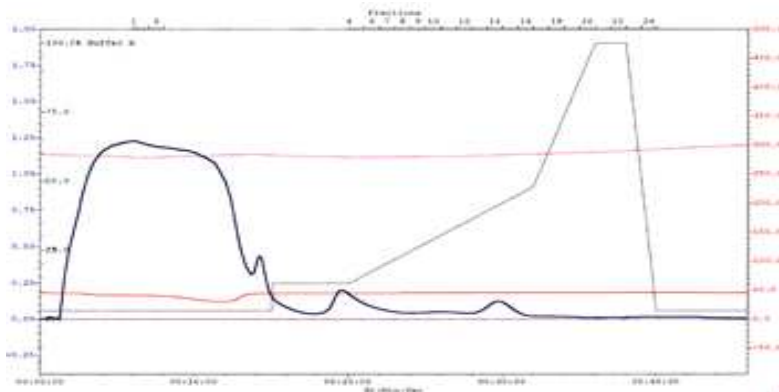
When examining the activity-screening results (Fig.12) of all the protein fractions that were collected for the WT and D185N mutant, a higher activity, compared to the blank was found in samples numbered 1-4. These samples corresponded to the first peak of proteins observed in the chromatogram, although the imidazol was at a sustained low concentration. Therefore, as expected, no clear band at the size of the sEH phosphatase was observed among the proteins/bands that appeared on the gels in lanes 2 and 3. Thus, the relatively higher activity observed in these fractions can be related to the dominant presence of bacterial phosphatases.

The second peak in the chromatogram, around fractions 6-9, showed no raise in O.D/ activity, and no clear band at the size of the sEH phosphatase on the gel.

The third peak of the eluted proteins appeared on the chromatogram around the 12<sup>th</sup> to the 20<sup>th</sup> fraction together with the linear raise of the imidazol. In parallel, a clear band at the expected size of 25 kDa began to appear on the gel at the 12<sup>th</sup>/13<sup>th</sup> (mostly around the 15<sup>th</sup>-21<sup>st</sup> fraction) and a significant higher phosphatase activity followed it accordingly. It could be therefore concluded that the band that was gradually isolated to be the only observed band, at a size of a 25 kDa consists of the sEH phosphatase.

In addition, it could be demonstrated that the chromatographic step clearly separated the human sEH phosphatase from the bacterial phosphatases.

a)



b)

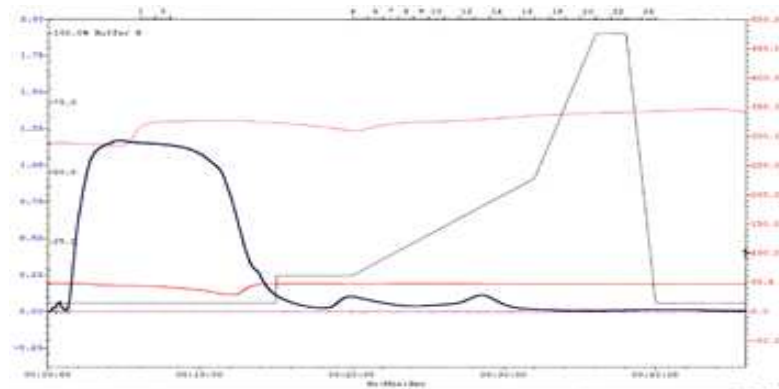


**Fig. 11. The “Run Report” (chromatogram) of the sEH phosphatase WT (a) and the D185N mutant (b) purification process as exhibited on the Bio-Logic Duo-Flow screen.** The elution of the recombinant proteins, tagged with (His)<sub>6</sub>, occurred from around the 12<sup>th</sup> sample (first peak from the right (blue line)) during the raise of the imidazol concentration (black line). Conductivity and acidity (red and pink lines) were kept relatively constant. Purification of all the rest of the different mutant proteins exhibited similar chromatograms implying of a proper and similar protein folding.

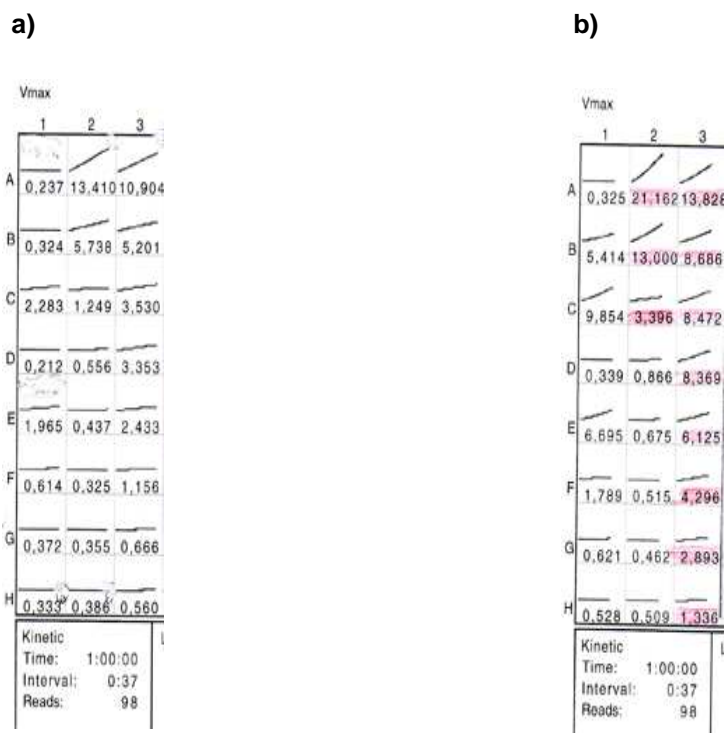


**Fig. 12. Activity-screening assay results of the sEH phosphatase WT proteins (a) and D185N mutant proteins (b) as appeared in the spectrophotometer print.** All fractions, which were collected during the purification procedure, were examined for phosphatase activity (product formation: 4-nitrophenol). The first square in a) and b) is the activity reading of the blank followed by the rest of the protein fraction readings in each of the other squares. A raise in activity was observed around the 12th sample (D2) and onwards for the WT proteins (a) and the D185N mutant proteins (b), corresponding to the elution and appearance of the sEH phosphatase band on the coomassie stained gels (Fig. 10), thereby supporting the identification of the sEH phosphatase containing fractions (and pointing out the active mutants).

As was written above the results presented here are representative examples, hence the other sEH mutant proteins were isolated in the same manner to more or less the same level of purity and showed same pattern of purification profile.

The chromatograms of the mutants were similar to the two chromatograms in Fig. 11. The coomassie gels of all the mutants exhibited a 25 kDa band that corresponded to the raise in the Imidazol concentration (during elution) and to the protein peak in the chromatogram. Similar behaviour upon chromatography of all examined active site mutants and WT proteins suggest that the proteins were similarly correctly folded, therefore, inactivity of a mutant could be later related to an involvement of the substituted amino acid in the catalytic process and not to a gross folding problem. Purification of most of the mutant proteins resulted in a main, clear, one band at the relevant lanes. Thus, altogether, WT and mutant proteins were successfully eluted and purified to a satisfying level for our needs. Subsequently, isolated sEH phosphatase-containing fractions of each mutant were pooled, concentrated and subjected to further investigations.

## 5.5 Characterization of the human sEH phosphatase mutants

### 5.5.1 Activity-screening assay

Following expression and purification of the human sEH phosphatase WT and mutant proteins, the biochemical properties of the 17 different sEH phosphatase mutant proteins and WT were initially examined by a phosphatase activity-screening assay. The activity-screening assay is a photometric assay that measures the formation of the product 4-nitrophenol (4-NP). During the activity-screening assay, all the fractions that were collected for each mutant during the purification process were scanned for product formation. The assay started with an addition of protein/ enzyme from each fraction to a reaction well that contained assay buffer and a substrate 4-nitrophenyl phosphate (4-NPP). Absorbance of the product was measured for one hour by the Spectromax-micrplate reader and presented by the spectrophotometer print, as shown in Fig. 11. The blank value (measured in wells that contain no enzyme/ protein fraction) was compared to the activity (absorbance) in other wells that contain the different protein fractions.

Detectable activity was revealed in 6 mutants out of 17: D11N, T123A T123N, N124A, N124D and D185N. The sEH phosphatase containing fractions in all of these mutants showed a higher activity values (to different extend) compare to the blank. As expected, the mutants mentioned above exhibited detectable activity in the same protein fractions, the ones that showed the highest purity of sEH phosphatase according to the coomassie stained polyacrylamide gels (usually the 15<sup>th</sup> to the 21<sup>st</sup> fraction). These fractions were collected for each of the “active” mutants, concentrated and further evaluated in kinetic activity measurements.

The other mutants, D9A, D9N, D11A, T123V, K160R, K160N, D184A, D184N, D185A, N189A, N189D, showed no detectable activity in their sEH phosphatase containing fractions.

### 5.5.2 Kinetic activity measurements and calculations

The sEH phosphatase mutants that exhibited any degree of activity in the phosphatase activity-screening assay were subjected to kinetic activity measurements and evaluations. After the sEH phosphatase containing fractions of each “active” mutant were pooled, concentrated and measured for their protein quantity, the collected sample (representing an “active” mutant) was examined in a photometric assay for product formation with different concentrations of substrate. In addition each assay was accompanied by two sub-assays that were done for scaling use: Absorbance of different concentrations of the model phosphatase substrate: 4-NPP and absorbance of different known concentrations of the product: 4-NP.

Table 2 summarizes the kinetic parameters calculated for the sEH phosphatase mutants and WT derived from the kinetic assay results (that measured the rate of catalysis at different substrate concentrations). The kinetic constants/ parameters that were calculated and presented in table 2 are  $K_m$  and  $V_{max}$ .  $V_{max}$  was chosen upon the  $K_{cat}$  parameter to represent the activity being in our view a more intuitive parameter (though  $K_{cat}$  was also calculated and presented in Table 4). The values of both parameters indicated in Table 2 are an average of at least three independent calculated measurements from separately purified protein batches.  $V_{max}$  is the maximal reaction rate /velocity and is termed limiting velocity. It is the velocity, which occurs at infinite substrate concentration and

can never be measured directly (but calculated). It is a direct measure of the enzyme's ability to convert a bound substrate to product and therefore presented in units of nmol of product divided to amount of enzyme in a well (mg) and to the duration of the catalysis reaction (the assay). The  $K_m$  is the substrate concentration that is needed to reach half-maximal rate or velocity ( $V_{max}$ ) and under certain conditions, it can describe the affinity of an enzyme to its substrate.

$V_{max}$  and  $K_m$  were calculated from the unprocessed kinetic assay results in four calculating techniques. The four techniques: **Lineweaver-Burk plot, Eadie-Hofstee plot, Hanes plot, and the direct linear plot** (see material and methods) are basically transforming the Michaelis-Menten equation to one that gives a straight-line plot by different algebraic conversions that result in an equation similar in structure to the straight-line equation ( $Y=MX+C$ ). Each one of the different calculating techniques has some advantages and disadvantages over the other. Not being sure which is the best method to choose (though the Lineweaver-Burk is the most popular method), the kinetic parameters were firstly calculated in all four techniques mentioned above (in Table 4, appendix) but only kinetic parameter results of the sEH phosphatase mutants and WT calculated in one chosen calculating method were compared to one another.

No significant differences were found between the results of the different calculated methods except for the ones calculated by the Lineweaver-Burk method. This difference was observed only when the enzyme was fully active, hence as the WT enzyme. When the first to the fourth concentration points were deducted from the Lineweaver-Burk plot, starting from the lowest concentration, the closer the result became to the expected  $V_{max}$  (according to the activity to substrate concentration graph) as can be seen in the Table 4 and in the calculation sheet detailed in material and methods. This is not surprising, as it is already known that there are relatively inaccuracies in the calculations for the lower concentration range in the Lineweaver-Burk method.

In Table 2 the average values of  $V_{max}$  and  $K_m$  were calculated by the direct linear plot method, which was the method of choice in this work, as it was the most recommended method in the literature (see discussion) though the most tedious one in practice (see 4.2.3.2 and 6.1)



**Table 2. The kinetic parameters obtained for WT and mutant sEH proteins.** Mutant and WT sEH phosphatase proteins were expressed, purified and analysed in a kinetic - photometric assay using different concentrations of 4-NPP as a substrate. The standard deviation was given for at least three independent measurements from separately purified protein batches. The kinetic constants presented here were calculated by the direct linear plot method by plotting velocity against substrate concentration (the method of choice, one of the four examined calculating methods). N.D.=not detectable, detection limit was determined to 1 nmol<sup>-1</sup> mg<sup>-1</sup> min. \* Significant changes in Km values (two-sided Student's t test) compared to the WT enzyme (D11N: P-value=0.016, N124D:P-value=0.016).

<b>ENZYME</b>	<b>Vmax (nmol<sup>-1</sup> mg<sup>-1</sup> min)</b>	<b>Km (mM)</b>
<b>WT</b>	<b>77.34 ± 8.77</b>	<b>1.3 ± 0.3</b>
<b>D9A</b>	<b>ND</b>	<b>ND</b>
<b>D9N</b>	<b>ND</b>	<b>ND</b>
<b>D11A</b>	<b>ND</b>	<b>ND</b>
<b>D11N</b>	<b>8.1 ± 3.9</b>	<b>0.54 ± 0.05 *</b>
<b>T123A</b>	<b>4.9 ± 3.3</b>	<b>1.03 ± 0.24</b>
<b>T123N</b>	<b>1.85 ± 0.3</b>	<b>0.80 ± 0.17</b>
<b>T123V</b>	<b>ND</b>	<b>ND</b>
<b>N124A</b>	<b>3.9 ± 2.2</b>	<b>0.95 ± 0.24</b>
<b>N124D</b>	<b>6.0 ± 1.0</b>	<b>2.7 ± 0.65 *</b>
<b>K160A</b>	<b>ND</b>	<b>ND</b>
<b>K160N</b>	<b>ND</b>	<b>ND</b>
<b>K160R</b>	<b>ND</b>	<b>ND</b>
<b>D184A</b>	<b>ND</b>	<b>ND</b>
<b>D184N</b>	<b>ND</b>	<b>ND</b>
<b>D185A</b>	<b>ND</b>	<b>ND</b>
<b>D185N</b>	<b>32.3 ± 15.3</b>	<b>1.9 ± 0.3 *</b>
<b>N189A</b>	<b>ND</b>	<b>ND</b>
<b>N189D</b>	<b>ND</b>	<b>ND</b>

The obtained values of the WT enzyme (Vmax-77.34 (nmol<sup>-1</sup> mg<sup>-1</sup> min), Km-1.3 (mM) are of the same order of magnitude as was previously found for the sEH phosphatase (Cronin et al., 2003). All the obtained kinetic results of the mutant proteins were compared to it.

As can be seen in Table 2 most of the 18 mutants (exchanges) were inactive or lost a major part of the enzyme's activity (vmax) in comparison to the WT enzyme, which is consistent with an important function in catalysis for the substituted amino acids. Loss of activity was unlikely to be due to a loss of structural integrity in any of the mutants since the WT and the mutated proteins had kept the same behaviour upon chromatography.

At least one of the exchanges of the amino acid candidates led to a completely inactive enzyme or to an enzyme with a strongly reduced activity. Part of the substituted amino acid candidates were standing the harsh criteria of exhibiting a completely inactive enzyme for all their alternative amino acid exchanges - to alanine or to an amino acid which is structurally similar to the one in the WT enzyme (an amino acid exchange to alanine was usually the non- conservative exchange except in the case of T123V): Both active- site mutations of Asp9 (D9), D9A and D9N, resulted in a complete loss of activity against 4-NPP, demonstrating that Asp9, the first of the two aspartates within loop1 (part of the DXDST motif), is crucial to the sEH phosphatase activity which fits very well the notion that Asp9 would participate in catalysis as a nucleophile. Additionally, all exchanges of amino acids Lys160

(motif 3), as well as Asp184 (D184) and Asn189 (N189) (motif 4) with non-functional amino acid residues resulted in a complete loss of enzymatic activity, proving their essential- vital function for catalysis.

Exchanges of several amino acids (Asp11 (D11), Thr123 (T123), Asn124 (N124) and Asp185 (D185)) resulted not only in an inactive enzyme but also in mutant proteins with retained activity - detectable activity to different extend (usually in exchanges that were considered characteristically similar to the WT). Amino acids of this group are also necessary for the catalysis process, though somehow less position sensitive due to their role in catalysis. Part of the exchanges that resulted in mutant proteins with detectable activity were accompanied with a significant change in the  $K_m$  values compare to the WT (marked in a star in Table 2). Our analysis show that the active site mutants of the second asparate in motif 1, Asp11 (D11), are on the contrary to the Asp9 (D9) mutants, either inactive (D11A) or strongly reduced (D11N) in their catalytic activity, with a significant twofold decrease in  $K_m$  (P-value-0.014, two-sided Student's test) compared to the WT enzyme. The Asp11 (D11) substitution results could be therefore in line with the possibility that Asp11 plays a possible role as a base-acid catalyst.

A substitution of Asp185 (D185) with alanine resulted in a completely inactive sEH phosphates, which is in line with the predicted role of Asp185 (D185) in coordination of the  $Mg^{2+}$  cation. On the other hand, a replacement with asparagine reduced the  $V_{max}$  of the enzyme to 40% while leaving the  $K_m$  unchanged. Substitution of T123A, T123N (T123V proved to be inactive) and both Asn124 mutations, resulted in proteins with significantly reduced catalytic activity compared to the WT enzyme while only the N124D mutant showed a significant twofold increase in  $K_m$ .

## 6 Discussion

### 6.1 The kinetic properties of the sEH phosphatase mutant proteins further characterize the catalytic mechanism of phosphorylation

Following site directed mutagenesis, the resulting WT and mutant sEH proteins were analysed for their kinetic properties. The kinetic-activity analysis showed among others that several amino acid exchanges led to a completely inactive enzyme. Some of the substituted amino acids resulted in an inactive mutant enzyme in all of their performed substitutions: D9A/N, K160R/N/A, D184A/N, N189A/D. Some of the substituted amino acids resulted in an inactive mutant enzyme in only part of their substitutions (usually in what was considered as the less conservative exchange): D11A, T123V, and D185A. The rest of these amino acids substitutions and all the Asn124 (N124) performed substitutions resulted in mutant enzymes with strongly reduced activity. These findings indicate as a whole, that all the investigated amino acids, which were suspected to be active site amino acids, are necessary in the catalytic mechanism and participate in forming the active site. Moreover, interpretation of the obtained kinetic determinants of the mutant enzymes that exhibited detectable activity could enlighten and specify the stages of the sEH phosphatase dephosphorylation process especially in the case of amino acid Asp11 (D11). The possible contribution to the catalytic process of each investigated amino acid or at least the correlation of our findings with other accumulated data is detailed in the following.

Altogether, the findings of this work approved the identity and the interactions of the active-site amino acids residues observed in the human sEH crystal structure using biochemical techniques (Gomez *et al.*, 2004) and are consistent with the crystal structure, which was elucidated during the work on this project. The 3D structure shows the magnesium to be nearly octahedral coordinated by Asp9, Asp185, the backbone oxygen of Asp11 (D11), two water molecules and the phosphate oxygen. This phosphate forms several hydrogen bond interactions with Lys160 (K160), Thr123 (T123), the backbone NH group and carbonyl oxygen of Asn124 (N124). These interactions can be viewed in Fig. 13 (section 6.3).

#### Asp9 (D9)

All exchanges of Asp9 (D9) in motif 1 resulted in inactive enzymes implying a vital role for Asp9 (D9). This supports the notion that Asp9 (D9) is the catalytic nucleophile of the sEH phosphatase which is much in line with the structural alignment done by Cronin *et al.*, (2003) and with some investigations that analysed the relation of sEH to other members of the HAD family (Burroughs *et al.*, 2006).

In continuation to this project, further biochemical investigations showed a direct phosphorylation of Asp9 during the catalytic cycle of the enzyme, proving Asp9 (D9) to be the catalytic nucleophile of the sEH active site (Cronin *et al.*, 2008). A direct identification of the phosphorylated intermediate by LC-MS/MS proved to be difficult and required firstly trapping of the very labile phosphorylated intermediate (the aspartylphosphates) by derivatisation with sodium borohydride resulting in corresponding alcohol homoserines. Only then, a distinguished difference (in mass shift) could be observed between the WT and the Asp9 (D9) mutant (which could not form an acylphosphate intermediate). The subsequent MS/MS fragment spectra further showed that the specific site of

modification in the sEH peptide is the Asp9 (D9), therefore proving the Asp9 (D9) to be the catalytic nucleophile.

### Asp11 (D11)

In some HADs, Asp11 (D11), the second Asp in loop 1 is replaced by threonine, tyrosine or alanine (Allen *et al.*, 2004). Accordingly, as can be seen in Fig. 5, Asp11 (D11) is not as well conserved as some of the other indicated amino acids. Therefore, requirement and nature of Asp11 (D11) and its function as a general acid / base catalyst were left questionable.

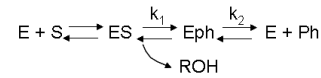
Results of this work proved an involvement of Asp11 (D11) in the dephosphorylation reaction. Moreover, the kinetic analysis showed that the mutants of Asp11 (D11) are inactive (D11A) or strongly reduced in their catalytic activity with a significant reduction in  $K_m$  (D11N), implying that Asp11 (D11) or Asp11 (D11) carboxylic side chain is specifically required and directly involved in catalysis which explains the strongly reduced  $V_{max}$ . This finding was found particularly interesting as it is not only challenging the doubts that were raised before concerning the necessity and art of Asp11 (D11) but also what was already observed in the human sEH crystal structure, showing that the Asp11 (D11) side chain is not directed to the reaction center but away from it (see Fig. 13), in contrary to what is expected from an amino acid/ amino acid side chain which is directly involved and absolutely required in catalysis.

A possible scenario that might explain/bridge on one hand the work results implying a direct involvement of Asp11 (D11) side chain in the dephosphorylation reaction and on the other hand, according to the human sEH crystal, the position of the Asp11 (D11) side chain directed away from the catalytic center structure, would be if Asp11 (D11) was able to undergo a substrate – induced conformational change as was observed for a homologous phosphoglucomutase (Lahiri *et al.*, 2002, 2003). Examination of Asp11 (D11) interactions (see Fig. 13) can suggest indeed that this scenario is possible. Asp11 (D11) interacts not only with the  $Mg^{2+}$  ion and the substrate phosphate oxygen through its backbone oxygen and NH groups but also obtains a hydrogen bond through its side chain with a water molecule coordinating the  $Mg^{2+}$  ion and with the side chain of the amino acid Arg99 (R99) which is part the cap domain. As the cap domain was already implicated in substrate recognition (Allen *et al.*, 2004, Lahiri *et al.*, 2004), it seems possible that with a quite flexible cap domain a substrate binding inducing a conformational change is feasible. Following this scenario, Asp11 (D11) side chain is able to participate in the catalysis, Asp11 (D11) could in the first step protonate the substrate leaving group of the substrate phosphate and in the second step it could activate solvent water (by deprotonation) that attacks the acylphosphate (enzyme phosphate intermediate) leading to hydrolysis (a rapid hydrolysis) of the enzyme phosphate intermediate and release of the phosphate group. A similar way of action for Asp11 (D11) operating in an acid / base –catalysed manner was already proposed for the PSP from *M. Jannaschii* (Wang *et al.*, 2002). Thus, according to the proposed scenario a replacement of the Asp11 (D11) side chain by asparagine or alanine will most likely interrupt Asp11 (D11) hydrogen bonds leading to conformational changes in the coordinating  $Mg^{2+}$  metal sphere (through the  $Mg^{2+}$  coordinating water molecule and the positioning of the cap domain), resulting in inability of the replaced amino acid to activate a water molecule (second step of the catalytic process) or directly protonate the substrate leaving group (first step of the catalytic process).

A further analysis of the kinetic results of the Asp11 (D11) mutants, as detailed below, supports the assumption that Asp11 (D11) is involved at least in the second step of the phosphorylation reaction. In particular, understanding the conditions that might lead to the obtained kinetic results of D11N - a

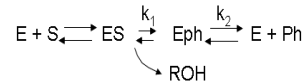
strong decrease in  $V_{max}$  and a significant reduction in  $K_m$  is a key factor in concluding the nature of the Asp11 (D11) involvement in the reaction.

The Michaelis constant  $K_m$  of the sEH dephosphorylation reaction, a reaction that involves a covalent intermediate



is  $K_m = K_d \times K_2 / (K_1 + K_2)$  where  $K_1$  describes the velocity of the acylphosphate formation and release of substrate (first step) and  $K_2$  describes the release of phosphate (second step).

When  $K_1$  is orders of magnitudes smaller than  $K_2$  ( $K_1 \ll K_2$ )



it becomes negligible and as can be figured out by the formula  $K_m$  equals then to  $K_d$ . This is the case described for the WT human sEH phosphatase (De Vivo et al., 2005);  $K_1$  is negligible in comparison to  $K_2$  so that the first step becomes the rate limiting step in the reaction. When  $K_m$  equals  $K_d$  ( $K_m = K_d$ ) in a reaction where the first step is the rate limiting step ( $K_1 \ll K_2$ ), the  $K_m$  can be a measure of affinity as in the case of the WT/ sEH phosphatase enzyme or other enzymes that obey the condition ( $K_1 \ll K_2$ ) (which practically means that the  $K_m$  values calculated for a certain enzyme with different substrates could be used as an affinity measurement and be compared between the different). We assume that if a mutant of the WT phosphatase is affecting/disturbing the enzyme activity through the first step of the reaction ( $K_1$ ), which is already considered the rate limiting step of the WT phosphatase, no significant change in  $K_m$  would be observed though the  $V_{max}$  would decrease. A glimpse at the Michaelis constant  $K_m$  equation in the case of  $K_1 \ll K_2$  ( $K_m$  resolves to  $K_d$ ) can approve the latter description for the hypothetical mutant.

What are the consequences in the opposite case, when a mutant is affecting/disturbing the enzyme activity through its second step, in a way that the second step of the reaction slows down and becomes a rate limiting step, where  $K_2$  ( $K_2 \ll K_1$ ) is much smaller than  $K_1$  (which is already small being the rate limiting step of the WT enzyme/phosphatase). According to the  $K_m$  equation written above,  $K_m$  will resolve to  $K_m = K_d \times K_2 / K_1$  which obviously means an expected reduction in  $K_m$ .

Hence, a mutation that affects/disturbs the enzyme's activity through a strong affect on the second step of the reaction (to a level of a rate limiting step) will result not only in a significant  $V_{max}$  reduction but also in a significant decrease in  $K_m$ . Such a reduction, has been seen in the D11N mutant. Therefore it can be assumed that in the case of D11N mutant as was described above for a hypothetical phosphatase mutant, the second step of the catalytic cycle is affected, it is blocked and the remaining activity is only due to a spontaneous hydrolysis of the acylphosphate. It could be additionally assumed that a mutant protein showing a  $V_{max}$  smaller than that of the D11N would imply an impairment of the first reaction step.

Although, following a replacement of aspartic acid with asparagine the D11N mutant is not supposed anymore to activate solvent water (second step) or to directly protonate the leaving group of the substrate (first step), a change in  $K_1$  (first step) would not be recognized when  $K_2$  becomes rate limiting. Therefore Asp11 (D11) affect on the first step of the reaction (and not only on the second step of the reaction) is possible. It was therefore concluded that Asp11 (D11) is involved at least in the second step of the dephosphorylation reaction (assisting in the hydrolysis process of the intermediate). In addition, no further indication could be obtained from the D11A mutant protein as its activity was completely lost therefore no  $K_m$  could be measured and interpreted for the way the mutant enzyme (or the replaced amino acid, Asp11 (D11)) might have affected the catalytic reaction. Thus, Asp11 involvement in the acid-catalysed substrate release (first step) is left possible. The D11A loss of activity might be then explained in the level of impaired  $Mg^{2+}$  and phosphate coordination and

interruption of the hydrogen bridges to R99 which strongly disturbed the positioning of the cap domain and the  $Mg^{2+}$  coordinating water.

Further biochemical studies (measurements of homoserine formation by LC-MS / MS analysis after reduction with borohydride (Cronin *et al.*, (2008)) indicated that the hydrolysis of the acyl intermediate is most likely slowed down in the D11N protein mutant compare to the WT. In the WT phosphatase, the homoserine formation most likely competes with the rapid hydrolysis of the acylphosphate facilitated by Asp11 (D11), and therefore the homoserine formation is only detectable in the mutated Asp11 protein where the hydrolysis of the acylphosphate intermediate is slowed down. This supports again the notion that Asp11 (D11) is involved in the second step of the reaction, hydrolysis of the covalent enzyme acylphosphate intermediate.

### **Tht123 (T123), Asn124 (N124)**

Both substitutions of Asn124 (N124) and two of the three substitutions of Thr123 (T123), T123A and T123N, resulted in a strongly reduced catalytic activity, 2 – 8% of the WT activity, except for the T123V mutant that was completely inactive. Although the exchanges of the Asn124 (N124) and Thr123 (T123) resulted in a reduced  $V_{max}$  in a factor of 13 to 40 the  $K_m$  only varied in a factor of not greater than 2. As was described before mutant proteins that show a smaller  $V_{max}$  than the  $V_{max}$  obtained for the D11N proteins in combination with unchanged or an increased  $K_m$ , are likely to show an altered first and second step of the reaction cycle, suggesting that both examined amino acids, Thr123 (T123) and Asn124 (N124), are involved in substrate positioning and phosphate turn-over. As the phosphate and the  $Mg^{2+}$  ion are multiply coordinated by few other active site amino acids and water molecules, the effect of the Thr123 (T123) substitutions, T123A and T123N mutants, showing a detectable residual activity, might have been compensated by other components of the active site or water molecules. Opposed to T123A/N, the mutant protein T123V was completely inactive being probably structurally slightly more impaired affecting the phosphate positioning. As in the case with T123N/A the Asn124 (N124) exchanges might have been compensated by other components of the active site or water molecules therefore showing a detectable activity though residual in all Asn124 (N124) selected exchanges. This might be expected when the connections of Asn124 connections are examined, as Asn124 (N124) forms hydrogen bonds with the phosphate oxygen through its backbone NH and CO groups. Thus, Asn124 (N124) is probably needed for a proper catalytic activity but not essential as expected from an amino acid that its exchanges lead to an impaired backbone conformation.

### **Lys160 (K160)**

Amino acid Lys160 (K160) in motif 3 was expected to have a vital role in substrate positioning within the active site, due to the lysine charged side chain that strongly interacts with the substrate-phosphate moiety. The activity assay results of K160N and K160R, supports this assumption. Both mutants K160N and K160R showed a total loss of activity, even though that the exchange to arginine is just an exchange to another basic amino acid (a relatively conservative exchange). Moreover, the K160A mutant failed to express which implies that, amino acid Lys160 (K160) is not only vital in the maintenance of the active site and the operation of the catalysis process but also in keeping the integrity of the whole protein structure.

### **Asp184 (D184)**

All exchanges of Asp184 (D184) in motif 4 (loop 4) with non-functional amino acids, resulted in a complete loss of activity, confirming the amino acid essential function in catalysis. The 3D structure

shows that Asp184 forms hydrogen bonds to Lys160 (K160) and to solvent water that coordinates the divalent  $Mg^{2+}$  cation (Fig. 12). Both interactions are probably needed to shield the charge of the phosphoryl group while being attacked by the catalytic nucleophile, therefore the loss of these interactions was probably the cause for the complete loss of activity in mutants D184A and D184N.

### **Asp185 (D185)**

Asp185 (D185) is the second Asp in motif 4. An exchange of Asp185 (D185) with alanine resulted in a completely inactive mutant enzyme, whereas the exchange of Asp185 (D185) with asparagine, which is structurally similar to aspartic acid but uncharged (a relatively conserved exchange), resulted in a partly active enzyme. One possible explanation might be that the mutant protein D185N was initially inactive and slowly regenerated itself after some time to an active enzyme by deamination, as it was shown for the epoxide hydrolase from *aspargillus niger* (Arand *et al.*, 1999) and for the glutamate dehydrogenase (Joshi *et al.*, 2002), after replacement of the catalytic nucleophile aspartic acid with asparagine. This possibility was examined in later biochemical investigations made in our lab by MS analysis of tryptic peptides derived from the sEH phosphatase mutant Asp185 (D185), but no such self-regeneration-activation of the D185N mutant was detected (Cronin *et al.*, 2008). The complete loss of activity of D185A protein mutant and the partly loss of activity of the D185N protein mutant proved the necessity of Asp185 amino acid in the catalytic process. Any replacement of Asp185 (D185) with a non-functional amino acid would interfere with the  $Mg^{2+}$  ion coordination sphere which would alter the enzyme activity in the first step of catalysis.

The replacement of Asp185 (D185) with asparagine in contrary to the replacement with alanine did not result in a complete loss of enzyme's activity, retaining almost 40% of the activity. This might be due to the similar structural characteristics of Asp and Asn (though uncharged) and the ability of Asn to compensate the presence of Asp with the two uncoupled nitrogen electrons. Asp185 (D185) can therefore be considered to be less position-sensitive compared to other amino acids where exchanges to a relatively characteristically similar amino acid (a conservative exchange) resulted in a complete loss of activity.

### **Asn189 (N189)**

Both exchanges of Asn189 (N189) with non-functional amino acids resulted in a complete loss of enzyme's activity, demonstrating an important function for Asn189 (N189) in catalysis. The exchange of Asn with Asp introduced an additional charge that could have increased the electrostatic repulsion of the three aspartates, thereby, interfering with the enzyme activity. A replacement of Asn189 (N189) could in general strongly interfere with the catalytic activity in a sequential way by disturbing the hydrogen bonds with Asp184 (D184) leading to a conformational change affecting the hydrogen bridge that Asp184 (D184) has with one  $Mg^{2+}$ -coordinating solvent water that further stabilizes Lys160 (K160).

### **The amino acids in loop/motif 4**

It is unique to sEH that all three amino acid residues (Asp184 (D184), Asp185 (D185), Asn189 (N189)) from the conserved motif in the metal binding loop 4 are needed to stabilize the active site, whereas, usually in HAD's, only two aspartic acid residues seem to be critical in loop 4 (Burroughs *et al.*, 2006).

### **Additional biochemical results that contributed in elucidating the sEH phosphatase catalytic mechanism using the WT sEH phosphatase and same mutant proteins**

In the work of Cronin *et al.*, (2008) the dephosphorylation reaction was further analysed by  $^{18}O$  incorporation and liquid mass chromatography – tandem mass spectrometry (LC –MS/MS). During the second step of the reaction cycle, the covalent enzyme acylphosphate intermediate is hydrolysed via



a nucleophilic attack by an activated water molecule either on the phosphorous atom of the phosphate moiety or at the aspartate carbonyl. If the site of attack is the phosphorous,  $^{18}\text{H}_2\text{O}$  would lead to incorporation of  $^{18}\text{O}$  into the phosphate leaving group. In contrast, if the  $^{18}\text{H}_2\text{O}$  binds to the aspartic acid carbonyl, an incorporation of  $^{18}\text{O}$  into the D9-containing sEH peptide would be detectable due to a small mass shift after one or two catalytic turnovers. Thus, phosphorylation of the WT sEH with 4-NPP in the presence of  $^{18}\text{H}_2\text{O}$  and subsequent analysis of the resulting peptides after by LC-MS/MS revealed that the nucleophilic attack occurs at the phosphorous, as no incorporation of  $^{18}\text{O}$  was detectable in the corresponding peptides.

Other biochemical results which completed or supported the interpretation of the kinetic results of D9A/N and D11N were indicated before under the results analysis of Asp9 (D9) and Asp11 (D11).

## 6.2 The deduced enzymatic reaction mechanism

A combined data of the results analysis of this work, the 3D structure (Gomez *et al.*, 2004), the structural and mechanistic similarities between the HAD members and the results of further biochemical investigations obtained later led to a presentation of a dephosphorylation reaction mechanism for the sEH phosphatas, detailed in the following.

The dephosphorylation reaction cycle of the enzyme includes a sequence of reactions:

Phosphorylation of the enzyme occurs as a result of a nucleophilic attack of the substrate phosphorous by the active site nucleophile, Asp9 (D9), leading to formation of an enzyme phosphate intermediate complex (a covalent enzyme acylphosphate intermediate). In the second step, a nucleophilic attack on the phosphorous atom of the phosphate moiety by a water molecule that is activated by Asp11 (D11) leads to hydrolysis of the enzyme phosphate intermediate, resulting in a release of the phosphate group from the enzyme and freeing the active site to the next coming phosphorylated substrate.

In Fig.13 an illustrated description of the active-site complex and the enzymatic reaction mechanism is presented. The first step of the catalytic cycle consists of a nucleophilic attack by the Asp9 (D9) on the substrate phosphoester group under formation of phosphoenzyme intermediate, supported by the absolute requirement of Asp9 (D9) for activity and by LC-MS/MS analysis showing phosphorylation of Asp9 (D9). The protonation of the substrate living group is likely provided by the side chain of Asp11 after it passes a substrate-induced rearrangement together with the cap domain. Another possibility is that acidified solvent water molecule would donate a proton to the substrate.

In the second step of the reaction cycle, the covalent intermediate is hydrolysed via a nucleophilic attack by D11-activated solvent water on the phosphorous atom. The role of Asp11 (D11) in the second step of the catalysis was strongly supported by the results of the kinetic analysis of the D11N mutant as detailed before and was additionally supported later by a LC-MS/MS analysis.

All of the other amino acids examined were proven in this work to be essential for the catalytic process, probably by substrate and / or  $\text{Mg}^{2+}$  binding, maintaining the active site complex stable and in the right position/ coordination for the performance of the catalytic reaction as described before for each of the amino acids (Thr123 (T123), Asn124 (N124), Lys160 (K160), Asp184 (D184), Asp185 (D185), Asn189 (N189)) in the kinetic analysis (section 6.2).

All in all, the presented findings support a mechanism that is in line with the catalytic scaffold described for HAD phosphotransferases and proves unexpectedly an involvement of Asp11 in the dephosphorylation process.

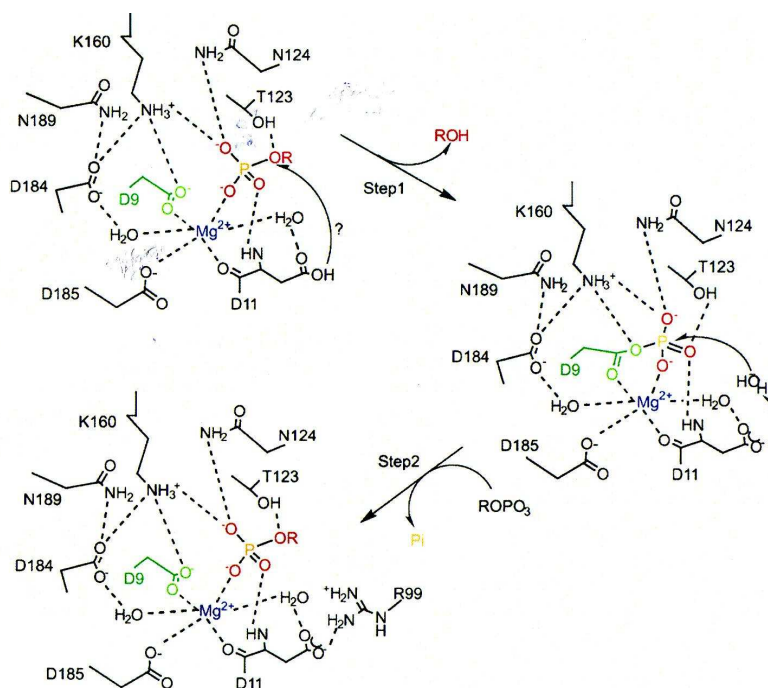


**Fig. 13. The deduced enzymatic mechanism of phosphate hydrolysis by the sEH phosphatase and a schematic view of the catalytic complex.** In the first step of the catalytic cycle of dephosphorylation, the active-site nucleophile Asp9 (D9) attacks the substrate phosphorous under formation of covalent enzyme acylphosphate intermediate and release of the dephosphorylated substrate. In the second step, the enzyme phosphate intermediate is hydrolysed via a nucleophilic attack of the phosphorous atom by a water molecule activated via proton abstraction by Asp11 (D11). The phosphate group is released and the enzyme is regenerated.

### 6.3 Comparison between the activity results of the sEH phosphatase active site mutants and the activity results of the active site mutants of few other HAD enzymes

The presented comparison was based on a comparison that was already made between three HAD enzymes: phosphoserine phosphatase (PSP)  $\text{Ca}^{2+}$ ATPase, and *Pseudomonas* sp. haloacid dehalogenase (Dehal.) by Kollet *et al.*, (1999). In order to compare the results of the active site mutants of the three HAD enzymes to the ones of the sEH phosphatase, the equivalent substituted amino acids of all the enzymes had to be at first matched. The sequence alignments in Table 3 assisted in matching these amino acids. The sequence alignments were taken from Collet *et al.*, (1999), based on the work of Koonin and Tatusov (1994) and Aravind *et al.*, (1998), the sEH phosphatase sequence was taken from Cronin *et al.*, (2003). It should be noticed that the search for equivalent mutants had also to consider the type or degree of substitution (by means of conservative or non-conservative substitution).

**Table 3. Sequence alignments of the sEH phosphatase and three other HAD enzymes (PSPase, ATPase, Dehal.).** The alignments revealed the parallel location of the conserved or partly conserved amino acids (marked in red) that were gathered in three conserved motifs. Most of the marked amino acids (suspected to be active-site amino acids) were substituted (see Table 4), thereby assisting in matching the different mutants of the four enzymes.

		Motif 1		Motif 2		Motif 3			
sEH phos.	7	FDLDGVL	106	LTNTW	32	V KPE	19	FLDDIGA NL	32
PSPase	19	FDVDSTV	82	I SGGF	43	GGKGK	16	IGDGATDM	184
ATPase	350	SDKTGTL	266	I TGDN	53	SHKSK	14	TG DGVNDA	707
Dehal.	9	FDLYGTL	101	LSNGS	27	VYKPD	20	VSSNAWDA	181

Matching the mutants in which their substituted amino acids were originated in motif 3 was not a straightforward task (see Table 3, three options for matching motif 3 amino acids), therefore few possibilities were indicated in Table 4 for motif 3 mutants.

**Table 4. A comparison table of the activity results of the active site amino acid mutants of the sEH phosphatase and three other enzymes of the HAD superfamily.** The sEH results were added to the original table taken from Collet et al (1999). Each sEH phosphatase mutant was compared, if possible, to its equivalent mutant in each one of the other enzymes. Few matching possibilities were indicated in the table for the sEH mutants in motif 3.

sEH phosphatase		Phosphoserine phosphatase		Ca <sup>2+</sup> ATPase		Haloacid Dehalogenase	
Mutation	Hydrolytic activity (%WT)	Mutation	Hydrolytic activity (%WT)	Mutation	Hydrolytic activity (%WT)	Mutation	Hydrolytic activity (%WT)
None (WT)	100	None (WT)	100	None (WT)	100	None (WT)	100
<b>Motif 1</b>		<b>Motif 1</b>		<b>Motif 1</b>		<b>Motif 1</b>	
		D20E	0	D351E	0	D10E	0
D9N	0	D20N	0	D351N	0	D10N	0.42
D9A	0					Y12F	40
		D22E	50	T353S	20		
D11N	10	D22N	0	T353A	0		
D11A	0						
<b>Motif 2</b>		<b>Motif 2</b>		<b>Motif 2</b>		<b>Motif 2</b>	
T123N	2	S109T	115	T625S	79		
T123A	5	S109A	6	T625A	Low Exp.	S118A	30
T123V	0						
N124							
<b>Motif 3</b>		<b>Motif 3</b>		<b>Motif 3</b>		<b>Motif 3</b>	
K160R	0	K158R	1			K151R	0.03
		K158A	<0.4				
K160N	0						
D184A	0	G178A	74	G702A	20	S175A	0.07
	0	D179E	78	D703E	31	S176A (D185A/D184A sEH)	92
D184N/D185N	0/ 40	D179N	0.6	D703N	<5		
		G180A (D185A sEH)	15 0			N177D (D185N sEH)	0 40
		D183E	63	D707E	<5	D180E	0.1
N189D	0	D183N	<0.4	D707N	<5	D180N/S/G	0
N189A	0						

Altogether, the comparison showed similar results for the equivalent active site mutants of all the enzymes. Amino acids that were firstly suspected and later proved to be part of a (common) catalytic mechanism in all of the four enzymes, managed to stand the stringent requirement of reduction of activity also in what can be considered as a conservative exchange (like Asp to Asn). As expected, the comparison emphasized the importance of the conserved and relatively conserved amino acids in the common catalytic mechanism of all four enzymes. The comparison could support future analogy regarding the catalytic mechanism/ triad of any other member or candidate member of the HAD superfamily, that is found with similar motifs. The results of the equivalent mutants show the same tendency and the small differences between the relatively equivalent mutants are acceptable being part of differences that are expected to be found between enzyme members of a superfamily. In addition, the comparison simply supports the selection that was initially made of the sEH amino acids as candidates for being active site amino acids and for substitution to non-functional amino acids.

#### **6.4 Current knowledge on the sEH phosphatase (other than the catalytic mechanism) and possibilities for further investigations**

It is known that within each superfamily, considerable structural diversity is generated by the attachment of regulatory and targeting domains and/or subunits to the protein catalytic domain. Regulatory subunits and domains serve to localize the protein to particular sub cellular localization and modulate protein specificity and activity, for example through second messengers (Lodish *et al.*, 2001). As the catalytic mechanism of the sEH phosphatase has been rather elucidated with the contribution of this work and further investigations (e.g., Cronin *et al.*, 2008), it seems that in the area of catalytic mechanism, what is left to be investigated is related to the regulation processes that govern the sEH phosphatase activity.

The physiological role of the phosphatase activity is not yet clear as well as other points that are associated with a role, the sEH phosphatase substrates and the way the enzyme operates as a bifunctional enzyme. These research topics are considered nowadays to be very appealing as they present a potential therapeutic application, due to the involvement of the epoxide hydrolase in hypertension (Fang *et al.*, 2001, Imig *et al.*, 2005) and in a growing number of pathologies as inflammatory diseases (Liu *et al.*, 2005, Schmeltzer *et al.*, 2005, Inceoglu *et al.*, 2006), pain, diabetes and stroke (Ohtoshi *et al.*, 2005, Schmelzer *et al.*, 2006, Zhang *et al.*, 2007).

##### **Substrates**

There is still much to investigate in the area of the sEH phosphatase substrates, mainly of the endogenous, physiological substrates. The enzyme has been shown to accept lipid phosphates as substrates and therefore a role in lipid metabolism was suggested for the sEH phosphatase. In the first work, which investigated the sEH phosphatase substrates, Newman *et al.*, (2003), assuming a functional association between the two catalytic sites, rationalized dihydroxy lipid phosphates as potential endogenous substrates. A series of phosphorylated hydroxyl lipids were therefore synthesized and found to be excellent substrates for the human sEH. Thus, dihydroxy lipid phosphates were suggested as possible endogenous substrate candidates for the sEH phosphatase, which would represent a novel branch of fatty acid metabolism (fatty acid epoxides) with potential signalling functions. In a later work, isoprenoid phosphates were identified as substrates for the sEH

phosphatase, supporting a possible connection of the sEH phosphatase to lipid metabolism or cholesterol biosynthesis (Enayetallah *et al.*, 2006).

The sEH phosphatase belongs to the HAD class 1 subfamily of phosphotransferases that contain a small cap domain and therefore tend to small phosphate substrates (Kuznetsova *et al.*, 2006). Nevertheless, it has been shown that some HADs can accept both small substrates (as by prokaryotic HADs) and larger substrates like proteins (as by HADs of higher organisms) (Peisach *et al.*, 2004). Same phenomenon was shown for other enzymes like the tyrosin phosphatase and the tumour suppressor PTEN that can act on both polypeptide and phosphoinositide phosphates (Lee *et al.*, 1999). Due to the diversity in substrate acceptance within the HAD superfamily and to the possibility of a diversity of substrate acceptance within one HAD's enzyme itself, it might be that the sEH phosphatase is playing an additional role to the one implied above, broadening by that the possibilities for substrate and role investigations.

### **The bifunctional character of the human sEH**

The bifunctional character of the human sEH implies that the sEH may have a regulatory function in connection with the epoxide hydrolase activity, though it is not yet known how the sEH operates as a bifunctional enzyme, on which level the two catalytic sites communicate, and how they combine their actions to one role. The role might be one that is already known for the epoxide hydrolase or a role that is not yet known.

In the work of Cronin *et al.*, (2003), it was suggested with analogy to the P-type ATPase that the phosphatase domain might regulate the activity of the sEH domain via a conformational rearrangement. However, results of activity experiments with substrates and inhibitors of both catalytic sites showed that direct interaction of the two active sites does not seem to take place, which is probably expected due to the large distance between the sEH and the phosphatase active centers. Thus, the way that the sEH operates as a bifunctional protein is still left open.

The sort of communication mechanism between the two catalytic sites of the sEH might be one of three different known types of active sites communication mechanisms (detailed below), as was already found for few other bifunctional enzymes that are relatively close to the sEH, the trehalose 6-phosphate synthase/ trehalose 6-phosphate phosphatase (a member of the HAD superfamily of enzymes) (Collet *et al.*, 1998) and the mammalian epoxide hydrolase Leukotriene A4 hydrolase (LTA4H)/ aminopeptidase (Chen *et al.*, 2004)

- 1) Two active sites, which are catalyzing consecutive reactions of a metabolic pathway and exhibiting substrate channelling. The clear advantage seems to be by having (for the second reaction in a row) a higher catalytic rate, achieved by lowering the time of diffusion, the time in which an enzyme encounter substrate in solution (as the substrates and products are confined in a limited volume)
- 2) Active sites of one protein that are catalyzing consecutive reactions without substrate channelling
- 3) Enzymes (active sites) that are catalyzing opposed reactions (Nagradova, 2003).

Considering the points written above and the results showing that the epoxide hydrolase of the sEH accepts lipid epoxide while the phosphatase of the sEH accepts lipid phosphates as substrates, it could be speculated that the sEH as a whole protein (the two active sites together) are involved in balancing levels of lipid mediators. Likewise, it is also possible that the sEH phosphatase is involved in regulation of any of the roles, which are already known for the epoxide hydrolase, especially in light of the possibility that the sEH phosphatase could accept diverse substrates. This again leaves a wide area for further investigations, which will enlighten the physiological interplay of the two sEH activities.

Regarding the cooperation of the two activities/ active sites it is suggested here (see below) that the sEH phosphatase active site in cooperation with the epoxide hydrolase active site is involved in regulation of blood pressure which is already a known role for the sEH (the epoxide hydrolase activity).

#### **6.4.1 A suggestive role for the sEH phosphatase in regulation of blood pressure through the eNOS enzyme**

We have speculated, that the enzyme eNOS and the sEH phosphatase function together in regulation of blood pressure. Blood pressure regulation is a complex system as it is regulated in different organs and through different pathways, which one of them is via the NO synthase (NOS) activity. The enzyme NOS has three isoforms that form NO. The endothelial NOS (eNOS) is the isoenzyme, which is particularly involved in regulating blood pressure (and in vascular remodelling and angiogenesis). The generation of NO by eNOS was proved to serve as a classical endothelial-derived relaxing factor that dilates blood vessels (Kurihara *et al.*, 1998), in contrary to the effect of the epoxide hydrolase activity of the sEH. eNOS is activated in two ways: It can be activated through receptors by a variety of receptor agonists in a Ca<sup>2+</sup> dependent manner or it can be activated by sheer stress, produced by flowing blood (the most important physiological pathway for eNOS activation), probably in a Ca<sup>2+</sup> independent fashion.

Lately, it has been reported, that eNOS is activated by sheer stress through phosphorylation of its Ser-1177 by kinase Akt/PKB. Inactivation by dephosphorylation is done by an unknown phosphatase (Dimmeler *et al.* 1999).

Knowing that sEH has been detected in endothelial cells and thus, localized in the same cell type as the eNOS (Fang *et al.*, 2001), makes the sEH phosphatase a very interesting candidate for being the Ser-1177 phosphatase, counteracting the activation of eNOS induced by sheer stress. This hypothesis implies that the sEH phosphatase activity is downstream to the NO synthase activity in regulating blood pressure and that the phosphatase domain of the sEH plays a synergistic role with the EH in regulation of blood pressure (as was already described for the epoxide hydrolase in the introduction: 2.3.1). It is not clear, if the synergistic role of both enzymes, the epoxide hydrolase and the phosphatase follows the communication patterns already known for bifunctional enzymes (see section 6.4). It might be that finding a role for the sEH phosphatase (as in regulation of blood pressure according to the hypothesis above) will lead to finding a new way of communication and action for bifunctional enzymes.

### **6.5 Processing the kinetic assay results: via which technique should the kinetic determinants be calculated?**

Four possible techniques for calculating the kinetic determinants, V<sub>max</sub> and K<sub>m</sub>, out of the kinetic assay results were used and compared. Obviously, the difference between the WT V<sub>max</sub> and K<sub>m</sub> the V<sub>max</sub> and K<sub>m</sub> of the different mutant proteins should be evaluated by comparing the calculated values obtained by one calculating technique.

According to the literature, it was not very clear which the best calculating technique is. It was therefore decided initially, to calculate the kinetic determinants in four well-established possible

techniques and only then to decide which one technique is best to follow. Based on the calculated results obtained from that technique, interpretations of results would be performed. In the following, the advantages and disadvantages of each of the methods used are discussed.

Undoubtedly the **Lineweaver-Burk** (L.-B.) method is the most popular and familiar technique for calculating kinetic parameters. Its familiarity gives the technique a great advantage as many biochemists and people from other disciplines will probably know and easily understand the method. In addition, the understanding of the plot is more intuitive and more obviously related to the velocity versus substrate concentration curve from which it was observed, because the substrate concentration and velocity are plotted on separate axes. Against all that, and most important in this case, is that L.-B. is probably the worst method to use for determination of kinetic parameters ([www.bio.paisley.ac.uk/kinetics/ chapter\\_2/contents\\_chap2.html](http://www.bio.paisley.ac.uk/kinetics/chapter_2/contents_chap2.html)). It has some real drawbacks in dealing with data containing significant experimental error. The L.-B. plot exaggerates the error at a low substrate levels where measurements are often less accurate as velocities are lower. A good example for that could be recognized when the  $V_{max}$  of the WT (WT1 and WT 2) was calculated by the L.-B. method. When all the different (eight) substrate concentrations which were used in the assay as required, for calculating the  $V_{max}$  of the WT resulted in an unreasonable  $V_{max}$  value. The obtained  $V_{max}$  was then much higher than expected (from the activity (velocity) versus substrate concentration curve). Deletion of the lowest substrate concentrations from the plot resulted in a more reasonable values for the  $V_{max}$ . This kind of manipulation was not necessary when  $V_{max}$  values were calculated by other calculating techniques.

By the **Eadie-Hofstee** (E.-H.) calculating technique the error is not as severe as in the L.-B. plot and it is generally regarded as being a better technique. The problem with the E.-H. plot is that the figures are plotted on the horizontal axis, which should be for the independent data, but the data plotted on the E.-H. horizontal axis is not truly independent as it contains an element of the velocity of the reaction, therefore any error, which occurs in the experiment, will be present on both axes. Nevertheless, the calculations obtained with this method were reasonable and quite similar to the ones from the Hanes plot.

The **Hanes** plot is probably the most recommended method compare to the L.-B. Moreover, the E.-H. method copes with errors (experimental errors are almost impossible to avoid) much better than the commonly used L.-B., and avoids the difficulties of velocity being included in the independent axis as by the E.-H.

The **Direct Linear** plot is different from the other three methods (see in material and methods 4.2.3.2). It was originally designed to be carried out in the lab while the assay is in process, as it requires only a graph paper and no calculations are needed for plotting the graph. It gives a direct read out of both  $K_m$  and  $V_{max}$ . It copes very well with error particularly with outliers who are obviously far from the correct value and gives a very good indication of where the error lies. In this work the direct linear plot results were obtained by using the excel program (see materials and methods 4.2.3.3). Although the calculations are quite tedious (which is the method's only clear disadvantage), the results obtained in this methods are reliable, straight forward and compatible to the expected  $V_{max}$ .

## 7 References

- Altschul, S. F., Madden, T. L., Schaffer, A. A., Zhang Z., Zhang, A., Miller, W. and Lipman D. J., 1997. Gapped BLAST and PSI-BLAST: a new generation of protein database search programs. *Nucleic Acids Res.* 25, 3389-3402.
- Arand, M., Kneht, M., Thomas, H., Zeller, H.D. and Oesch, F., 1991. An impaired peroxisomal targeting sequence leading to an unusual biocompartmental distribution of cytosolic epoxide hydrolase., *FEBS Lett.* 294: 19-22.
- Arand, M., Grant, D. F., Beetham, J. K., Friedberg, T., Oesch, F. and Hammock, B. D., 1994. Sequence similarity of mammalian epoxide hydrolases to the bacterial haloalkane dehalogenase and other related proteins-Implication for the potential catalytic mechanism of enzymatic epoxide hydrolysis, *FEBS Lett.* 338: 251.256
- Arand, M., Wagner, H., Oesch, F., 1996. Asp333, Asp495, and His523 form the catalytic triad of rat soluble epoxide hydrolase. *J Biol Chem.* 271(8):4223-9.
- Arand, M., Müller, F., Mecky, A., Hinz, W., Urban, P., Pompon, D., Kellner, Oesch, F., 1999. Catalytic triad of microsomal epoxide hydrolase: replacement of Glu404 with Asp leads to a strongly increased turnover rate. *Biochem J.* 337 ( Pt 1):37-43.
- Arand, M., and Oesch F. 2002 Mammalian xenobiotic epoxide hydrolase In : *Enzyme systems that metabolise drugs and other xenobiotics.* Edited by C.Ioannides John Wiley & Sons Ltd
- Aravind L., Galperin M.Y., and Koonin E.V., 1998. The catalytic domain of the P-type ATPase has the haloacid dehalogenase fold. *Trends biochem. Sci.* 23, 127-129.
- Argiriadi, M.A., Morisseau, C., Hammock, B.D. & Christianson, D.W., 1999 Detoxification of environmental mutagens and carcinogens : structure, mechanism and Evolution of liver epoxide hydrolase. *Proc. Natl.Acad.Sci.Usa* 96, 10637-10642
- Asano, S., Tega, Y., Konishi, K., Fujioka, M. and Takeguchi, N., 1996. Functional expression of gastric H<sup>+</sup>,K<sup>(+)</sup>-ATPase and site-directed mutagenesis of the putative cation binding site and catalytic center. *J.Biol.Chem.* 271, 2740-2745
- Barford, D., Amit, K.D and Egloff, M.P., 1998. The structure and mechanism of protein phosphatases: insight into catalysis and regulation. *Annu.Rev.Biophys.Biomol.Stru.* 27:133-64
- Beetham, J.K., Grant, D., Arand, M., Garbarino, J., Kiyosue, T., Pinoet, F., Oesch, F., Belknap, W.R., Shinozaki, K and Hammock, B.D 1995. Gene evolution of epoxide hydrolases and recommended nomenclature. *DNA Cell Biol.* 14, 61-71.
- Borhan, B., Jones, A.D., Pinot, F., Grant, D.F., Kurth, M.J. and Hammock, B.D. 1995. Mechanism of soluble epoxide hydrolase. Formation of an  $\alpha$ -hydroxy ester-enzyme intermediate through Asp-333. *J.Biol.Chem.* 270, 26923-30
- Brockmüller J. Dissertation, 1999. Interindividual variability of cytosolic and microsomal epoxide hydrolase in human and functional effects of amino-acid polymorphism in microsomal epoxide hydrolase.
- Chacos, N., Capdevila, J., Flack, J.R., Manna, S., Martin-Wixtrom, C., Gill, S.S., Hammock, B.D. and Estabrook, R.W. 1983. The reaction of arachidonic acid epoxides with a cytosolic epoxide hydrolase. *Arch.biochem.Biophys.* 223, 639-48.
- Chen X, Wang S, Wu N, Yang CS. 2004 Leukotriene A4 hydrolase as a target for cancer prevention and therapy. *Curr Cancer Drug Targets*;4(3):267-83. Review.
- Collet, J. F., Gerin, I., Rider, M. H., Veiga-da-Cunha and van Schaftingen, E., 1997. Human L-3-phosphoserine phosphatase: sequence, expression and evidence for a phosphoenzyme intermediate. *FEBS Lett.* 408, 281-284
- Collet, J. F., Stroobant, V., Pirard, M., Delpierre, G. & Van Schaftingen, E. 1998. A new class of phosphotransferases phosphorylated on an aspartate residue in an amino-terminal DXDX(T/V) motif. *J. Biol.Chem.* 273, 14107-14112
- Collet, J. F., Stroobant, V. & Van Schaftingen, E. 1999 Mechanistic studies of phosphoserine phosphatase, an enzyme related to P-type ATPases *J.Biol.Chem.* 274, 33985-33990
- Cronin, A., Mowbray, S., Dürk, H., Homburg, S., Fleming, I., Fisslthaler, B., Oesch, F., Arand, M., 2003. The N-terminal domain of mammalian soluble epoxide hydrolase is a phosphatase. *Proc Natl Acad Sci U S A.* 100(4):1552-7.
- Dahms, A. S., Kanazawa, T. and Boyer, P. D., 1973. Source of the oxygen in the C-O-P linkage of the acyl phosphate in transport adenosine triphosphatases. *J.Biol. Chem.* 248. 6592-6595.
- Davis BB, Morisseau C, Newman JW, Pedersen TL, Hammock BD, Weiss RH. Attenuation of vascular smooth muscle cell proliferation by 1-cyclohexyl-3-dodecyl urea is independent of soluble epoxide hydrolase inhibition. *J Pharmacol Exp Ther.* 2006 Feb;316(2):815-21.
- Delinger, C.L. and Vessel, E.S. 1989 Hormonal regulation of the developmental pattern of epoxide hydrolases. *Studies in rat Liver. Biochem. Pharmacol.* 38, 603-610.
- De Vivo, M., Ensing, B. and Klein, M.L., 2005. Computational study of phosphatase activity in soluble epoxide hydrolase: High efficiency through water bridge mediated proton shuttle. *J. Am. Chem.Soc* 127, 11226-11227



- De Vivo, M., Ensing, B., Peraro, M. D., Gomez, G. A., Christianson, D. W. and Klein, M. L., 2007. Proton shuttles and phosphatase activity in soluble epoxide hydrolase. *J. Am. Chem.Soc* 129, 387-394
- Dreyer, C., Krey, G., Keller, H., Givel, F., Helftenbein, G. and Wahli, W., 1992. Control of peroxisomal  $\beta$ -oxidation pathway by a novel family of nuclear hormone Receptors. *Cell*, 68, 879-87
- Dietze, E.C., Casas, J., Kuwano, E. and Hammock, B.D. 1993a The interaction of cytosolic epoxide hydroilase from human, monkey, bovine, rabbit and murine liver by trans-3-phenylglycidols. *Comp.biochem.Physiol.* 104B, 309-314
- Dorrance AM, Rupp N, Pollock DM, Newman JW, Hammock BD, Imig JD. 2005. An epoxide hydrolase inhibitor, 12-(3-adamantan-1-yl-ureido)dodecanoic acid (AUDA), reduces ischemic cerebral infarct size in stroke-prone spontaneously hypertensive rats. *J Cardiovasc Pharmacol.*;46(6):842-8.
- Drapper, A.j. and hammock, B.D. 1999b. Soluble epoxide hydrolase in rat inflammatory cells is indistinguishable from soluble epoxide hydrolase in rat liver. *Toxicol.Sci.*50, 30-35.
- Eriksson,L., Verhaar,H.J.M.,Sjöström,M. and Hermens,J.L.M. 1993. Multivariate characterization and modelling of the chemical reactivity of epoxides. Part 2 :extension to di-and trisubstitution. *Quant.Struct.Act.Relat.* 12, 357-366
- Fahlstadius, P., Wrensch M. R., Petrakis N. L., Gruenke L. D., Mike R.,Ernster, 1988. cis-9,10-epoxystearic acid in human leukocytes: isolation and quantitative determination. *lipids* 23, 1015-1018 ;
- Fisslthaler, B., Popp, R., Kiss, I., Potente, M., Harder, D. R., Fleming, I. and Busse, R., 1999. Cytochrome P450 2C is an EDHF synthase in coronary arteries. *Nature* 401, 493-497
- Fornage, M., Hinojos, C. A., Nurowaska, B. W., Boerwinkle, E., Hammock, Morisseau, C. H. P., Doris, P. A., 2002. Polymorphisim in soluble epoxide hydrolase and blood pressure in spontaneously hypertensive rats. *Hypertension.* 40:485-90
- Fornage, M., Boerwinkle, E., Doris, PA.,Jacobs, D., Liu, K., Wong, N. D., 2004 Polymorphisim of the soluble epoxide hydrolase is associated with coronary artery calcification in African-American subjects : \_coronary artery risk development in young adults (CARD\_ )study. *Circulation.* 27 ; 109(3):335-9
- Franken, S. M., Rozeboom, H. J., Kalk, K. H. and Dijkstra, B. W., 1991. Crystal structure of haloalkane dehalogenase: an enzyme to detoxify halogenated alkanes, *EMBO J.* 10:1297-1302
- Friedberg,T., Lollmann,B.,Becker,R.,Holler,R., and Oesch,F. 1994. The microsomal epoxide haydrolase has a single membrane signal ancjor sequence which is dispensable for the catalytic activity of this protein. *Biochemistry.J.* 303: 967.972.
- Gill, S.S. and Hammock, B.D. 1980 Distribution and properties of a mammalian soluble epoxide hydrolase. *Biochem.Pharmacol.* 29, 389-395.
- Gill, S.S. and Hammock, B.D. 1981b Epoxide hydrolase activity in the mitochondrial fraction of mouse liver. *Nature* 291, 167-168.
- Goldman; P., Milne; G. W: and Keister; D. B:; 1968. Carbon-halogen bond cleavage. *J.Biol.Chem.* 243. 428-434.
- Gomez; G. A., Morisseau; C., Hammock; B.D and Christianson; D.W.; 2004. Structure of human epoxide hydrolase reveals mechanistic inferences on bifunctional catalysis in epoxide and phosphate ester hydrolysis. *Biochemistry* 43, 4716-4723.
- Gould, S.J., Keller,G.a., Schneider,M., Howel,S., Garrard,L., Goodman,J.M., diestel,B., Tabak,H.F. and Subramani, S. 1990b Peroxisomal protein import is conserved between yeast, plants, insects and mammals. *EMBO J.* 9, 85-90.
- Gould, S.J., Keller,G.a., Schneider,M., Howel,S., Garrard,L., Goodman,J.M., diestel,B., Tabak,H.F. and Subramani, S. 1990b Peroxisomal protein import is conserved between yeast, plants, insects and mammals. *EMBO J.* 9, 85-90.
- Grant, D.F., Storms, D.H. and Hammock, B.D. 1993, Molecular cloning and expression of murine liver soluble epoxide hydrolase
- Guo,A., Durner,J. and Klessing, D.F. 1998 Characterization of a tobacco epoxide hydrolase gene induced during the resistance response to TMV. *Plant J.*15, 647-656.
- Halarncar,P.P., Wixtrom,R.N., Silva,M.H. and Hammock,B.D. 1989. Catabolism of epoxy fatty esters by the purified epoxide hydrolase from mouse and Human liver. *Arch.Biochem.biophys.* 272, 226-236.
- Hammock, B. D. and Ota, K., 1983. Differential induction of cytosolic epoxide hydrolase, microsomal epoxide hydrolase, and glutathione S-transferase activities. *Toxicol Appl Pharmacol.* 1983 Nov;71(2):254-65.
- Hammock, B. D., Rinot, F., Beetham, J. K., Grant, D. F., Arad, M. E., and Orsch, F. 1994. Isolation of a putative hydroxyacyl enzyme intermediate of an epoxide hydrolase, *Nature.* 363: 693-698.
- Hassett, C., Aicher, L., Sidhu, J. S., and Omiecinski, C., 1994b. Human microsomal epoxide hydrolase : genetic polymorphism and functional expression. In vitro of amino acids variants, *Hum.mol.Genet.* 3, 421-428.

- Hengstler, J. G., Arand, M., Herrero, M. E. and Oesch, F.; 1996. Polymorphism of N-Acetyltransferases, Glutathione S transferase, Microsomal Epoxide Hydrolase and Sulfotransferases : Influence on cancer susceptibility. *Recent Results in Cancer Research*, Vol.154. Springer-Verlag Berlin. Heidelberg.
- Hollinshead, M. and Meijer, J. 1988 Immunocytochemical analysis of soluble epoxide hydrolase and catalase in mouse and rat hepatocytes demonstrates a peroxisomal localization before and after clofibrate treatment. *Eur.J.Cell Biol.* 46, 394-402
- Huang, Q., Yeldani, A. V., Alveres, K., Ide, H., Reddy, J. K. and Rao, M. S., 1995. Localization of peroxisome proliferator-activated receptor in mouse and rat tissues and demonstration of its nuclear translocation in transfected CV-1 cells. *Int.J.Onc.* 6, 307
- Imig J.D. 2005 Epoxide hydrolase and epoxygenase metabolites as therapeutic targets for renal diseases. *Am J Physiol Renal Physiol.* 289(3):F496-503.
- Ingelman\_Sundberg, M., Oscarson, M and McLellan, R.A. 1999. Polymorphic human cytochrome P450 enzymes: an opportunity for individualized drug treatment. *TIPS* 20, 342-349
- Inoue, N., Yamada, K., Imai, K. and Aimoto, T., 1993. Sex hormone related control of hepatic epoxide hydrolase activities in mice. *Biol.Pharm.Bull.* 16, 1004-1007
- Issemann, I and Green, S. 1990. Activation of a member of the steroid hormone receptor superfamily by peroxisome proliferators. *Nature* 347, 645-650
- Ivanov, Y. D., Izotov, A. A., Rukavishnikov, I. G. and Uvarov, V. Y., 1993. Determination of the secondary structure of epoxide hydrolase by Raman spectroscopy, *Biochim.Biophys. Acta.* 1162:217-220.
- Janssen, D. C., Fries, F., van der Ploeg, J., Kazemier, B., Terpstra, P. and Witholt, B., 1989. Cloning of 1,2-dichloroethane degradation genes of *Xanthobacter autotrophicus* GJ10 and expression and sequencing of the dhLA gene. *J. Bacteriol.* 171:6791-6799.
- Knehr, M., Thomas, H., Arand, M., Gebel, T., Zeller, H-D. and Oesch F. 1993 Isolation and characterization of a cDNA encoding rat liver cytosolic epoxide hydrolase and its functional expression in *Escherichia coli*. *J.Biol.Chem.* 268, 17623-27
- Koonin, E. V. and Tatusov, R. L., 1994. Computer analysis of bacterial haloacid dehalogenase defines a large superfamily of hydrolases with diverse specificity *J.Mol. Biol* 244, 125-132. .
- Kosaka, K., Suzuki, K., Hayakawa, M., Sugiyama, S. and Ozawa, T., 1994. Leukotoxin, a linoleate epoxide: Its implication in the late death of patients with extensive burns. *Mol.Cell.Biochem.* 139, 141-148
- Krämer, A., Frank, H., Setiabudi, F., Oesch, F. and Glatt, H., 1991. Influence of the level of cytosolic epoxide hydrolase on the induction of sister chromatid exchanges by trans- $\beta$ -ethylstyrene 7,8-oxide in human lymphocytes. *Biochem.Pharmacol.* 42, 2147-2152
- Lancourciere, G.M and Armstrong, R.N. 1993 Microsomal and soluble epoxide hydrolase are members of the same family of C-X bond hydrolase enzymes. *Chem.Res.Toxicol.* 7, 121-124.
- Liu, J. Q., Kurihara, T., Miyagi, M., Tsunasawa, S., Nishiara, M., Esaki, N. and Soda, K., 1997. Paracatalytic inactivation of L-2-haloacid dehalogenase from *Pseudomonas* sp. YL by hydroxylamine. Evidence for the formation of an ester intermediate. *J.Biol.Chem* 272, 3363-3368.
- Liu, J. Q., Kurihara, T., Miyagi, M., Esaki, N. and Soda, K., 1995 Reaction mechanism of L-2-haloacid dehalogenase of *Pseudomonas* sp. YL. Identification of Asp10 as the active site nucleophile by  $^{18}O$  incorporation experiments. *J.Biol.Chem* 270, 18309-18312.
- Li, Y. F., Hata, Y., Fujii, T., Hisano, T., Tishilara, M., Kurihara, T. and Esaki, N., 1998. Crystal structures of reaction intermediates of L-2-haloacid dehalogenase and implications for the reaction mechanism. *J.Biol.Chem* 273, 15035-15041
- Lodish, H., Berk, A., Zipursky, S. L., Matsudaira, P., Baltimore, D., Darnell, J., 2001. *Molecular cell biology*. Fourth edition, Freeman
- Meijer, J., Lundqvist, G. and DePierre, J. W., 1987b. Comparison of the sex and subcellular distributions and immunochemical reactivities of Hepatic epoxide hydrolases in seven mammalian species. *Eur.J.cell Biochem.* 167,269-279.
- Meijer, J. and DePierre, J. W., 1988. Cytosolic epoxide hydrolase, *Chem.Biol.Interact.* 64, 207-49
- Meijer, J., Starkerud, C. and Afzelius, B. A., 1993. Effects of clofibrate withdrawal on peroxisomes in mouse hepatocytes. *Eur.J.CellBiol.* 60,291-299
- Mertes, I., Fleischmann, R., Glatt, H. R. and Oesch, F., 1985. Interindividual variations in the activities of cytosolic and microsomal epoxide hydrolase in human liver. *Carcinogenesis* 6, 219-223- from Sandbergs paper
- Misawa, E., Chan Kwo chion, C.K.C., Archer, I.V., Woodland, M.P., Zhou, N.-Y., Carter, S.F., Widdowson, D.A. and Leak, D.J. 1998. Characterization of catabolic epoxide hydrolase from a *Corynebacterium* sp. *Eur.J.Biochem.* 253, 173-183
- Miyata, M., Kudo, G., Lee, Y-H., Yang, T.J., Gelboin, H.V., Fernandez-salguero, P., Kimura, S and Gonzales, F.J. 1999. Targeted disruption of the microsomal epoxide hydrolase gene. *J.Biol.Chem.* 274, 23963-68.

- Moghaddam, M.F., Motoba, K., Borhan, B., Pinot, F. and Hammock, B.D. 1996. Novel metabolic pathways for linoleic and arachidonic acid metabolism. *Biochim. Biophys. Acta* 1290, 327-339.
- Moghaddam, M.F., Kudo, G., Lee, Y.H., Yang, T.J., Gelboin, H.V., Fernandez-Salguero, P., Kimura, S and Gonzales, F.J. 1999. Targeted disruption of the microsomal epoxide hydrolase gene. *J. Biol. Chem.* 274, 23963-23968.
- Morais, M. C., Zhang, W., Baker A. S., Zhang, G., Dunaway-Mariano, D. and Allen, K. N., 2000. The crystal structure of *Bacillus cereus* phosphonoacetaldehyde hydrolase: insight into catalysis of phosphorous bond cleavage and catalytic diversification within the HAD enzyme superfamily. *Biochemistry* 39, 10385-10396.
- Morisseau, C., Goodrow, M.H., Dowdy, D., Zheng, D., Greene, J.F., Sanborn, J.R. and Hammock, B.D. 1999. Potent urea and carbamate inhibitors of soluble epoxide hydrolases. *Proc. Natl. Acad. Sci. USA* 96, 8849-8854.
- Mullin, C.A and Hammock, B.D. 1982. Chalcon oxides-potent selective inhibitors of cytosolic epoxide hydrolase. *Arch. biochem. Biophys.* 216, 423-439.
- Nagradova, N., 2003 Interdomain communications in bifunctional enzymes: how are different activities coordinated? *Biochem. Pharmacol* 15; 66(8):1381-91
- Ndubuisil, M. I., Kwok, B. H., Vervoort J., Koh, B. B., Eloffson, M. & Crews, C. M., 2002. Characterization of a novel mammalian phosphatase having sequence similarity to *Schizosaccharomyces pombe* PHO2 and *Saccharomyces cerevisiae* PHO13. *Biochemistry* 41, 7841-7848
- Newman, J. W., Morisseau, Harris, T. R., Hammock, B. D., 2003. The soluble epoxide hydrolase encoded by EPXH2 is a bifunctional enzyme with novel lipid phosphatase activity. *PNAS* vol.100, no.4, 1558-1563
- Newman, J. W., Morisseau, C., Hammock, B. D., 2005. Epoxide hydrolases: their roles and interactions with lipid metabolism. *Prog. Lip Res* 44 1-51
- Noris, K. K., DeAngelo, T. M. and Vessel, E. S., 1989. Genetic and environmental factors that regulate cytosolic epoxide hydrolase activity in normal lymphocytes. *J. Clin. Invest.* 84. 1749-56
- Oesch F. 1973. Mammalian epoxide hydrolases : inducible enzymes catalysing the inactivation of carcinogenic and cytotoxic metabolites derived from aromatic and olifinic compounds. *Xenobiotica.* 3, 305-340
- Ollis, D. L., Cheah, E., Cygler, M., Dijkstra, B., Frolow, F., Franken, S. M., Harel, M., Remington, S. J., Silman, I., Schrag, J., Sussman, J. L., Verschuere, K. H. G., and Goldman, A., 1993. The alpha/beta hydrolase fold, *protein Eng.* 197-211
- Ota, K. and Hammock, B. D., 1980. Cytosolic and microsomal epoxide hydrolases: Differential properties in mammalian liver *Science.* 207: 1479-1481
- Patel BN, Mackness MI, Nwosu V, Connock MJ. 1986. Subcellular localization of epoxide hydrolase in mouse liver and kidney. *Biochem Pharmacol.* 15;35(2):231-5.
- Pieper Annette, 2000. Ph.D. Synthesis and functional Characterization of fertilin.
- Pinot, F., Grant, D. F., Beetham, J. K., Parker, A. G., Borham, B., Landt, S., Jones, A. D. and Hammock, B. D., 1995. Molecular and biochemical evidence for the involvement of the Asp-333-His-523 pair in catalytic mechanism of soluble epoxide hydrolase, *J. Biol. Chem.* 270: 7968-7974.
- Pinot, F., Grant D, F., Spearow, J. L., Parker, A. G. and Hammock, B. D., 1995b. Differential regulation of soluble epoxide hydrolase by clofibrate and sexual hormones in the liver and kidneys of mice. *Biochem. Pharmacol.* 50, 501-508.
- Pirard, M., Collet, J. F., Matthijs, G. and van Schaftingen, E., 1997. Comparison of PMM1 with the phosphomannosidases expressed in rat liver and in human cells. *FEBS Lett.* 411, 251-254
- Pluth, J. M., Ramsey, M. J., Tucker J. D., 2000. Role of maternal exposure and newborn genotypes on newborn aberration frequencies. *Mutat. Res.* 16 :465 (1-2) : 101-11.
- Przybyla-Zawislak, B. D., Srivastava, P. K., Vazquez-Antias, J., Mohrenweiser, H. W., Maxwell, J. E., Hammock, B. D., Bradbury, J. A., Enayetallah, A. E., Zeldin, D. C and Grant, D. F., 2003. Polymorphisms in human soluble epoxide hydrolase. *Mol. Pharmacol.* 64: 482-490
- Raaka, S., Hassett, C. and Omiecinski, C.J. 1998. Human microsomal epoxide hydrolase: 5'-flanking region genetic polymorphisms. *Carcinogenesis* 19, 387-393.
- Ridder, I. S., Rosenboom, H. J., Kalk, K. H., Janssen, D. B. and Dijkstra, B. W., 1997. Three-dimensional structure of L-2-haloacid dehalogenase from *Xanthobacter autotrophicus* GJ10 complexed with the substrate-analogue formate. *J. Biol. Chem.* 272, 33015-33022
- Ridder, I. S., and Dijkstra, B. W., 1999. Identification of the Mg<sup>2+</sup>-binding site in the P-type ATPases and phosphatase members of the HAD (haloacid dehalogenase) superfamily by structural similarity to the response regulator protein CheY *Biochem. J.* 339, 223-226.
- Rink, R., Fennema, M., Smids, M., Dehmel, U. and Janssen, D.B. 1997. Primary structure and catalytic mechanism of the epoxide hydrolase from *Agrobacterium radiobacter* Ad1. *J. Biol. Chem.* 272, 14650-14657.

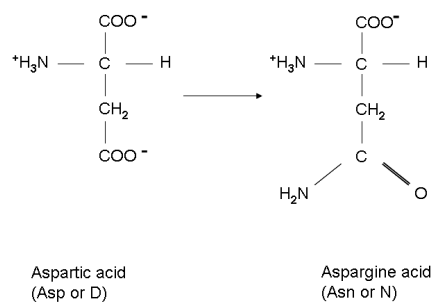
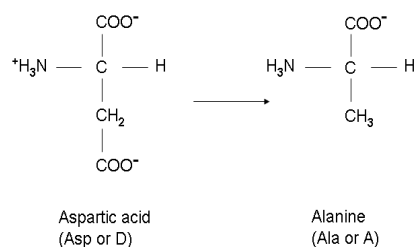
- Sandberg, M., Adman, E. T., Meijer, J. and Omiecinski, C. J. 2000. Identification and functional characterization of human soluble epoxide hydrolase genetic polymorphisms. *J.Biol.Chem.* vol.275, 37, 28873-28881
- Sandberg, M. and Meijer, J. 1996. Structural characterization of the human soluble epoxide hydrolase gene (EPHX2). *Biochem.Biophys.Res.Commun.* 221, 333-339.
- Sato, K., Emi, M., Ezura, Y., Fujita, Y., Takada, D., Ishigami T., Umemura, S., Xin, Y., Wu, L. L., Larrinaga-Shum, S., Stephenson, S. H., Hunt, S. C. and Hopkins, P. N., 2004. Soluble epoxide hydrolase variant (Glu287Arg) modifies plasma total cholesterol and triglyceride phenotype in familial hypercholesterolemia: intrafamilial association study in an eight-generation hyperlipidemic kindred. *Journal of human genetics.* 49(1):29-34
- Saito, S., Lida, A., Sekine, A., Eguchi, C., Minura, Y., Nakamura, Y., 2001. Seventy genetic variations in human microsomal and soluble epoxide hydrolase genes (EPHX1 and EPHX2) in the Japanese population. *J.Hum Genet.* 46(6):325-9
- Schladt, L., Thomas, H., Hartmann, R. and Oesch, F. 1988. Human liver cytosolic epoxide hydrolases. *Eur.J.Biochem.* 176, 715-723.
- Schanstra, J. P., Rink, R., Pries, F. and Jansen, D. B., 1993. Construction of an expression and site-directed mutagenesis system of haloalkane dehalogenase in *Escherichia coli*. *Protein expression and purification* 4, 479-489
- Schmeltzer, K. R., Kubala, L., Newman, J. W., Kim I. H., Eisereich, J. P., Hammock, B. D., 2005. Soluble epoxide hydrolase is a therapeutic target for acute inflammation. *Proc.Natl.Acad.Sci U.S.A* 102, 9772-9775
- Schneider, B., Muller, R., Frank, R., Lingens, F. 1993. Site directed mutagenesis of the 2-haloalkanoic acid dehalogenase 1 gene from *Pseudomonas* sp. strain CBS3 and its effect on the catalytic activity. *Biol.Chem. Hoppe-Seyler.* 374, 489-496.
- Seidegard, J., DePierre, J. W. and Pero, R. W., 1984. Measurements and characterization of membrane-bound and soluble epoxide hydrolase activities in resting mononuclear leukocytes from human blood. *Cancer Res.* 44, 3654-3660.
- Singh, I., 1997. Biochemistry of peroxisomes in health and disease. *Mol.Cell.Biochem.* 167, 1-29.
- Siniosoglou, S., Hurt, E. C., Pelham, H. R. B., 2000. Psr1/psr2p, two plasma membrane phosphatases with an essential DXDX(T/V) motif required for sodium stress response in yeast. *J. Biol Chem.* 2000 23;275(25):19352-60.
- Stapleton, A., Beetham, J. K., Pinot, F., Garbarino, J. E., Rockhold, D. R., Friedman, M., Hammock, B. D. and Belknap, W. R. 1994. Cloning and expression of soluble epoxide hydrolase from potato. *Plant J.* 6, 251-258
- Stock, A. M. and Mowbray, S. L., 1995. Bacterial chemotaxis: a field in motion. *Curr.Opin.Struct. Biol.* 5, 744-751
- Svinarov, D. A. and Pippenger, C. E. 1995. Valproic acid-carbamazepine interaction: is valproic acid a selective inhibitor of epoxide hydrolases? *Ther.Drug Monit.* 17, 217-220
- Thomas, H., Timms, C. W. and Oesch, F., 1990. Epoxide hydrolases: Molecular properties, induction, polymorphisms and function. In: K. Ruckpaul and H. Rein (eds.), *Frontiers in Biotransformation*, Vol. 2, pp. 278-337. Berlin: Akademie-Verlag.
- Tran, K. L., Aronov, P. A., Tanaka, H., Newman, J. W., Hammock, B. D., Morisseau, C., 2005. Lipid sulfates and sulfonates are allosteric competitive inhibitors of the N-terminal phosphatase activity of the mammalian soluble epoxide hydrolase. *Biochemistry* 44, 12179-12187
- Van Dyke, D. C., Ellingrod, V. L., Berg, M. J., Niebyl, J. R., Sherbondy, A. L., Trembath, D. G., 2000. Pharmacogenetic screening for susceptibility to fetal malformation in women. *Ann Pharmacother.* 34 (5): 639-45
- Verschuere, K. H., Seljee, F., Rozeboom, H. J., Kalk, K. H., and Dijkstra, B. W., 1993. Crystallographic analysis of the catalytic mechanism of haloalkane dehalogenase. *Nature* 363:693-698.
- Wittinghofer, A., 2006. Phosphoryl transfer in Ras proteins, conclusive or elusive? *Trends Biochem sci* 31, 20-23
- Yu Z, Xu F, Huse LM, Morisseau C, Draper AJ, Newman JW, Parker C, Graham L, Engler MM, Hammock BD, Zeldin DC, Kroetz DL. 2000. Soluble epoxide hydrolase regulates hydrolysis of vasoactive epoxyeicosatrienoic acids *CircRes.* 24; 87(11):992-8.
- Zheng J, Plopper CG, Lakritz J, Storms DH, Hammock BD. 2000. Leukotoxin-diol: a putative toxic mediator involved in acute respiratory distress syndrome. *Am J Respir Cell Mol Biol.* 25(4):434-8.

## 8 Appendix

### 8.1 The amino acid exchanges

Asp - 9, 11, 184, 185 → Ala

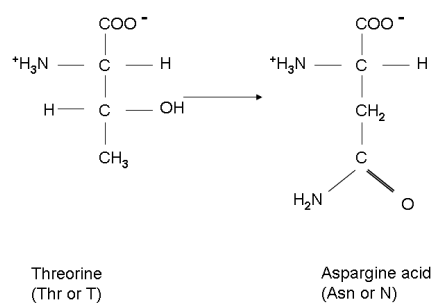
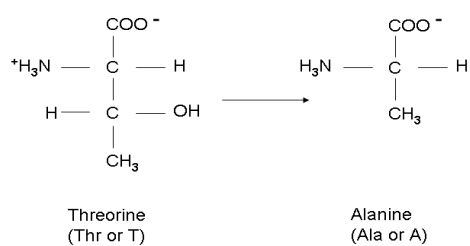
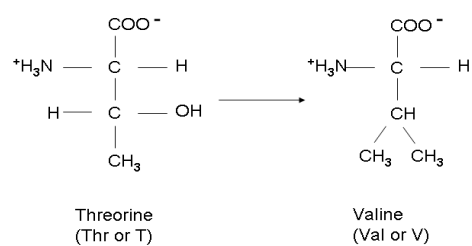
Asp - 9, 11, 184, 185 → Asn



Thr - 123 → Val

Thr - 123 → Ala

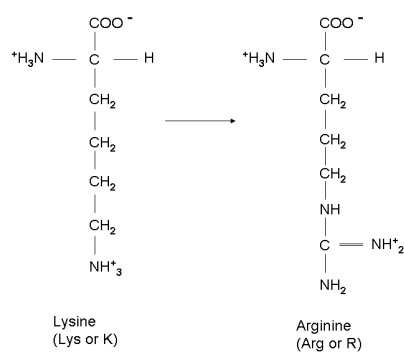
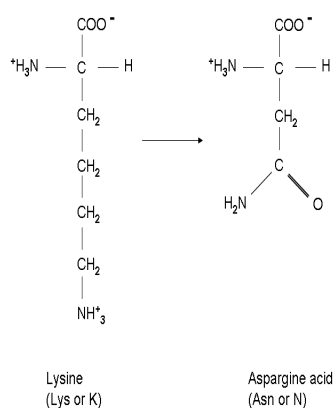
Thr - 123 → Asn

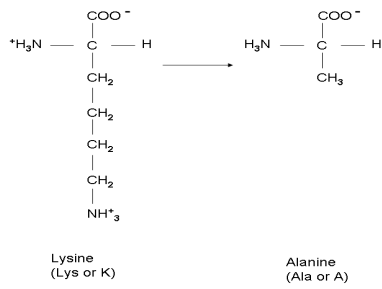


Lys - 160 → Arg

Lys - 160 → Asn

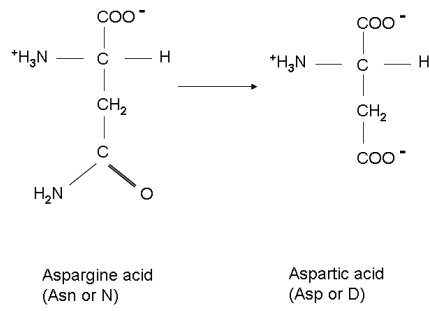
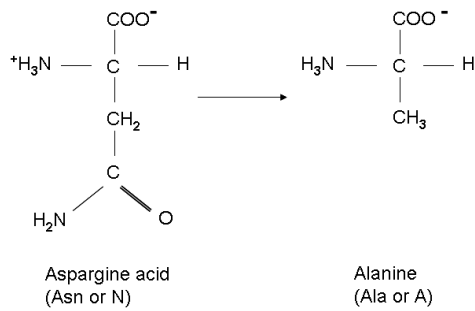
Lys - 160 → Ala





Asn – 189, 124 → Ala

Asn – 189, 124 → Asp



## 8.2 The different combinations of the amino acids genetic code

		Second letter				
		U	C	A	G	
First letter	U	UUU } Phe UUC } UUA } Leu UUG }	UCU } UCC } Ser UCA } UCG }	UAU } Tyr UAC } UAA Stop UAG Stop	UGU } Cys UGC } UGA Stop UGG Trp	U C A G
	C	CUU } CUC } Leu CUA } CUG }	CCU } CCC } Pro CCA } CCG }	CAU } His CAC } CAA } Gln CAG }	CGU } CGC } Arg CGA } CGG }	U C A G
	A	AUU } AUC } Ile AUA } AUG Met	ACU } ACC } Thr ACA } ACG }	AAU } Asn AAC } AAA } Lys AAG }	AGU } Ser AGC } AGA } Arg AGG }	U C A G
	G	GUU } GUC } Val GUA } GUG }	GCU } GCC } Ala GCA } GCG }	GAU } Asp GAC } GAA } Glu GAG }	GGU } GGC } Gly GGA } GGG }	U C A G

### 8.3 The oligonucleotide primers

**Table 1. The oligonucleotide primers that were successfully used for site directed mutagenesis are listed in the table below.** The amino acid exchange which was induced by each one of the specific primers is indicated in the left side. The nucleotide bases that introduced a point mutation leading to an amino acid substitution are marked in red. Marked in green, are the bases responsible for a modified restriction site. For comparison, the relevant WT sequence is written above each primer sequence.

The mutants	Mutation primer
Asp9→Ala (D→A)	<u>Asp</u>
Asp 9 ("W.T")	gcc gtc ttc gac ctt gac ggg gtg ctg gcg ctg
	<u>Ala</u>
Ala 9 (Mutant)	gcc gtc ttc <b>gc(c)</b> c ctt gac ggg gtg ctg gcg ctg
Asp9→Asn (D→N)	<u>Ala</u> <u>Asp</u>
	cgc gcg gcc gtc ttc gac ctt gac ggg gtg ctg gcg
	<u>Ala</u> <u>Asn</u>
	cgc gcg <b>gct</b> gtc ttc <b>aac</b> ctt gac ggg gtg ctg gcg
Asp11→Ala (D→A)	<u>Asp</u> <u>Gly</u>
	ttc gac ctt gac ggg gtg ctg gcg ctg cca gcg g
	<u>Ala</u> <u>Gly</u>
	ttc gac ctt <b>gcc</b> <b>ggc</b> gtg ctg gcg ctg cca gcg g
Asp11→Asn (D→A)	<u>Asp</u> <u>Leu</u> <u>Asp</u>
	cc gtc ttc gac ctt aac ggg gtg ctg gcg ctg cc
	<u>Asp</u> <u>Leu</u> <u>Asn</u>
	cc gtc ttc gat <b>tta</b> <b>aac</b> ggg gtg ctg gcg ctg cc
Thr123→Ala (T→A)	<u>Thr</u>
	t gcc atc ctc acc aac acc tgg ctg gac gac cg
	<u>Ala</u>
	t gcc atc ctc <b>gcg</b> aac acc tgg ctg gac gac cg
Thr123→Asn (T→N)	<u>Ala</u> <u>Ile</u> <u>Leu</u> <u>Thr</u>
	ct act gcc atc ctc acc aac acc tgg ctg gac gac c
	<u>Ala</u> <u>Ile</u> <u>Leu</u> <u>Asn</u>
	ct act <b>gca</b> <b>ata</b> <b>tta</b> <b>aac</b> aac acc tgg ctg gac gac c
Thr123→Val (T→V)	<u>Thr</u>
	t gcc atc ctc acc aac acc tgg ctg gac gac cg
	<u>Val</u>
	t gcc atc ctc <b>gtt(t)</b> aac acc tgg ctg gac gac cg
Lys160→Ala (K→A)	<u>Lys</u>
	g gga atg gtc aaa cct gaa cct cag atc tac aag
	<u>Ala</u>
	g gga atg gtc <b>gcg(g)</b> cct gaa cct cag atc tac aag
Lys→160 Asn (K→N)	<u>Lys</u> <u>Pro</u>
	a atg gtc aaa cct gaa cct cag atc tac aag tt ctg
	<u>Asn</u> <u>pro</u>
	a atg gtc <b>aat</b> <b>ccg</b> gaa cct cag atc tac aag tt ctg
Lys160→Arg (K→R)	<u>Val</u> <u>lys</u>
	g gga atg gtc aaa cct cag atc tac aag
	<u>Val</u> <u>arg</u>
	g gga atg <b>gtg</b> <b>cgc</b> cct gaa cct cag atc tac aag
Asp184→Ala (D→N)	<u>Asp</u>

The mutants	Mutation primer
	c gtt ttt ttg gat gac atc ggg gct aat ctg aag
	<u>Ala</u>
	c gtt ttt ttg g <b>cc</b> (c) gac atc ggg gct aat ctg aag
Asp184→ Asn (D→ N)	<u>Asp</u> Asp
	c gtt ttt ttg gat gac atc ggg gct aat ctg aag cca
	<u>Asn</u> Asp
	c gtt ttt ttg <b>a</b> at gat atc ggg gct aat ctg aag cca
Asp185→ Ala (D→ A)	<u>Asp</u>
	ttt ttg gat gac atc ggg gct aat ctg aag cca
	<u>Ala</u>
	ttt ttg gat g <b>cg</b> atc ggg gct aat ctg aag cca
Asp185→ Asn (D→ N)	<u>Asp</u> Ile
	ttt ttg gat gac atc ggg gct aat ctg aag cca gc
	<u>Asn</u> Ile
	ttt ttg gat <b>a</b> at att ggg gct aat ctg aag cca gc
Asn189→ Ala (N→ A)	Ala <u>Asn</u>
	ac atc ggg gct aat ctg aag cca gcc cgt gac ttg
	Ala <u>Ala</u>
	ac atc ggg gca <b>gcg</b> ctg aag cca gcc cgt gac ttg
Asn189→ Asp (N→ D)	Ala <u>Asn</u>
	ac atc ggg gct aat ctg aag cca gcc cgt gac
	Ala <u>Asp</u>
	ac atc ggg gca <b>g</b> at ctg aag cca gcc cgt gac





## 8.5 Declaration

I hereby declare that the submitted dissertation was completed by myself and no other.

Moreover, I declare that the following dissertation has not been submitted further in this form or any other form, and has not been used to obtain any equivalent qualifications at any other organisation/institution. Additionally, I have not applied for, nor will I attempt to apply for any other degree or qualification to this work.

Shirli Homburg

## 8.6 Curriculum Vitae

### Shirli Homburg

Born: April 2, 1969, Israel  
Nationality: Israeli and British  
Family status: Divorced, mother of two sons (9 and 4 years)  
Address: Am Roren Tor 79  
55232 Alzey (06731-648021, 0171-6262295)

#### Education

2000 - 2010 Ph.D, Department of Toxicology, Johannes Gutenberg University, Mainz, Germany  
Thesis: "Biochemical analysis of the phosphatase domain of the human soluble epoxide hydrolase (sEH)"  
1995 – 1998 Master of Science (M.Sc), Department of Biochemistry, Faculty of Life Sciences and Department of Physiology and Pharmacology, Faculty of Medicine, Tel- Aviv University, Israel  
Thesis: "The effect of a depolarising signal on the activity of the enzyme poly (ADP-ribose) polymerase and the enzyme's involvement in signal transduction of the depolarising signal in rat neuronal cells and cardiac myocytes in primary cultures"  
1991 – 1994 Bachelor of Science (B.Sc), Faculty of Life Sciences, Tel- Aviv University, Israel

#### Work experience

2008 – present Working in the field of toxicology, regulatory toxicology and REACH in SCC (Scientific Consulting Company), Wendelsheim, Germany  
2003 – 2007 Basic and clinical scientific writing for medical journals and internet sites (www.adhesions.de and www.endogyn.com); organization of courses for a gynaecological endoscopic institute (Endogyn) and the "12<sup>th</sup> Regional Meeting of the International Society for Gynecological Endoscopy"  
2004 – 2006 Work in in-vitro fertilization (IVF) laboratory, Free University Medical Centre, Amsterdam, Holland  
1999 – 2001 Intelligence work for the Israeli embassy, Frankfurt, Germany  
1997 – 1998 Teacher of biology and science, Avney Hahoshen High School, Rishon Lezion, Israel  
1995 – 1998 Assistant professor in the Biochemistry Department, Life Science Faculty and the Physiology and Pharmacology Department, Faculty of Medicine, Tel-Aviv University (required for a master degree scholarship)  
1988 – 1991 Compulsory army service, IDF, officer dealing with education and knowledge of Israel

**Publications**

1. Cohen-Armon M., Hammel I., Anis Y., Homburg S., Dekel N.  
Evidence for endogenous ADP-ribosylation of GTP-proteins in neuronal cell nucleus.  
Journal of Biological Chemistry. 271:26200-26208, 1996.
2. Homburg S., Visochek L., Moran N., Danzer F., Priel E., Asculai E., Schwartz D., Rotter V., Dekel N., Cohen-Armon M.  
A fast signal-induced activation of poly (ADP-ribose) polymerase: A novel downstream target of phospholipidase C.  
Journal of Cell Biology. 150:293-307, 2000.
- 3\* Cronin A., Mowbray S., Durk H., Homburg S., Fleming I., Fisslthaler B., Oesch F., Arand M.  
The N-terminal domain of mammalian soluble epoxide hydrolase is a phosphatase.  
Proceedings of National Academy of Science USA. 100:1552-1557, 2003.
4. Kruschinski D., Homburg S., Wockel A., Kapur A., Reich H.  
Lift-laparoscopic total hysterectomy as a routine procedure.  
Surgical Technology International. 13:147-156, 2004.
5. Kruschinski D., Homburg S.  
Lift-(gasless) laparoscopic surgery under regional anesthesia.  
Surgical Technology international. 14:193-6, 2005.
6. Kruschinski D., Homburg S., D'souza F., Campbell P., Reich H.  
Adhesiolysis in severe and recurrent cases of adhesion related disorder (ARD)- a novel approach utilizing lift (gasless) laparoscopy and SprayGel adhesion barrier  
Surgical Technology International. 15:131-9, 2006.
- 7\*. Cronin A., Homburg S., Dürk H., Richter I., Adamska M., Frere F., and Arand M.  
Characterization of human sEH phosphatase by site directed mutagenesis and LC-MS/MS analysis  
Journal of Molecular Biology. 383: 627-40, 2008.

\* Related to my thesis.